International Atomic Energy Agency

INDC(NDS)-173/GI
INT(85)-7

INDC INTERNATIONAL NUCLEAR DATA COMMITTEE

STATUS REVIEWS OF 14 MEV NEUTRON INDUCED CROSS SECTIONS: MEASUREMENTS AND CALCULATIONS

Text of lectures delivered during the second Research Co-ordination Meeting (Gaussig, GDR, November 1983) for the Co-ordinated Research Programme on measurement and analysis of 14 MeV neutron nuclear data needed for fission and fusion reactor technology

Compiled by
M.K. Mehta

September 1985

IAEA NUCLEAR DATA SECTION, WAGRAMERSTRASSE 5, A-1400 VIENNA

INDC(NDS)-173/GI
INT(85)-7

STATUS REVIEWS OF 14 MEV NEUTRON INDUCED CROSS SECTIONS: MEASUREMENTS AND CALCULATIONS

Text of lectures delivered during the second Research Co-ordination Meeting (Gaussig, GDR, November 1983) for the Co-ordinated Research Programme on measurement and analysis of 14 MeV neutron nuclear data needed for fission and fusion reactor technology

Compiled by
M.K. Mehta

September 1985

Reproduced by the IAEA in Austria
September 1985

85-04282

Foreword

This report contains the text of invited review lectures delivered during the second research co-ordination meeting of the co-ordinated research programme on measurement and analysis of 14 MeV neutron nuclear data needed for fission and fusion reactor technology. The meeting was held at Gaussig (GDR) during 21-25 November 1983 and was hosted by TUD Dresden. Concurrently with the meeting an International Symposium on Fast Neutron Reactions, and review lectures were a part of the programme of the Symposium. Since the meeting there have been many requests from laboratories participating in the Interregional Project INT/1/018 on Nuclear Data Techniques and Instrumentation to make the texts of the lectures available in the printed form as the review lectures have been found to be very useful both as guidelines and for planning experimental programmes with 14 MeV neutron generator. It was then decided to publish the texts as an INDC(NDS)- report as part of the series of reports generated by the work done under the Interregional Project. The texts are reproduced directly from the Authors' manuscripts without any editing.

Table of Contents

Present 14 MeV nuclear data needs for fission and fusion reactor technology *

J.J. Schmidt
Nuclear Data Section
International Atomic Energy Agency
Vienna, Austria

Abstract

The requirements for improved 14 MeV neutron cross sections for fission and fusion reactor technology are reviewed on the basis of the requests contained in the 1981/82 issue of the World Request List for Nuclear Data, WRENDA, published by the IAEA. Reactor neutronics calculations, neutron and γ-shielding design, material activation, and the prediction and monitoring of radiation damage are the most prominent application areas, where the major requirements occur for improved partial neutron reaction, neutron- and γ-production cross sections, and energy and angular distributions of secondary emitted neutrons and charged particles.

* Invited paper presented at the XIIIth International Symposium on Nuclear Physics - Fast Neutron Reactions, organized by the Technical University Dresden in Gaussig, German Democratic Republic, 21-25 November 1983.

I. Introduction

14 MeV neutrons have a rather singular threefold importance:

(i) They represent about the upper energy limit of neutrons occurring in nuclear fission reactors;

(ii) The (D,T) reaction in which 14 MeV neutrons are generated represents the basis for all contemporary fusion reactor designs based on magnetic plasma confinement;

(iii) The (D,T) reaction used in neutron generators allows the measurement of absolute and relative 14 MeV neutron cross sections.

Requests for improved 14 MeV neutron nuclear data therefore frequently occur in the most recent IAEA World Request List for Nuclear Data, WRENDA 81/82 [1]. Almost half of the total number of individual requests contained in WRENDA 81/82; i.e. 838, is directly for 14 MeV neutrons or includes the 14 MeV "point" as part of a larger energy range, and covers 66 different nuclear data types for 108 different elements and isotopes. In the following we shall use the WRENDA 81/82 requests, subdivided into several more important areas of application, as a guideline to the explanation of 14 MeV neutron nuclear data requirements for fission and fusion reactor technology.

II. Standards

Most neutron cross section measurements are performed relative to a standard reference cross section; this has the advantage that one does not need to measure the neutron flux. On the other hand, known standard neutron cross sections can be used to measure the neutron flux. Three important standard neutron cross sections are requested in WRENDA 81/82 with the following accuracies:

$^{1}H(n,n)(\theta_n)$ $\pm$ 1 %

$^{6}Li(n,t)\alpha$ $\pm$ 5 %

$^{235}U(n,f)$ $\pm$ 1-2 %

III. Neutron transport calculations for nuclear fission reactors

In the present stage of the development of nuclear fission reactor technology one can broadly discern between thermal power and research reactors and fast breeder reactors and critical facilities. The analysis and design of these reactors are performed with two major calculational methods:

(i) multigroup diffusion or transport theory, and

(ii) the Monte Carlo method.

The first method needs multigroup neutron cross sections, the second collision probabilities as input data. These input data are computed from large evaluated neutron cross section computer files which in turn are generated from experimental data complemented by theoretical calculations.

In fission reactor design and safety analysis the following characteristic quantities are being computed:

- energy- and space dependent neutron flux density $\phi(\vec{r},E)$ all over the reactor;
- effective neutron multiplication factor K_{eff};
- breeding (or conversion) ratio;
- nuclear fuel composition and enrichment;
- critical mass of nuclear fuel;
- critical reactor size;
- absorption and activation of coolant and structural materials;
- safety coefficients, i.e. changes of K_{eff} as a function of temperature, $\delta K_{eff}/\delta T$:
  - (i) Doppler coefficient;
  - (ii) Na-void coefficient;
  - (iii) fuel thermal expansion coefficient

  etc.

Typical fission reactor materials are:

- fissile isotopes: ^{235}U, $^{239,241}Pu$ etc.
- fertile isotopes: ^{238}U, ^{240}Pu etc.
- structural materials: Fe, Cr, Ni, Zr and other metals
- coolants: H_2O, D_2O, CO_2, He, Na
- control rod materials: B, Ta
- shielding materials: Fe, Pb, Si, Ba etc.
- oxide fuel: O
- carbide fuel: C

III.1. Thermal fission reactors

In thermal fission reactors the largest neutron nuclear interaction rates occur for neutrons from below 1 meV to several eV and concern (n,γ), (n,f) and (n,n) processes, in addition neutron capture and fission resonance integrals and thermal scattering law data are needed.

The very small number of 14 MeV neutrons in thermal fission reactors is reflected by a very small number of data requests in WRENDA 81/82. We quote a few higher priority requests and their purpose:

- $^{2}H(n,2n)$, ± 5 %, for computing neutron multiplication in D_2O-cooled reactors;
- $Zr(n,nem)$ $(E_{n'},\theta_{n'})$, ± 10 %, for estimating neutron emission by the structural material Zr;
- $^{233}U(n,f)$, ± 5 %, used as fuel in ^{232}Th - ^{233}U reactors.

III.2. Fast fission reactors

In fast fission reactors the neutrons cover a much larger energy range from eV to about 15 MeV. In addition to (n,γ), (n,f) and (n,n), endothermic threshold reactions such as (n,n'), (n,p), (n,α) and (n,2n) as well as the energy and angular distributions of secondary emitted particles, and parameters over the full range of resolved and unresolved resonances become important. The larger number of 14 MeV neutrons in fast reactors and the greater diversity of neutron nuclear reactions is reflected in a larger number and diversity of requests in WRENDA 81/82.

Inelastic neutron scattering is the major neutron slowing-down mechanism in fast reactors, and, because of its usually large fraction in the nuclear fuel and strong excitation of its low-lying levels, inelastic neutron scattering on ^{238}U is the process which influences most strongly the neutron energy spectrum of a fast reactor. Total neutron inelastic scattering cross sections, level excitation cross sections, and spectra of inelastically scattered neutrons are therefore required with a high accuracy of ± 5 %. The same quantities are requested for Fe(± 5-10 %), Cr, Ni (± 10-30 %), Na(± 10 %), and fissile materials (± 10-15 %) with less accuracy reflecting the smaller importance of these materials for the neutron spectrum.

Highest priority still at 14 MeV have the fission and neutron multiplication properties of the main fissile and fertile isotopes, i.e. the (n,f) process, the prompt number of fission neutrons, $\bar{\nu}$, the energy spectrum of prompt fission neutrons, $N_f(E)$, and the (n,2n)-process. The following table summarizes the most important accuracy requirements.

Isotope	Accuracy (± %)			
	(n,f)	$\bar{\upsilon}$	$N_f(E)$	(n,2n)
^{235}U	1-2	1	5	-
^{238}U	2-5	1	2	5-10
^{239}Pu	2	0.5-1	1	10-15
^{240}Pu	3-5	1	3	-
^{241}Pu	10	5	-	20

Neutron absorption in Fe, Cr and Ni, the main components of stainless steel which is the commonly used structural material in fast reactors, has a similarly strong influence on the neutron economy of fast reactors, and is therefore requested with similarly high priority and an accuracy of ± 5 %.

Secondary actinides, such as ^{237}Np, ^{238}Pu, $^{241,242,243}Am$ and $^{242,243,244,245}Cm$ isotopes, built up during reactor operation in successive neutron capture processes and radioactive decays starting from the primary actinides, have much lower concentrations in the nuclear fuel than the primary actinides and thus a much smaller influence on neutron economy. Neutron fission and multiplication parameters of secondary actinides need therefore to be known only to accuracies of ± 10-30 %.

IV. Neutron transport calculations for nuclear fusion reactors

All currently considered magnetic confinement fusion devices such as tokamaks, mirror machines and others are based on the T(d,n)α reaction which produces 14 MeV neutrons and 3.5 MeV α-particles. A typical tokamak-type fusion reactor contains a plasma composed of deuterons and tritons surrounded by a first wall of toroidal shape which in turn is surrounded by a shielding blanket in which, through interaction of the neutrons produced in the plasma with lithium, tritium is produced and fed back into the plasma.

Neutron transport theory is used to calculate the neutron flux density, $\phi(\vec{r},E)$, throughout the reactor; such calculations are also called neutronics, neutron balance or neutron economy calculations.

The following materials are typical for fusion reactors:

Fuel:	D,T
Tritium breeding materials:	^{6}Li, ^{7}Li compounds
Coolant:	e.g. FLiBe compound (F,Li,Be)

First wall materials:	Fe, Cr, Ni, Ti, V, Mo, Nb, W
Other structural materials:	C (Carbid), Al
Neutron multipliers:	Be, Pb
Magnet conducting materials:	Cu, Be, Al, Sn
Reflectors and moderators:	Be, B, C, O
Shielding materials:	B, C, O, Si

The 14 MeV neutrons produced in the plasma are slowed down in the first wall and in the blanket. A typical spectrum of the neutrons entering the blanket extends down to KeV energies, with the bulk of the neutrons centered in the MeV range and a strong component of 14 MeV neutrons. For neutronics calculations therefore all neutron cross sections of the above materials have to be known from KeV energies to about 15 MeV, with an emphasis on partial reactions such as (n,p), (n,np), (n,α), (n,nα), (n,2n) etc. and on energy and angular distribution of secondary particles (neutrons and charged particles) emitted in these reactions. We consider now various aspects of fusion reactor design calculations for which specific classes of neutron data are required.

IV.1. Multiplication of neutrons

(n,xn)($x \geq 2$) and (n,f) reactions can be used to enhance the neutron flux through neutron multiplication and thus the breeding of fuel in the following ways.

In normal (d,t)-fusion reactors, materials with high (n,2n) cross sections such as Be, Fe, V, Zr, Mo, Nb, Pb and Bi, used as main or additional materials in the first wall, can lead to a significant multiplication of the neutrons impinging on the blanket and thus to enhanced tritium breeding.

In fission-fusion hybrid reactors, addition of inner blankets of ^{232}Th or ^{238}U is being considered for two purposes:

(i) breeding of ^{233}U or ^{239}Pu (via (n,γ) reaction in ^{232}Th or ^{238}U and two subsequent β-decays);

(ii) multiplication of neutrons through (n,2n), (n,3n) and (n,f) reactions for enhanced tritium breeding in the outer Li blanket.

For all of the above materials WRENDA 81/82 contains requests for (n,2n), (n,3n) and (n,f) reaction cross sections with accuracies ranging from $\pm$ 10-15 %.

IV.2. Neutron activation

Also in fusion reactors neutron activation represents a serious problem: calculations of neutron-induced radioactivities are essential to assess radiation hazards and thus reactor safety, and the requirements for radioactive waste disposal. Thus for all fusion reactor materials all neutron activation cross sections for processes

leading to radioactive nuclei are requested with ± 10-20 % accuracies. In this context also reactions with smaller cross sections such as (n,t) or (n,nd) reactions can be important as exemplified by requests with ± 20 % accuracy for these reactions on ^{56}Fe and ^{60}Ni nuclei.

IV.3. Parasitic neutron absorption

Neutrons captured in (n,p), (n,α), but also (n,γ), (n,d), (n,t) and (n,^{3}He) reactions with lower cross sections are lossed for tritium breeding. Major parasitic neutron absorbers are the structural materials used in the first wall and in the blanket through (n,p) and (n,α) reactions which are requested with ± 10-20 % accuracy. Other typical requests are for (n,α) cross sections of ^{12}C and ^{19}F with ± 10-15 % accuracy and for the (n,p) cross section of ^{52}Cr with ± 10-25 % accuracy.

IV.4. Coolant effect calculations

The compound FLiBe is considered simultaneously as tritium breeding material and as coolant for the blanket. ^{19}F is thus one of the constituents of FLiBe and will influence the neutron economy as well as the tritium breeding in the blanket. For this element neutron elastic scattering angular distributions, absorption, activation and double-differential neutron emission cross sections are requested with ± 10-15 % accuracy.

IV.5. Structural materials

Stainless steel with Fe, Cr and Ni as major constituents is the main structural material foreseen for first wall, blanket etc. of fusion reactors, but Ti, V, Mo and W are also under consideration. (n,n'), (n,2n) and (n,3n) processes with these materials are mainly responsible for the degradation in energy of the neutrons produced in the plasma and thus largely determine the energy spectrum of the neutrons impinging on the blanket. This explains the large number of high priority ± 10 % accuracy requests for neutron inelastic scattering cross sections and energy distributions and for double-differential neutron emission cross sections

$$\sigma_{n,nem} = \sigma_{n,n'} + 2\,\sigma_{n,2n} + 3\,\sigma_{n,3n} + \ldots$$

IV.6. Tritium breeding and blanket calculations

Tritium is bred through the following neutron reactions with Li isotopes:

$$^{6}Li(n,t)\alpha \text{ and } ^{7}Li(n,n't)\alpha$$

The cross sections for these two reactions are requested with highest priority and a high accuracy of ± 5 %.

However, in tritium breeding calculations also all competing neutron reactions with these two isotopes must be known and are requested in WRENDA 81/82 with high priority, e.g. for both isotopes

(n,n), $(n,n)(\theta_n)$ with $\pm$ 10-20 % accuracy,
(n,n'), $(n,n')(\theta_{n'})$, $(n,n')(E_{n'})$ with $\pm$ 20 % accuracy,
$(n,2n)$, $(n,2n)(\theta_{n'})$ with $\pm$ 15-20 % accuracy, and

for ^{7}Li

(n,np), $(n,np)(\theta_p)$
(n,nd), $(n,nd)(\theta_d)$
} with $\pm$ 20 % accuracy.

V. Shielding of fission and fusion reactors

Shielding materials have several effects:

(i) they absorb (and thus shield) neutrons essentially through (n,γ), (n,p) and (n,α) reactions.

But they also

(ii) scatter neutrons through (n,n) and (n,n') processes;

(iii) multiply neutrons through $(n,2n)$ and $(n,3n)$ processes; and

(iv) produce gamma rays through the (n,γ) process and as a byproduct of almost all particle emitting reactions which do not lead to the groundstate of a stable residual nucleus.

This explains the following three classes of requests listed in WRENDA 81/82 for a number of shielding materials for fission as well as fusion reactors, mostly with high priority:

(i) Requests for neutron scattering cross sections

Fe $(n,n)(\theta_n)$ $\pm$ 10 % accuracy
Bi $(n,n)(\theta_n)$, $(n,n')(E_{n'})$ $\pm$ 20 %

(ii) Requests for neutron emission cross sections

Al, Si, Ca, Pb (n,nem) (n,nem) $(\theta_{n'},E_{n'})$ $\pm$ 5-15 %

(iii) Requests for γ-production cross sections

Fe, Ni, Zr, Pb, Bi $\pm$ 10-15 %
(n,totaly), $(n,totaly)(E_\gamma)$, $(n,totaly)(\theta_\gamma,E_\gamma)$

For fast fission reactors the same quantities are requested with high priority and $\pm$ 5-10 % accuracy for the main fissile and fertile isotopes which in core and blanket act as γ-sources.

VI. Radiation damage in fission and fusion reactors

VI.1. Displacements and nuclear transmutations

Nuclear reactions cause two major types of radiation damage to reactor structural materials:

(i) displacement of atoms from their normal lattice positions (only partially remedied through temperature-dependent annealing); and/or

(ii) nuclear transmutations leading to new elements and to the build-up of hydrogen and helium.

The displacement effect is of course the more pronounced the higher the energy is of the neutrons colliding with the structural material nuclei. For fast fission reactor neutrons with energies typically in the higher KeV and lower MeV range, below the threshold of (n,charged particle reactions), displacement is the major damage mechanism. This effect is still much more pronounced at the higher MeV energies typical for fusion reactor neutron spectra.

Nuclear transmutations mostly through (n,p) and (n,α) reactions take place in fast fission reactors, but are also much more important in fusion reactors, due to the harder neutron energy spectra and larger neutron cross section values in these spectra. It should be noted that transmutation reactions also always cause displacements.

Displacements and transmutations lead to

- embrittlement,
- radiation-enhanced creeping, and
- surface blistering and bulk swelling

of reactor structural materials and are thus the main factors determining the life time of reactor structures and, in particular, of reactor pressure vessels. From the above it is evident that radiation damage in fusion reactors is much more severe than in fission reactors. Reliable computational estimates are still hampered not only by uncertainties in metallurgical data, but also by uncertainties and gaps in nuclear data. This is reflected in the large number of high priority WRENDA requests, particularly for fusion reactors. For all or most of the following elements and isotopes

Li, ^{6}Li, ^{7}Li, ^{9}Be, ^{10,11}B, C, N, O, F, Al, Si, Ti, V, Cr, Fe, Ni, Cu, Zr, Nb, Mo, Sn and W

the following neutron cross section data are requested:

(n,p) (n,α) with $\pm$ 10-20 % accuracy

(n,total p), (n,total p)(θ_p,E_p) } with $\pm$ 10 % accuracy

(n,total α), (n,total α)(θ_α,E_α) }

$(n,n)(\theta_n)$, $(n,nem)(\theta_{n'},E_{n'})$ with $\gtrsim \pm 10$ % accuracy

VI.2. Computational estimates of radiation damage caused by displacements

Computational estimates of radiation damage caused by displacements in fission or fusion reactor structures presuppose a knowledge of neutron energy spectra inside or close to these structures, e.g. close to the pressure vessels. Those in-pile spectra are usually deduced from multiple foil activation measurements in the following way. Neutron-induced radioactivities (A_i) are being measured for N different neutron reactions:

$$A_i^{exp} = \int_0^\infty \sigma_i(E)\, \phi\,(E)\, dE;\ i = 1, 2, \ldots., N$$

with

E = neutron energy,

$\sigma_i(E)$ = cross section for neutron dosimetry reaction i,

$\phi(E)$ = neutron energy spectrum.

From the above set of equations, for measured A_i and known σ_i, $\phi(E)$ can be obtained through an unfolding procedure. With known $\phi(E)$, the displacement rate can be obtained as

$$I_{Displ.} = \int_0^\infty \sigma_{Displ.}(E)\, \phi\,(E)\, dE$$

where

$\sigma_{Displ.}$ = sum of all neutron scattering and reaction cross sections of the structural material in question, each cross section weighted with its specific damage function.

$I_{Displ.}$ can be measured, e.g. in DPA = displacements per atom, and compared with calculated values.

WRENDA 81/82 contains a number of requests for neutron dosimetry reactions and damage cross sections as summarized below.

Reaction	Isotope	Accuracy (± %)
(n,γ)	^{45}Sc	10
(n,p)	^{32}S, $^{46,47,48}Ti$, ^{54}Fe, ^{59}Co, ^{58}Ni, ^{63}Cu	5
(n,np), (n,d)	$^{47,48}Ti$	5

Reaction	Isotope	Accuracy (± %)
(n,nd), (n,t)	^{56}Fe	5
(n,α)	^{54}Fe, ^{63}Cu	5
(n,n')	^{93}Nb, ^{103}Rh, ^{115}In, ^{199}Hg (leading to long-lived isomer states)	5-10
(n,2n)	^{55}Mn, ^{58}Ni, ^{93}Nb, ^{197}Au	$\gtrsim$5
(n,f)	^{237}Np	$\lesssim$5
Damage cross sections	C, Cr, Fe, Ni	10

Reference

1. WRENDA 81/82, IAEA World Request List for Nuclear Data; N. Dayday, IAEA, Editor; INDC(SEC)-78/URSF, July 1981.

STUDY OF (n,d), (n,t), (n,^{3}He) AND (n,α) REACTIONS BY ACTIVATION AND OTHER OFF-LINE TECHNIQUES

S.M. QAIM
Institut für Chemie 1 (Nuklearchemie),
Kernforschungsanlage Jülich GmbH,
5170 Jülich, Federal Republic of Germany

ABSTRACT

Some of the off-line techniques used in the study of (n, complex particle) reactions are outlined. The status of available cross section data is reviewed and a brief discussion of the possible reaction mechanisms is given.

INTRODUCTION

In the interactions of fast neutrons with nuclei complex particles like ^{2}H, ^{3}H, ^{3}He and ^{4}He are emitted with a low probability. This probability decreases with the increasing charge of the target nucleus. Studies of complex particle emitting reactions are of considerable significance, on the one hand for enhancing our understanding of nuclear theory and, on the other, for practical applications, especially for estimating nuclear heating and radiation damage effects. The information available on the emission of complex particles, with the exception of α-particles, however, is rather small. Since the cross sections are low, purely physical methods involving spectral investigations of the emitted particles are often inadequate and use of interdisciplinary techniques is essential. This paper gives a short review of some of the recent advances in this field of study, achieved by off-line methods of measurement.

OFF-LINE TECHNIQUES

Three techniques have been commonly used to study charged particle emission reactions by off-line methods. These are:

- Activation
- Gas accumulation
- Mass spectrometry

We discuss these below individually.

Activation Technique

This is a relatively simple technique and involves identification and radiometric determination of the radioactive reaction product. It is a highly sensitive method, especially in combination with specific radiochemical separations and high-resolution counting methods. It should, however, be mentioned that, despite its simplicity, the technique can lead to erroneous results if proper precautions are not taken. Most of the early cross section data at 14 MeV were obtained using this technique; many of them, however, show large discrepancies. Several of the steps involved and the various precautions needed in the precise measurements of cross sections by this technique were critically reviewed recently by Csikai [1] and Qaim [2]. In investigations on low-yield reactions like (n,t) and (n,^{3}He), high-purity substances (if possible as highly enriched isotopes) should be used as target materials. Since relatively thick targets are needed, use of internal standards for neutron flux monitoring is recommended. Clean radiochemical separations and low-level methods of counting are most essential [cf. 3-6].

The advantages of the activation technique are:

- Simplicity
- High sensitivity. In the case of (n,^{3}He) reactions at 14 MeV cross sections of $\sim$ 1 μb have been measured. Depending on the half-life of the activation product the detectable limit corresponds to $\sim 10^{2}$ atoms.
- Distinction between (n,x) and (n,n'x) type processes is possible.
- Cross section measurement of processes leading to the formation of even closely spaced isomeric levels (with measurable half-lives) is possible.

The limitations of the activation technique are:

- Non-applicability in the case of stable reaction products.
- Yields only integral data; information on reaction mechanism is rather small.
- Contributions of competing reaction channels leading to the formation of the same activation product are not distinguishable. At 14 MeV this is specially so in the case of (n,d) reaction where the same reaction product is also formed via (n,n'p) and (n,pn) processes.

Gas Accumulation

The activation technique can be somewhat modified when the product is a soft radiation emitting gas, like ^{3}H, ^{14}C, ^{37}Ar etc. The irradiated sample is generally opened in a vacuum apparatus and heated to high temperatures in the presence of some carrier gas. The radioactive gaseous product is then released and collected together with the carrier gas in a bulb. Part of this activity is then transferred to a gas counting tube which is then filled with methane to normal pressure and connected to an anticoincidence counting system. Some analytical check is necessary to ascertain that the collected gas

is really the investigated product. This is generally done by radiogas chromatography [cf. 7,8] but pulse height discrimination technique has also been used [cf. 9].

The advantages and limitations of this technique are somewhat similar to those described above for the activation technique. A series of studies on triton emission reactions has been performed using tritium separation and gas phase counting [cf. 7,9-12]. The detectable limit corresponds to $\sim 5 \times 10^7$ atoms. In these measurements, as expected, a sum of (n,t) and (n,xt) contributions is obtained.

Mass Spectrometry

This technique involves identification of the reaction product via its mass. As far as study of fast neutron induced reactions is concerned, the method has been applied to the estimation of ^{3}He and ^{4}He, the detection of ^{1}H, ^{2}H and ^{3}H being so far not attempted.

Two types of mass spectrometers have been used, viz. a magnetic spectrometer in a static mode for detecting ^{4}He [cf. 13] and a quadrupole spectrometer in a dynamic mode for detecting ^{3}He-particles [cf. 14]. Mass spectrometry constitutes a sensitive method for the detection of light mass gaseous products and $\sim 10^8$ atoms in about 2 g samples can be detected. The dynamic range of the system is generally $> 10^7$, which means that the intensity ratios of $1:10^7$ for neighbouring masses can be well distinguished.

Similar to the activation and gas accumulation techniques the mass spectrometric method yields only integral cross sections so that little information on the reaction mechanism is obtained. Furthermore, a sum of (n,x) and (n,n'x) type cross sections is obtained. The sensitivity of this method is lower than those

of the other two techniques. The superiority of mass spectrometry in comparison to the other two off-line methods, however, lies in the fact that even stable transmutation products can be measured.

STATUS OF INTEGRAL DATA

Some of the integral cross section data were deduced by an integration of the differential data [cf. 15]. However, a larger body of the data has been obtained using the off-line techniques described above. The agreement between the data obtained using various techniques is relatively good, thereby adding confidence to the more recent measurements. The four types of reactions considered here are discussed below.

(n,d) Reactions

Among the off-line methods so far only the activation technique has been used. The cross sections obtained at 14 MeV give a sum of (n,d), (n,n'p) and (n,pn) processes, all of which lead to the same product nucleus. The results of a systematic study carried out at Jülich have been recently summarized [16] and are shown in Fig. 1. The data fall distinctively on two curves: one for the lightest stable target nuclei, which are rather away from the stability line of the investigated elements, and the other for nuclei richer in neutrons. In the case of the lightest target nuclei the neutron separation energy (S_n) is higher than the proton separation energy (S_p) and the dominant process is the (n,n'p) reaction. For the neutron richer nuclei possibly all the three processes make appreciable contributions.

Using the activation technique a few measurements on [(n,d)+(n,n'p)+(n,pn)] reactions were also performed in the energy range of 15 to 2o MeV and with a 3o MeV d(Be) break-up neutron spectrum. However, so far not a single measurement covering the early rising part of an excitation function, i.e. in the energy range of 5 to 1o MeV, has been reported.

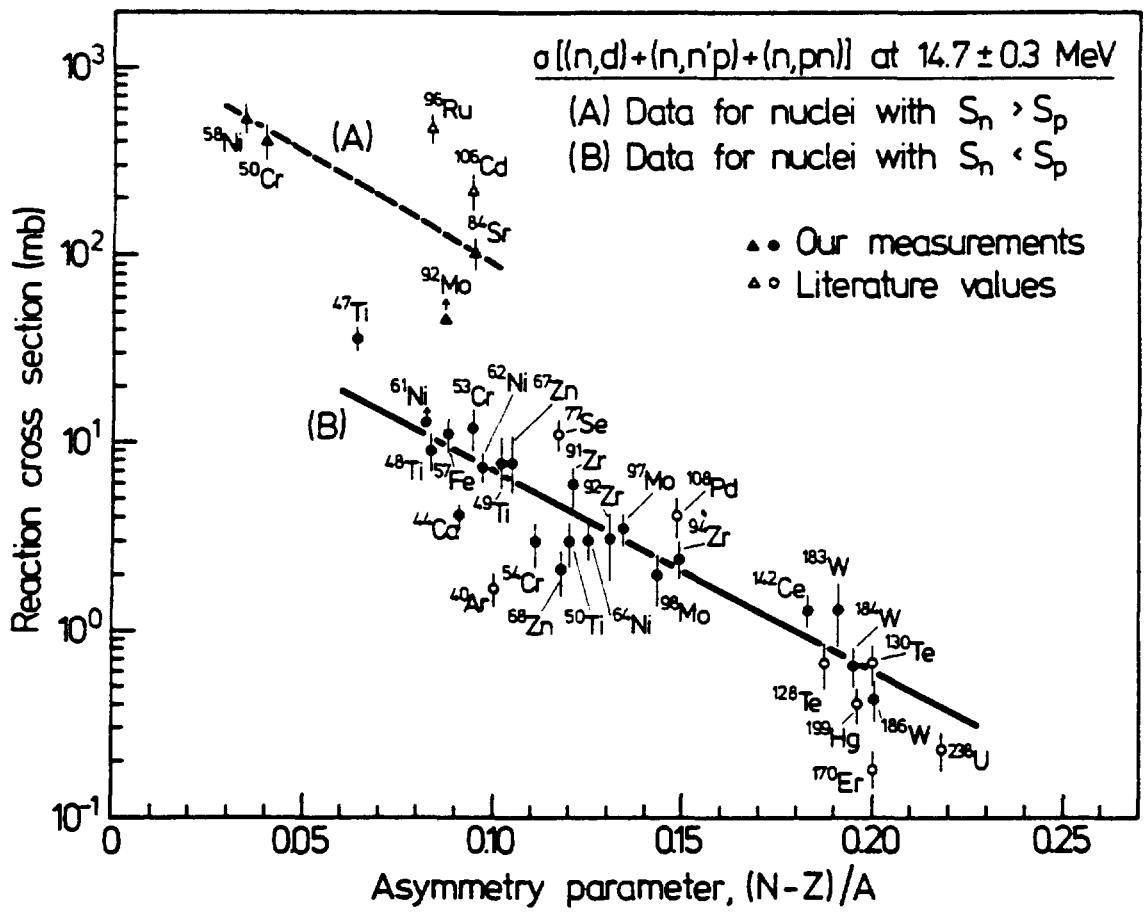

Fig. 1 Systematics of [(n,d)+(n,n'p)+(n,pn)] reaction activation cross sections induced by 14.7 ± o.3 MeV neutrons [16].

As far as the pure (n,d) cross sections are concerned, integral data exist only at 14 MeV and were obtained via spectral measurements [cf. 15,17,18]. Over the mass range of 27 to 96 the cross section is more or less constant (σ= 1o±3 mb). Hauser-Feshbach calculations have shown [16] that the contributions of statistical processes to the total (n,d) cross section are generally small, a result similar to that deduced from angular distribution measurements on the emitted deuterons.

(n,t) Reactions

Integral cross sections of (n,t) reactions at 14 MeV were obtained by an integration of the differential data, by radiometric analysis of the activation products as well as by tritium counting. The cross sections for very light nuclei are exceptionally large. In the medium and heavy mass regions first systematic studies were carried out at Jülich [cf. 3,5] and it was observed that the (n,t) cross section decreases rather slowly with (N-Z)/A of the target nucleus. Measurements at Debrecen [9,11] on several odd mass target nuclei gave much higher cross section values, suggesting the existence of an even-odd effect.

Extensive studies on triton emission reactions have been performed at Jülich also with broad neutron spectra [cf. 7,1o,19], especially those produced in the break-up of 53 and 3o MeV deuterons on Be. The trends in cross sections are somewhat similar: with the exception of a sharply decreasing trend in the light mass nuclei the cross section is practically constant over the region of Z = 2o to 82. The results for 3o MeV d(Be) break-up neutrons are shown in Fig. 2. Activation measurements showed that for medium and heavy mass elements the emission of three nucleons (p2n) is more favoured than the emission of a bound triton.

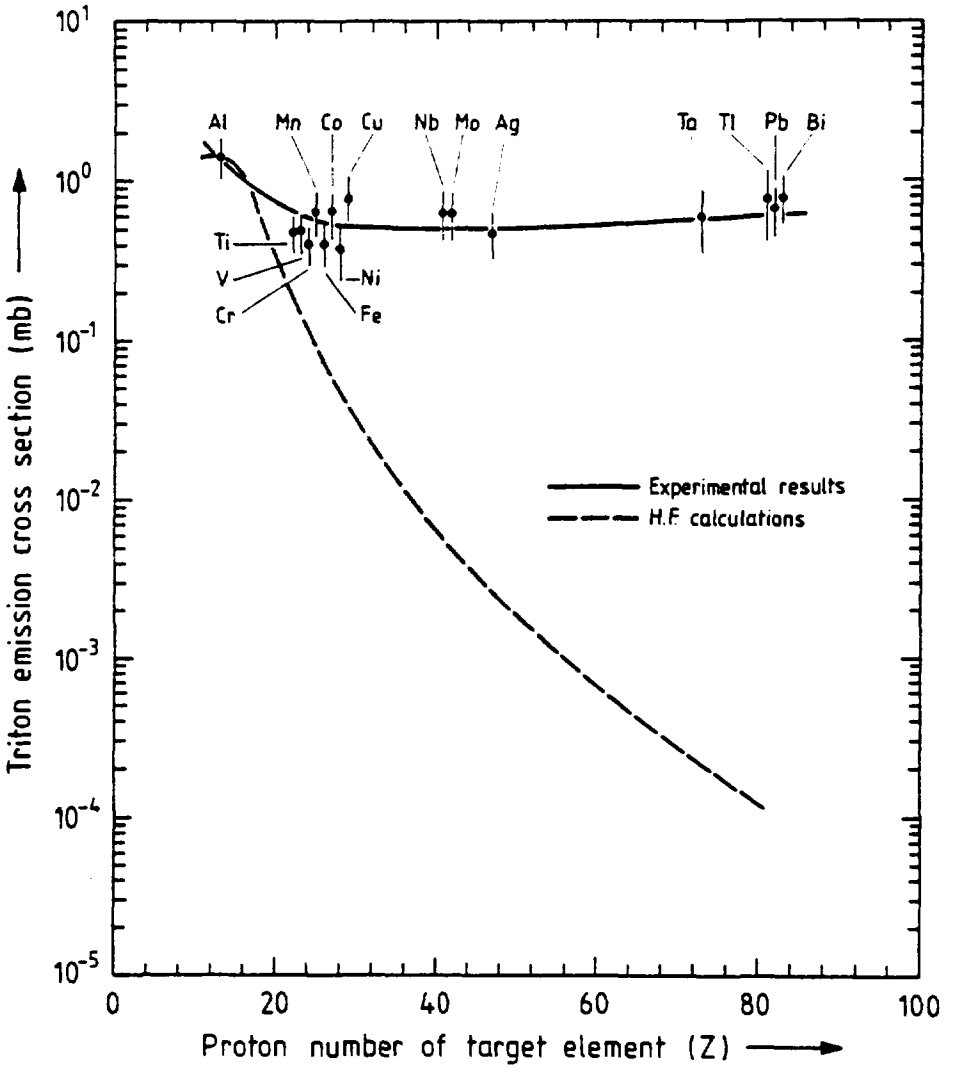

Fig. 2 Systematics of triton emission cross sections with 3o MeV d(Be) break-up neutron spectrum [19].

The energy dependence of the (n,t) cross section is known best for the $^{6}Li(n,t)^{4}He$ reaction, which serves as one of the basic standards for neutron flux monitoring. Furthermore, this reaction as well as the $^{7}Li(n,n't)^{4}He$ reaction are of primary importance for tritium breeding in fusion reactor technology. There has been some discrepancy in the data for the latter reaction. The cross section can be measured via neutron spectroscopy, ^{4}He assessment or by tritium counting. The latter process ought to yield more accurate results. Recently the data were redetermined as a Geel-Jülich collaboration [2o] and the discrepancy has now been solved. Very

recently first measurements on the excitation functions of (n,t) reactions on medium mass nuclei have been reported [12]. Those results are reproduced in Fig. 3.

It is known that the (n,t) reaction on light mass nuclei proceeds predominantly via direct processes. In the medium mass region, on the other hand, Hauser-Feshbach calculations have been attempted [cf. 11,21] to describe the total (n,t) cross section. The calculations performed at Jülich [21] showed that at 14 MeV the (n,t) cross section on nuclei in

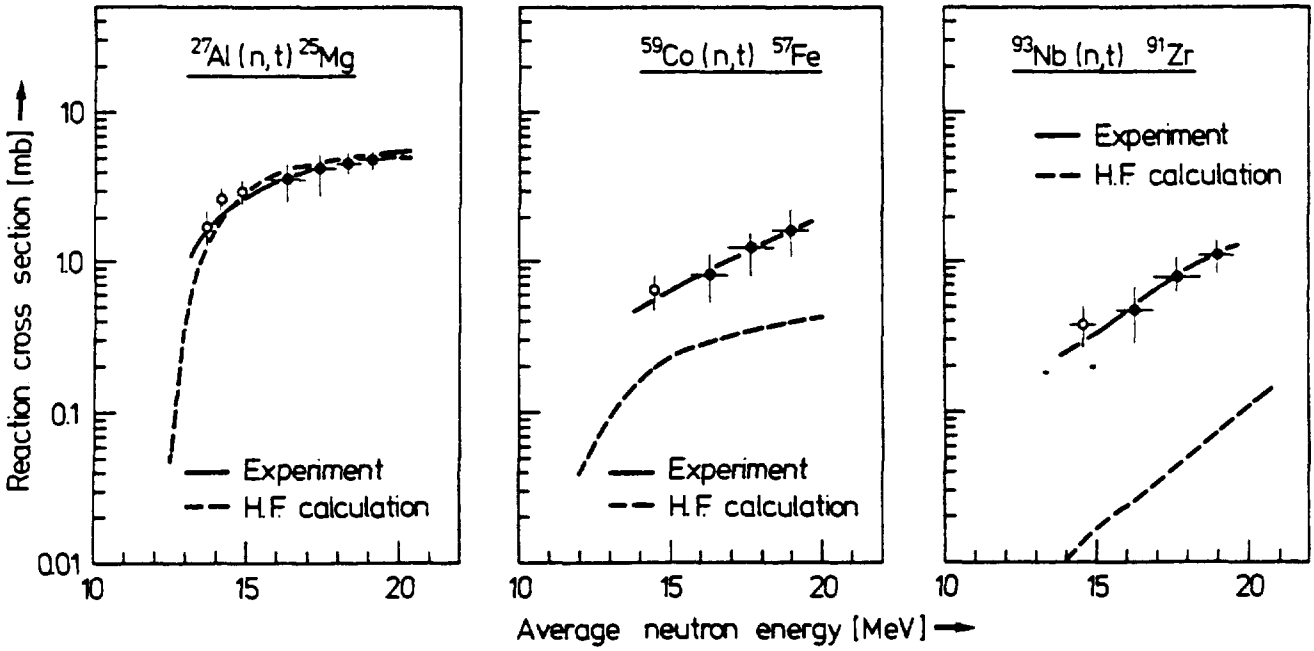

Fig. 3 Excitation functions of (n,t) reactions on ^{27}Al, ^{59}Co and ^{93}Nb [12].

the (2s,1d) shell is described by calculations within a factor of 2. A somewhat similar conclusion was drawn for 3o MeV d(Be) break-up neutrons [19] as can be seen in Fig. 2. The calculational results given in Fig. 3 show that the excitation function of the (n,t) reaction on ^{27}Al is described well by the statistical model; with the increasing mass of the target nucleus, however, the contribution of statistical processes decreases.

(n,^{3}He) Reactions

Systematic studies on (n,^{3}He) reactions at 14 MeV have been carried out mainly at Jülich [cf. 4,6]. Almost all the data were obtained using extensive radiochemical separations and low-level methods of counting. The trend was found to be similar to that for (n,t) cross sections; in absolute terms, however, the (n,^{3}He) cross section is at least by an order of magnitude smaller than the (n,t) cross section. At 14 MeV the (n,^{3}He) reactions have the smallest measurable cross sections (1 to 1o μb).

Extensive studies of (n,^{3}He) reactions have also been carried out with a 53 MeV d(Be) break-up neutron spectrum using both activation and mass spectrometric techniques [14,22]. Even at a relatively high excitation energy of about 3o MeV ^{3}He-emission from medium and heavy mass nuclei amounts to

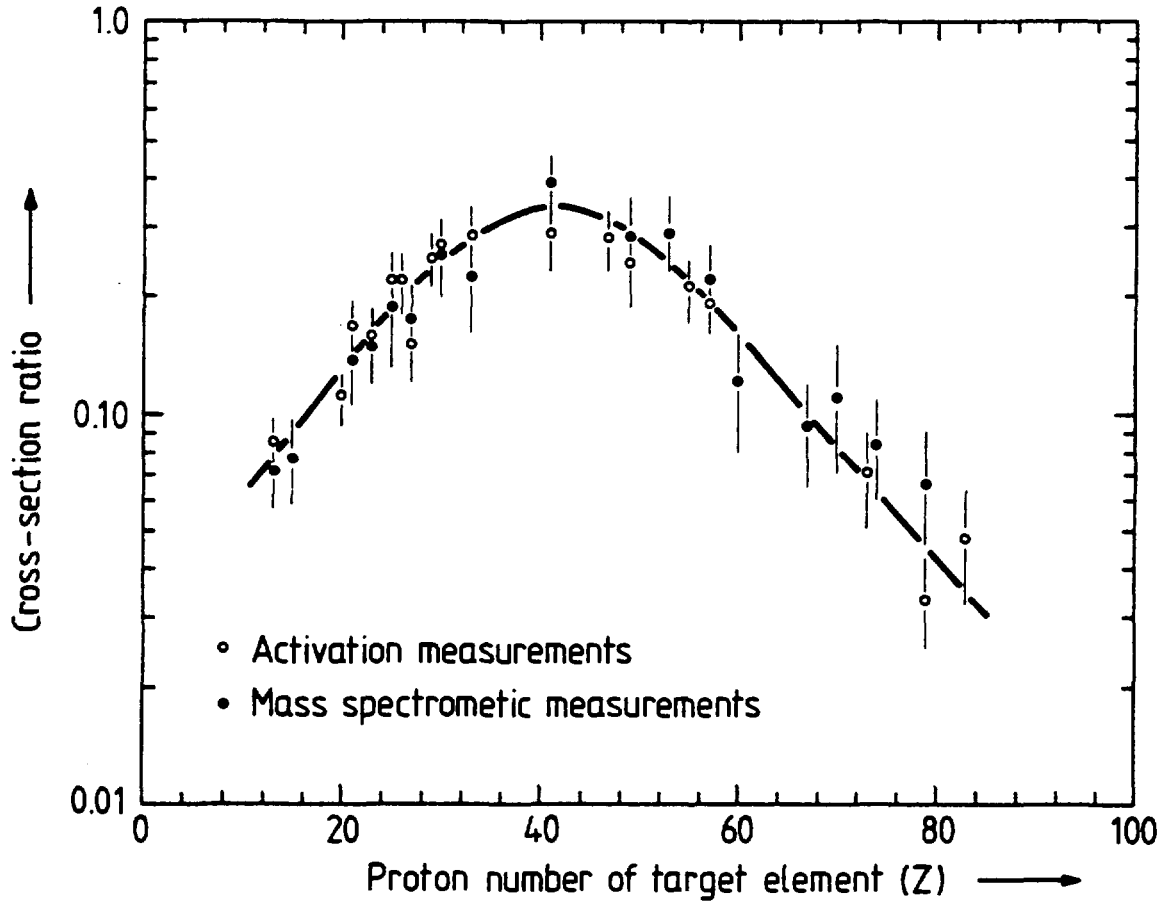

Fig. 4 ^{3}He/^{4}He emission cross section ratio as a function of Z of the target elements [22].

< o.1 % of the total inelastic cross section. The results on the measurement of ^{3}He to ^{4}He emission cross section ratios are shown in Fig. 4. Evidently, over the entire investigated mass range, the ratios obtained by the activation technique are identical within about 3o % with the mass spectrometric data. This may suggest that the activation products are formed predominantly via ^{3}He- and ^{4}He-emission. It may, however, also mean that in the ratio measurements described here the relevant processes contribute in such a way that an accidental agreement emerges.

For (n,^{3}He) reactions so far no excitation function has been reported.

Hauser-Feshbach calculations have shown [21] that at 14 MeV the contributions of statistical processes to (n,^{3}He) cross sections are small. The same conclusion was drawn in the case of (n,^{3}He) reactions induced by 53 MeV d(Be) break-up neutrons [22].

(n,α) Reactions

This type of reactions have been investigated in more detail as compared to the other reactions discussed above. Almost all the on-line and off-line techniques have been used and systematic trends in cross sections at 14 MeV have been studied. Some of the recent works using off-line methods deal with measurements in the rare-earth region [23] as well as mass spectrometric studies of helium production cross sections [cf. 24,25].

A considerable amount of information on the excitation functions of (n,α) reactions is also available. However, there are still some gaps in the data. One example was the $^{58}Ni(n,\alpha)^{55}Fe$ reaction. We studied this reaction recently [26] by separating ^{55}Fe radiochemically, preparing a thin source and assaying its radioactivity by X-ray counting. The results are shown in Fig. 5. The transition from low energy region to 14 MeV

is smooth. The 14 MeV results obtained by various techniques are in good agreement.

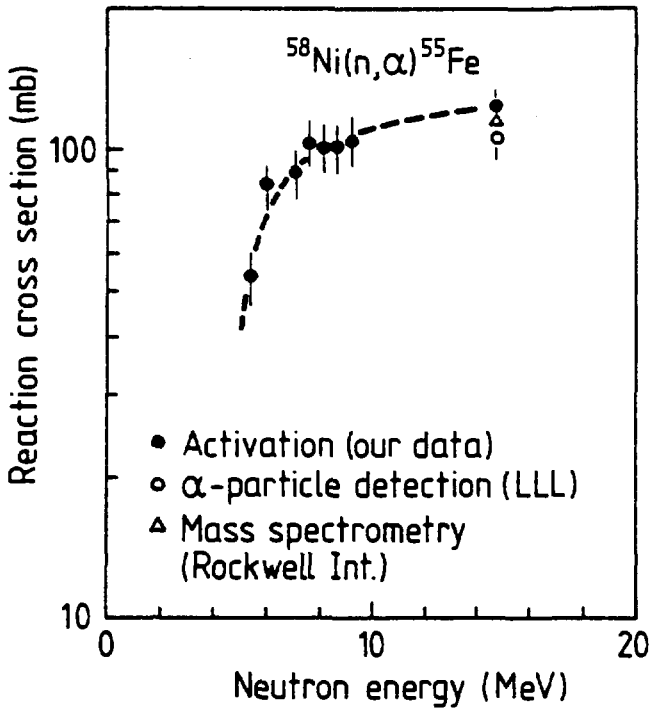

Fig. 5 Excitation function of the $^{58}Ni(n,\alpha)^{55}Fe$ reaction [26].

Detailed theoretical analyses of the spectral as well as integral data on (n,α) reactions suggest that in the light mass region direct processes appear to be dominant. In the medium mass region statistical contributions are important. Those contributions, however, decrease appreciably in the heavy mass region.

CONCLUSIONS

Off-line methods of measurement, involving interdisciplinary techniques, have proven to be very useful for the study of fast neutron induced reactions leading to the emission of complex particles, especially ^{3}H and ^{3}He. ^{3}H-emission from the (2s,1d)-shell nuclei seems to be described by the statistical model;

with the increasing mass, however, the statistical contribution decreases. In ^{3}He-emission non-statistical effects seem to be dominant. The cross section data for all the (n, complex particle) reactions are of practical importance for design calculations in fusion reactor technology.

REFERENCES

[1] J. Csikai, in Nuclear Theory for Applications-198o, IAEA-SMR-68/I (1981) p. 215
[2] S.M. Qaim, in Nuclear Theory for Applications-198o, IAEA-SMR-68/I (1981) p. 261
[3] S.M. Qaim and G. Stöcklin, J.Inorg.Nucl.Chem. 35 (1973) 19
[4] S.M. Qaim, J.Inorg.Nucl.Chem. 36 (1974) 239; Erratum p. 3886
[5] S.M. Qaim and G. Stöcklin, Nucl.Phys. A257 (1976) 233
[6] S.M. Qaim, Radiochimica Acta 25 (1978) 13
[7] S.M. Qaim, R. Wölfle and G. Stöcklin, J.Inorg.Nucl.Chem. 36 (1974) 3639
[8] S.M. Qaim, A. Rusheed, G. Stöcklin and R. Wölfle, Int.J. appl.Radiat.Isotopes 28 (1977) 585
[9] T. Biro, S. Sudar, Z. Miligy, Z. Dezsö and J. Csikai, J.Inorg.Nucl.Chem. 37 (1975) 1583
[1o] S.M. Qaim and R. Wölfle, Nucl.Phys. A295 (1978) 15o
[11] S. Sudar and J. Csikai, Nucl.Phys. A319 (1979) 157
[12] S.M. Qaim, R. Wölfle and H. Liskien, Phys.Rev. C25 (1982) 2o3
[13] H. Farrar IV, W.N. McElroy and E.P. Lippincott, Nucl.Techn. 25 (1975) 3o5
[14] C.H. Wu, R. Wölfle and S.M. Qaim, Nucl.Phys. A329 (1979) 63
[15] S.M. Grimes, R.C. Haight, K.R. Alvar, H.H. Barschall and R.R. Borchers, Phys.Rev. C19 (1975) 2127
[16] S.M. Qaim, Nucl.Phys. A382 (1982) 255
[17] S.M. Grimes, R.C. Haight and J.D. Anderson, Phys.Rev. C17 (1978) 5o8

[18] R.C. Haight and S.M. Grimes, in Proc. Symp. on Neutron Cross Sections from 10 to 50 MeV, Brookhaven 1980, Report BNL-NCS-51245 (1980) p. 245

[19] R. Wölfle, S. Khatun and S.M. Qaim, Nucl. Phys., in press

[20] H. Liskien, R. Wölfle and S.M. Qaim, Proc.Int.Conf. on Nuclear Data for Science and Technology, Antwerp, September 1982, p. 349

[21] S.M. Qaim, H.V. Klapdor and H. Reiss, Phys.Rev. C22 (1980) 1371

[22] S.M. Qaim, C.H. Wu and R. Wölfle, Nucl.Phys. A410 (1983) 421

[23] S.M. Qaim, Radiochimica Acta, in press

[24] H. Farrar IV and D.W. Kneff, Trans.Amer.Nucl.Soc. 28 (1978) 197

[25] D.W. Kneff, H. Farrar IV, F.M. Mann and R.E. Schenter, Nucl.Tech. 49 (1980) 498

[26] S.M. Qaim, R. Wölfle and G. Stöcklin, in Proc. Int. Conf. on Nuclear Data for Science and Technology, Antwerp, September 1982, p. 356

Measurements of Cross Sections and Spectra for Neutron Emitting Channels by Fast Neutron Spectroscopy

D. Seeliger

Technical University Dresden, GDR

Abstract:
A brief review is given for recent 14 MeV neutron spectroscopy experiments. Using as an example the voluminous data set determined at the TU Dresden it is shown, what type of neutron nuclear data informations can be derived from double differential secondary neutron emission spectra. Finally, some conclusions will be drawn about the further need of neutron spectroscopy experiments at 14 MeV.

1. Review of Recent Neutron Spectroscopy Experiments at 14 MeV

Secondary neutron spectra from the interactions of 14 MeV neutrons with nuclei have been investigated in a considerable number of experiments during the past 15 years [1 - 9]. New experiments are reported at this meeting by the groups from Osaka, Dresden and Rawalpindi.
Table 1 gives an overview for which elements these investigations have been carried out. A satisfactory situation has been achieved for the elements
Be, Al, Si, Ti, Cr, Fe, Ni, Cu, Zn, Zr, Nb, Mo, Su, Ta, W, Pb, and Bi
for which at least two independent high quality experiments have been reported. But this does not mean an agreement between different experiments in every detail.

A few data are available for the elements Li, O, F, Na, Mg, P, S, Ca, V, Mn, Co, Ga, Se, Br, Ag, Cd, In, Sb, I, Ba, Au, and Hg. In this cases only one experiment or measurement in a limited energy or angular region has been reported.

But there are still many elements for which no double differential neutron emission cross sections are available. This is the case for
B, N, Ne, Cl, Ar, K, Sc, Ge, As, Kr, Rb, Sr, Y, Tc, Ru, Rh, Pd, Te, Xe, Cs, all rare earth elements, Re, Os, Ir, Pt and Tl. In Table 2 some parameters are summarized of recent experiments from which the main contribution to this area of investigation since 1973 came [6,8,9]. In all cases the pulsed beam time-of-flight method was used, giving high enough intensity needed for systematic studies. At the TU Dresden in cylindric geometry for many elements measurements with moderate resolution in the spectra region 2 ... 14 MeV had been reported [6]. The investigations at the IRK Vienna concentrated on the measurement of the low energy part of the spectra 0.5 ... 6 MeV, also with moderate resolution and including angular integration within the experiment [8]. Recently high resolution ring geometry experiments within a broad energy range are reported by the Osaka University for many elements ([9] and this Symposium). The new experimental arrangement at the TU Dresden with a flight path of 5 meters allows measurements with improved energy resolution in a wide angular range.

The figures 1 and 2 give an example for the agreement between experiments of different groups. The angular integrated spectra for Fe determined by [1, 4, 6, 8] are in reasonable agreement between each other. An excess of low energy neutrons observed by the authors of [5] was not confirmed by other measurements. Fig. 2 shows that the former measurements at the TUD for lead are confirmed by the new Osaka results. Due-to the much higher resolution of the later experiment it shows pronounced structures at the high end of the spectra which are connected with the excitation of individual low-lying states in the lead isotopes. The new TUD results for lead presented at this meeting show similar structures like the Osaka measurement (see paper presented by Elfruth et al.).

Till now measurements have been reported only with scatterers having the natural isotope abundance.

Now let us consider the situation concerning the excitation of the low lying states, especially the first excited states. Also in this case many experiments had been reported [10-31], most of them using the associated particle tof-method with a comparatively high proton recoil energy bias. But if we look at the distribution of this experiments along the (Z,A)-scale it is evident, that such investigations are carried out mainly for light and medium mass gg-nuclei having a big distance between the ground state and the first excited state.

The data situation may be called satisfactory for light gg-nuclei like $^{12}_{6}C$, $^{24}_{12}Mg$, $^{28}_{14}Si$ and $^{32}_{16}S$. Some information about the excitation cross sections averaged over the first states for different isotopes for medium elements like Cr, Fe, Ni, Zn and also for Pb can be found in the literature. (As an example on fig. 3 the Stelson data [12] are shown together with data for $^{24}Mg(n,n'_1)$ at incident energies between 7 MeV and 12 MeV and a theoretical analyses of all data in the frame of CCC and HF theories [33].) Only a few new measurements are available. Having in mind this at the one hand and the circumstance of missing data for important nuclei at the other hand, new experimental investigations with high energy resolution could be very useful.

The general situation concerning investigations of particle-correlated neutron emission from (n,2n) and (n,xn) reactions is even more unsatisfactory. In a few experiments many years ago - Winter (59), Mjachkov (61), Jeramie (63), Bouchez (64) - mainly by associated-particle tof spectroscopy the correlated neutron spectra from $^{9}Be(n,2n)$ were measured. Voignier (71) investigated the Pb(n,2n) process in a similar manner. The only one recent measurement of this type was reported by Schroeder et al. [32], which determined the spectra of second neutrons from $^{127}I(n,2n)$ and $^{209}Bi(n,2n)$ with a double tof-Spectrometer. Measurements of this type need more than thousand hours measuring time, that is the main reason, why at this time only in a few cases a satisfactory pure experimental information about the spectra of

second neutrons is available.(This information usually is obtained from the inclusive secondary neutron emission spectra, subtracting a theoretically calculated (nn')-contribution.) Figs. 4, 5 and 6 show results from [32]: The quadro-differential cross sections $\delta(\Omega_1\Omega_2E_1E_2)$, neutron spectra from the (n,2n) reaction and angular distributions, respectively.

2. Nuclear data information from a double differential spectra measurement

Now, let us consider the question, what type of nuclear data information one can obtain from double differential spectra. As an example, this will be demonstrated for the voluminous data set measured at the TUD [6].

The direct result of experiments, after flux and efficiency normalization, geometry dead time , linearity, multiple scattering corrections and also elastic peak separation as well as transfer to the c.m.system, are the inclusive secondary neutron double differential spectra for all nonelastic neutron producing reaction channels as presented at fig. 7 for a few elements. Due-to the limited energy resolution of that experiment in the neutron energy region above 10 MeV these spectra represent a crude average over contributions from individual states. Even at this resolution and after a weak smoothing of the spectra a clear indication of structures in the spectra, which are out of statistical errors, is evident. A systematic physical study of such fluctuations is missing, as yet. Some-times for practical purposes also double-differential spectra, including the elastic scattering contribution,are published [9], which are strongly different from the former in the high energy range. From the double differential spectra as presented on fig. 7 as a next step the angular integrated nonelastic neutron emission spectra can be evaluated. In the present case this was done by integration of the ddcs in 0,25 MeV energy bins, the extrapolation to $\vartheta = 0^\circ$ and 180° basing on a Legendre polynomial fit and following integration over ϑ. The resulting spectra with the equidistant data points are shown on fig. 8. In this case spectra for all

the elements investigated in [6] will be given having in mind, that these spectra in the past have been used in many experimental as well as theoretical works like a standard experiment for comparisons. This might be the case also in the frame of the 14 MeV CRP.

Some-times for comparisons with theory also angular distributions averaged over a 1 MeV energy bin are determined - as shown for Zr and Bi on fig. 9.
In fig. 8 beyond the data points evaluated from the experimental ddcs also curves of a physical parametrization basing on equilibrium and pre-equilibrium models are shown [6]. The combination of experimental data plus physical parametrization allows the determination of further quantities: Extrapolation of the spectra to E = 0 and integration over the range E = 0 ... E_o yields emission cross section

$$\sigma_{nM} = \sigma_{n,n'} + 2\sigma_{n,2n} + \sigma_{n,pn} + \sigma_{n,\ n} + \cdots \ .$$

On the other hand holds . -

$$\sigma_{nM} = \sigma_{nX} + \sigma_{n2n} - \sigma_{n,\quad} - \sigma_{n,p} \ ,$$

so that with the well-known nonelastic cross sections σ_{nX} (and the usually small $\sigma_{n\alpha}$ and σ_{np} cross sections) the σ_{n2n} cross section can be determined, independently from activation measurements.

Resulting from the extrapolation procedure described σ_{nM} cross sections over the assymmetry parameter $\frac{N-Z}{A}$ are shown on fig. 10 for elements investigated in [6]. Elements with one dominating isotope (more than 90% abundance) data are presented by points. Open circles are averaged values for elements with several essential isotopes. Error bars include experimental uncertainties and estimated uncertainties of the extrapolation procedure. Obtained σ_{nM} in a wide mass number range have an almost linear dependence from the assymetry parameter. For heavy nuclei yielded σ_{nM} in most cases are

somewhat higher than twice the (n,2n) cross sctions from systematics.
Comparing σ_{nM} and $2\,\sigma_{n2n}$ one must take into account, that the theoretical extrapolation does not include the full contribution of the direct collective inelastic scattering to low-lying states (this is evident also at the high energy end of spectra on fig. 8). Therefore, in the order of magnitude 100 mb for heavy nuclei should be added to σ_{nM}-values presented on fig.10. A rough estimate of (nn') cross sections for heavy nuclei therefore is obtained from the rule $\sigma_{nn'} \simeq (\sigma_{nM} + 100\ \text{mb}) - 2\sigma_{n2n}$.

For light and medium nuclei having a high n,2n threshold a more direct and accurate determination of $\sigma_{nn'}$ possible using the physical parametrization of the spectra by equilibrium and pre-equilibrium-models [6]. Results of this exercise are presented on the insert of fig. 10. This numbers are in a general agreement with systematics on the base of measurements of γ-rays from the (n,n'γ) reaction at 14 MeV [34].

The physical parametrization procedure with equilibrium and pre-equilibrium models permits also a further, independent evaluation of the (n,2n) cross section and second neutron spectra. At first this was described for ^{93}Nb in the paper [35]. Fig 11 shows the separation of the spectrum of secondary neutrons from the difference between experimental (solid line) and the calculated emission spectrum of primary neutrons (broken line). The energy integration of $\sigma_{2nd}(E_o,E)$ yields a cross section value $\sigma_{n2n} = 1280 \pm 140$ mb in fair agreement with the results from systematics and from the difference $\sigma_{nM} - \sigma_{nX}$.

Finally, on fig. 12 those σ_{nM} cross sections from fig. 10 are shown, which belong to pairs of nuclei having the same neutron number N. In all this cases for N = const the experimentally determined cross sections σ_{nM} show the tendency of increasing with (N - Z)/A. This behaviour is similar to (N - Z)/A-

systematics observed for (n,2n) cross sections by Csikai and Petö for many nuclei [36]. In the present case this effect occurs, though the (n,2n) cross section for the light nuclei is only a small part of σ_{nM}. It is of interest to test neutron emission cross sections for other isotopes, whether this is a general systematical effect or not.

Summarizing this section one can state, that measurements of ddcs for neutron emission from nuclei together with a careful theoretical analysis in the frame of nuclear reactions models can provide a lot of different nuclear data information. Partially this information is not available through other experiments and partially this are informations like (n,2n) cross sections, which usually are determined by activation techniques, i.e. by a completely different method.

3. Some recommendations for further investigation of neutron emission

3.1. Data measurements

1. For laboratories equiped with tof spectrometers with moderate resolution ($2\tau \simeq$ 2-3 ns, L $\simeq$ 2 m) it might be a useful task filling out of data gaps in the emission energy range 2 ... 10 MeV for elements like
   Li, B, N, Na, K, V, Mn, Co, Ag, Y, Te, Cd, Ba, Tl
   and others for which data measurements are missing or carried out in one experiment only.

2. As standard spectra for checking the experimental procedures in different laboratories the scattering on carbon, iron and niobium should be used at least by all groups participating in the CRP. The accuracy of this standard spectra should be increased to 3 ... 5 %.

3. In experiments with moderate resolution but low detector threshold (0.1 ... 0.3 MeV) neutron emission spectra for important elements missed in the former IRK programme [8] would be very useful.

Beyond angular integrating measurement, for very important elements like Li, Be, C, Fe, Ni, Nb, Bi a.o. also the angular distribution of low emission energy neutrons, which is not completely isotropic (see figs. 6 and 9), would be of interest.

4. The high energy tail of nonelastic neutron spectra, where contributions to the spectra is coming from isolated levels, in general is still determined insufficiently. Very high resolution experiments ($2\tau \simeq 1.5$ ns, $L \simeq 10$ ...20 m) could give useful informations which is needed for all important elements for which isolated low lying states are not investigated at 14 MeV. Measurements with separated isotopes would be highly appreciated. Careful elastic peak separation procedures are needed in this case. At present only the experimental conditions at the Osaka University are close to the technical requirements for such investigations. The background conditions are likely to become easier if the proton recoil energy threshold in enlarged up to 5...7 MeV, but from the point of view of the overall consistency of the investigations, measurements will low threshold (<1 MeV) and a high dynamical range should be preferred.

5. Because-off the big number of candidates for further experimental investigations, those elements or nuclei should selected mainly, which are included in the WRENDA list.

3.2. Theoretical model approvement and basic research

1. Basing on experiments especially for the high energy part of the spectra further investigations applicability of direct reaction models, exciton model, generalized exciton model statistical model a.o. for ddcs description are useful, resulting in a recommended procedure for spectra and angular distribution calculations, which are consistent with their application to other neutron incident energies (E_o = 5 ... 20 MeV).

2. Investigations of fluctuations and physical structures in the neutron emission spectra and their physical interpretation could be of interest.

3. Studies of the influence of collective excitations or shell effects on the continuous emission spectra basing on measurements with separated isotopes of strongly deformed or near-magic nuclei could give a very useful information for model improvement.

3.3. Calculations and Compilations

1. A compilation of all existing neutron emission spectra measurements by different groups in a unique form including an analysis of the accuracies would be very useful for many applications and further improvement of the evaluated neutron nuclear data libraries.

2. Calculations basing on a well-defined and carefully checked procedure including angular distributions could give informations for non-measured (or non-measureable) isotopes (like fission products).

Finally, let me conclude, that still a lot of interesting and useful investigations in connection with the neutron spectroscopy has to be done in the future. Hopefully, an importent contribution to this area of investigations will be produced in the frame of the 14 MeV CRP.

Figure captions

fig. 1 Angle integrated secondary neutron spectrum from interactions of 14 MeV neutrons with iron; experimental results from [1], [4], [5], [6], [8] and statistical model calculations (indicated as ◇ o ⋈ ⧗ and +, respectively)

fig. 2 Comparison of ddcs for lead at $\vartheta = 122^{o}$ from Osaka-University [9] and TUD [6]

fig. 3 Differential inelastic cross section for the excitation of the first 2^{+} state in ^{24}Mg at different incident energies; experiments: Stelson et al. [12] and Foertsch et al. [33]; calculations by CCC method and HF theory [33].

fig. 4 Three-dimensional plots of the quadro-differential cross section for ^{127}I and ^{209}Bi [32]

fig. 5 Spectra of the first neutrons from the n,2n reaction determined from fig 4 calculations by statistical model with different level density parameters [32]

fig. 6 Angulardependence of (n,2n) cross sections for ^{127}I and ^{209}Bi [32]

fig. 7 Double-differential neutron emission spectra at 14.6 MeV incident energy [6]
a) for Zr
b) for Nb
c) for Bi

fig. 8 Angle integrated neutron emission spectra at 14.6 MeV incident energy [6]
a) for Na, Mg, Al, P, S
b) for Ti, V, Cr, Mu, Fe
c) for Co, Ni, Cu, Zn, Ga
d) for Se, Br. Zr, Nb, Cd
e) for In, Sn, Sb, J, Ta
f) for W, Au, Hg, Pb, Bi

fig. 9 Differential neutron emission cross sctions for 1 MeV emission energy bins [6]
a) for Zr
b) for Bi

fig.10 Systematics of the neutron production cross sections 6_{nM} determined by theoretical extrapolation of the integrated spectra presented on fig. 8 [6]; insert: $6_{nn'}$ cross sections estimated by the rule $6_{nn'} \simeq (6_{nM} + 100\ mb) - 26_{n,2n}$; points-isotopes; circles-elements

fig.11 Separation of the spectrum of second neutrons (right hand insert) from the difference between The experimental spectrum (solid line) and the calculated emission spectrum for the first neutrons (broken line) for ^{93}Nb [35]

fig.12 Systematical dependence of 6_{nM} cross sections for nuclei with the same neutron number N [6].

Table captions

Table 1 14 MeV neutron emission spectra measurements

Table 2 Experimental conditions of some 14 MeV neutron emission measurements

References:

[1] R. M. Schectman, J.D. Anderson,
Nucl. Phys. 77 (1966) 241

[2] C.S. Mathur, et al.
Phys. Rev. 186 (1969) 1038

[3] J.L. Kammerdiener, UCRL 51232 (1972)

[4] O.A. Salnikov et al.
Yad. Fiz. 122 (1971) 620
Yad. Konst. 7 (1972) 102

[5] G. Clayeux, J. Voignier, CAER 4279 (1972)

[6] D. Hermsdorf et al.
Kernenergie 17 (1974) 76
17 (1974) 259
18 (1975) 83
19 (1976) 241
ZfK, 277 Ü (1975)

[7] J.E. Kozyr et al.,ZfK 376 (1978) 82
Ukrain. Journ. Fiz. 20 (1975) 2061

[8] G. Stengl et al., Nucl. Phys. A 290 (1977) 109
A. Chalupka et al, ZfK, 410 (1980) p.25

[9] Takahashi et al. OKTAUIAN, A-83-01, 1983

[10] R.L. Clarke, W.G. Cross
Nucl. Phys. 53 (1964) 177
A 95 (1967) 320

[11] G.C. Bonazzola, E. Chiavassa
Nucl.Phys. 68 (1965) 369, 86 (1966) 378
Phys. Rev. 140,N4B (1965) 835
Lett Nuovo Cimento 2 (1969) 667

[12] P.H. Stelson et al.,Nucl.Phys. 68 (1965) 97

[13] B.E. Lechenko et al. Yad Fiz. 15 (1972) 15

[14] J.C. Alder et al. Helv. Phys. Act. 41 (1968) 433
42 (1969) 564
Nucl. Phys. A 147 (1970) 657

[15] R. W. Bauer et al., Nucl. Phys. 47 (1963) 241
A93 (1967) 673

[16] G.A. Grin et al. Helv.Phys.Acta 42 (1969) 990
39 (1966) 214
Phys. Lett. B 25 (1967) 387

[17] C. Joseph et al., Helv. Phys. Acta 40 (1967) 693

[18] J. Höhn et. al., Nucl. Phys. A 134 (1969) 289

[19] D. Meier et al.,Helv. Phys. Acta 42 (1969) 813

[20] M. Lutz et al.,Phys. Rev. 187 (1969) 1479

[21] J.M. Coon et al., Phys. Rev. 111 (1958) 250

[22] J. Voignier C.r.Acad. Sci B 733 (1968) 267

[23] C. Wong et al., Nucl.Phys. 33 (1962) 680

[24] Holland et al. Journ. Phys. G (1977) 1431

[25] Chen et al. C N P 3 (1981) 320

[26] J.E. Kozyr et al., Yad. Fiz. 28 (1978) 16
27 (1978) 616

[27] Klicewsky, Nucl.Phys. A 304 (1978) 269

[28] Mezetti et al., N C L 22 (1978) 91

[29] Winkler et al., Proc. Knoxville Conf. (1979) 150

[30] Benenson et al., A-ALB-7527 (1975)

[31] Deak et al., INDC (HUN)-18 (1981)

[32] Schroeder et al., Ztschr. Phys. A 287 (1978) 353

[33] H. Foertsch et al., Nucl. Phys. to be publ.

[34] S.M. Qaim, Proc. Conf. on Nuclear Cross Section 5
and Technology, Whashington, 1975, p 664

[35] D. Hermsdorf et al., Journ. Nucl. En. 27(1973) 747

[36] J. Csikai, G. Petö, Phys. Lett. 20 (1966) 52

Table 1

14 MeV Neutron Emission Spectra Measurements

Z	El.	labs. TUD [6]	IRK [8]	OSA [9]	other meas. 1-5;7
1	D			x	
2	He				
3	Li			x	
4	Be	x		x	
5	B				
6	C	x		x	
7	N				
8	O			x	
9	F			x	
10	Ne				
11	Na	x			
12	Mg	x			2x
13	Al	x		x	2x
14	Si	x		x	2x
15	P	x			
16	S	x			x
17	Cl				
18	Ar				
19	K				
20	Ca	x			
21	Sc				
22	Ti	x	x		
23	V	x			

Z	El.	labs. TUD	IRK	OSA	other meas.
24	Cr	x	x	x	
25	Mn	x			3x
26	Fe	x	x	x	4x
27	Co	x			2x
28	Ni	x	x	x	3x
29	Cu	x	x	x	3x
30	Zn	x	x		
31	Ga	x			
32	Ge				
33	As				
34	Se	x			2x
35	Br	x			
36	Kr				
37	Rb				
38	Sr				
39	Y				
40	Zr	x	x		x
41	Nb	x	x	x	4x
42	Mo		x	x	
43	Tc				
44	Ru				
45	Rh				
46	Pd				

Z	El	labs.			
		TUD	IRK	OSA	other meas.
47	Ag		x		
48	Cd	x			2x
49	In	x			
50	Sn	x	x		2x
51	Sb	x			2x
52	Te				
53	I	x			
54	Xe				
55	Cs				
56	Ba		x		
57-72	R.E.				
73	Ta	x	x		
74	W	x	x		2x
75	Re				
76	Os				
77	Ir				
78	Pt				
79	Au(x)		x		2x
80	Hg	x			
81	Tl				
82	Pb	x	x	x	3x
83	Bi	x	x	x	3x

Table 2

Experimental conditions of 14 MeV Neutron Emission Measurements

laboratory	N° of elements	method	L [m]	ΔE [MeV]	d.d.c.s. [dgr.]	publication
TUD	34	t.o.f. cyl.geometry pulsed beam	2	2-14	40-150	[6]
I R K	17	t.o.f. angular integr. pulsed beam	1	0,5-6	no	[8]
OSA	20	t.o.f. ring.geom. pulsed beam	9.5	(0,5... 2) -14	15-150	Gaußig 83 [9]
TUD	2	t.o.f. ring geom. pulsed beam	5	2-14	15-165	Gaußig,83

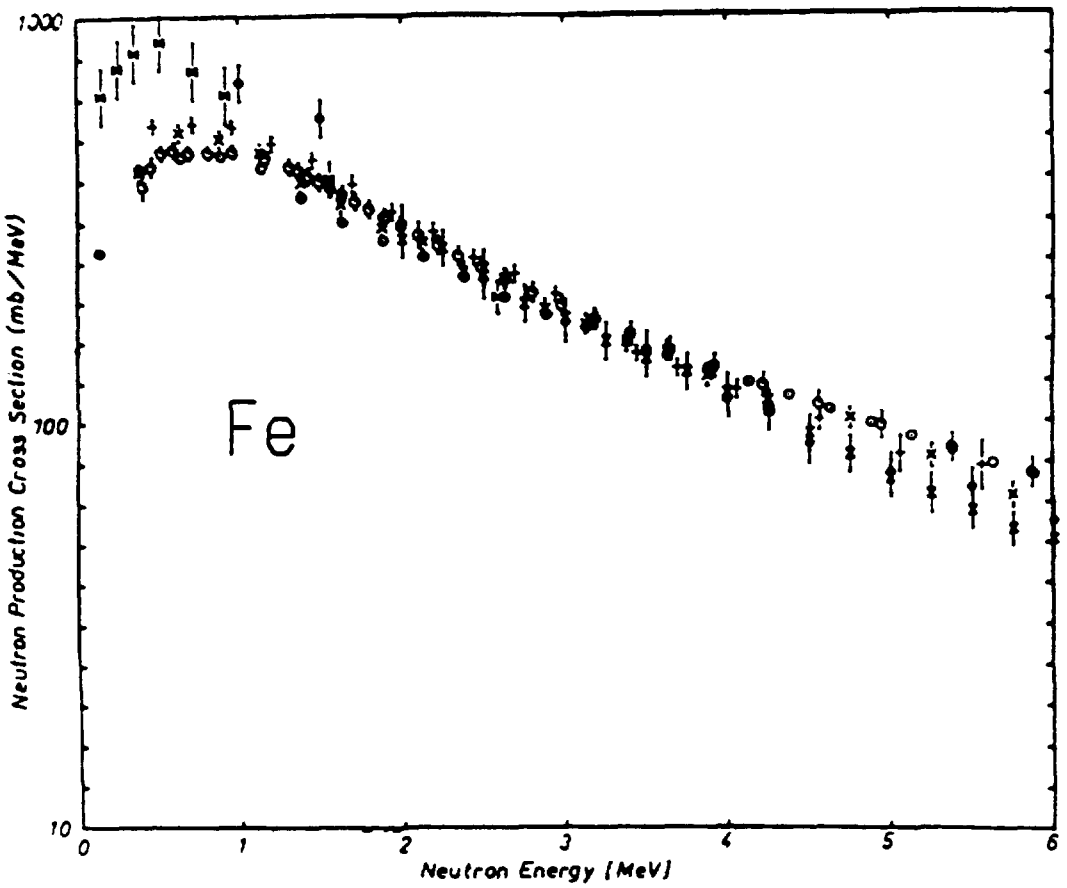

fig. 1 Angle integrated secondary neutron spectrum from interactions of 14 MeV neutrons with iron; experimental results from [1], [4], [5], [6], [8] and statistical model calculations (indicated as ◇ ○ ⋈ ⧖ and +, respectively)

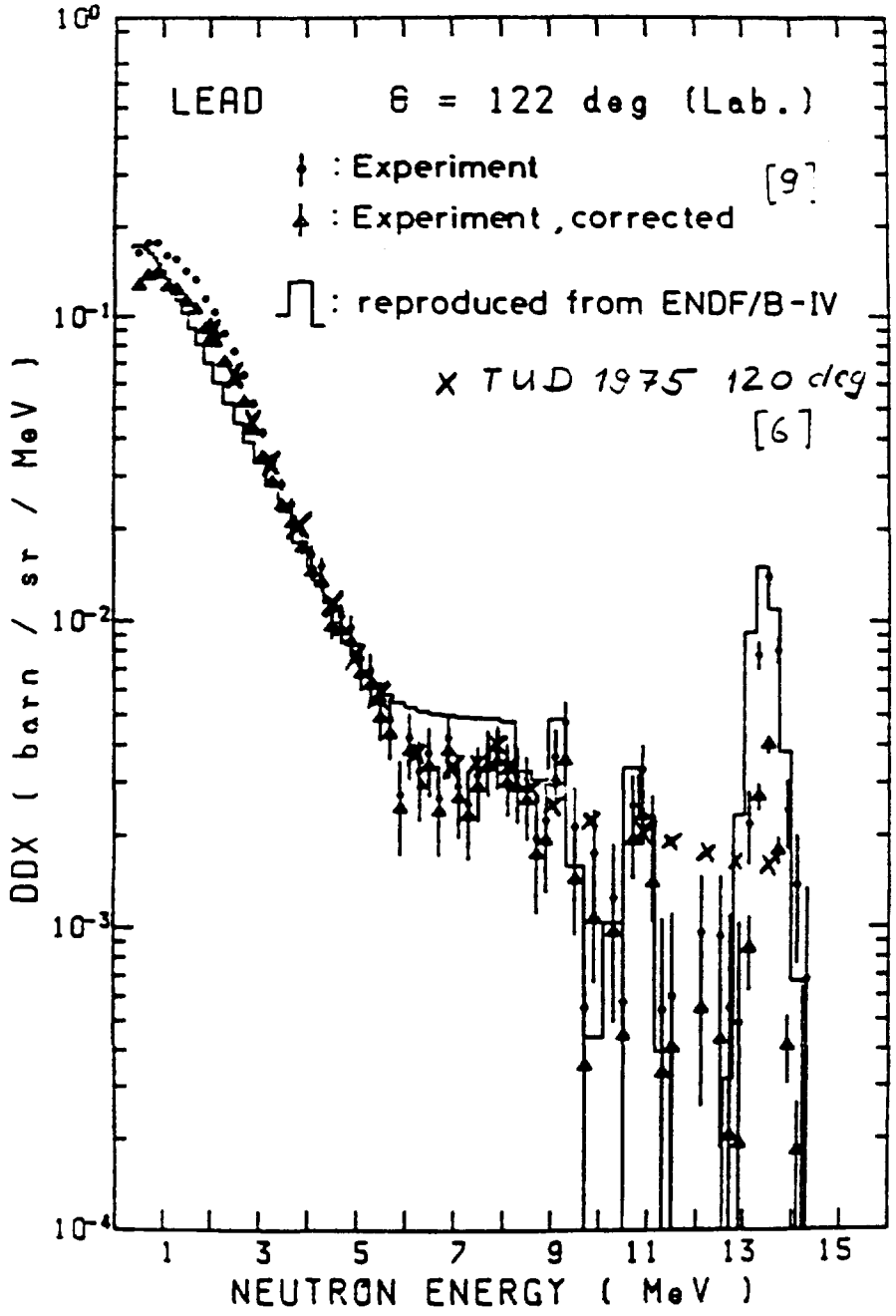

fig. 2 Comparison of ddcs for lead at $\vartheta = 122^{\circ}$ from Osaka- University [9] and TUD [6]

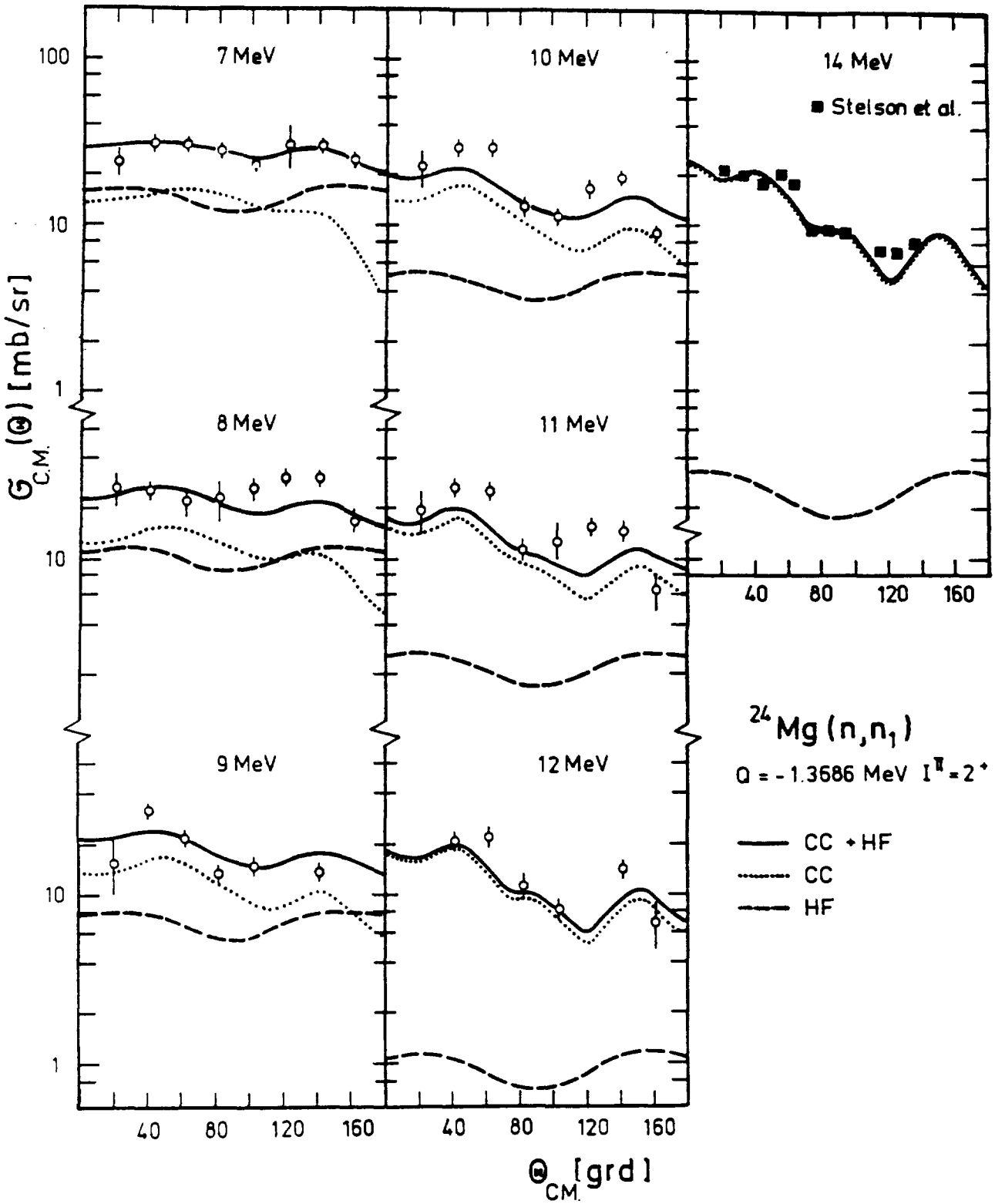

fig. 3 Differential inelastic cross section for the excitation of the first 2^+ state in ^{24}Mg at different incident energies; experiments: Stelson et al. [12] and Foertsch et al. [33]; calculations by CCC method and HF theory [33].

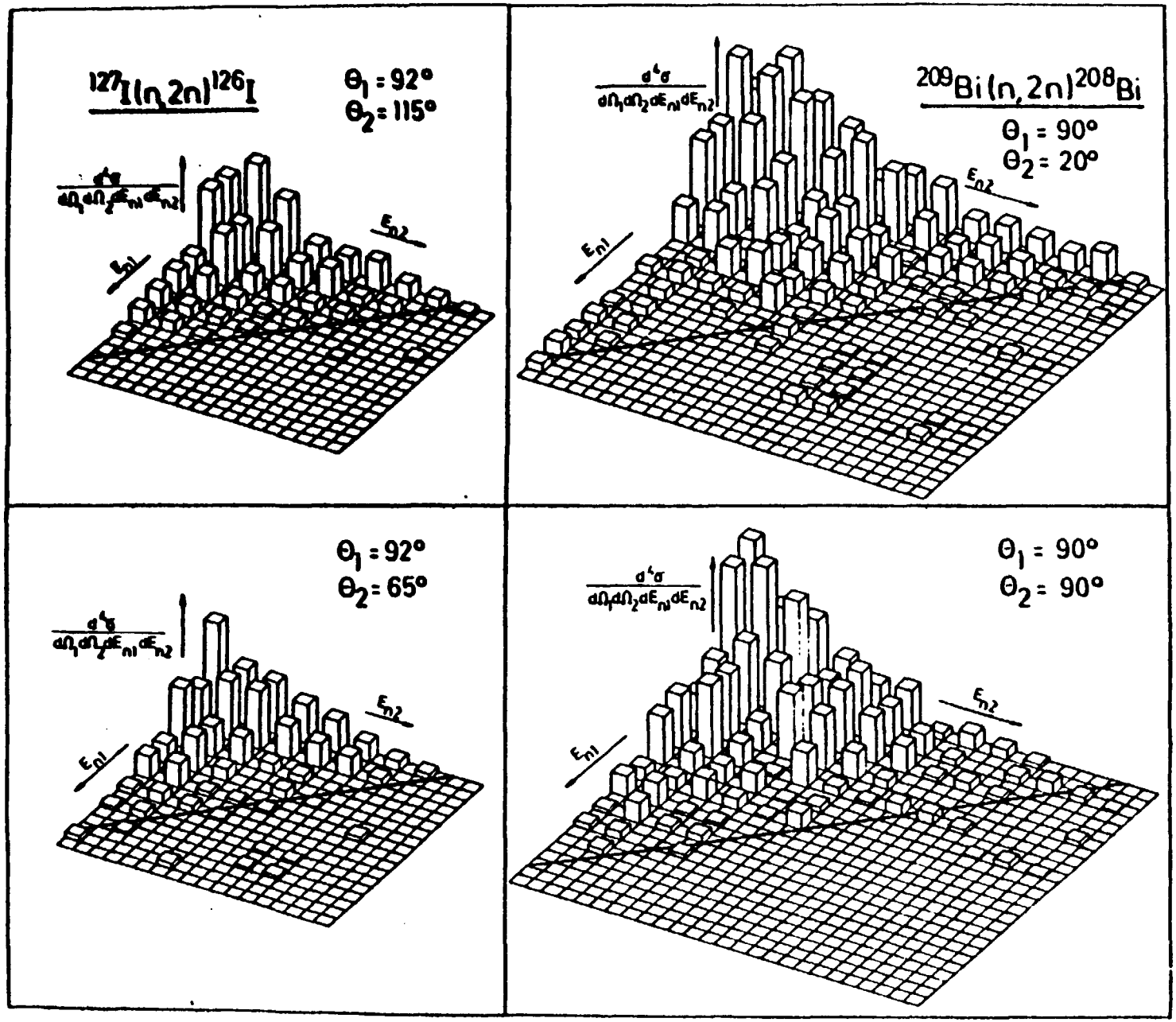

fig. 4 Three-dimensional plots of the quadro-differential cross section for ^{127}I and ^{209}Bi [32]

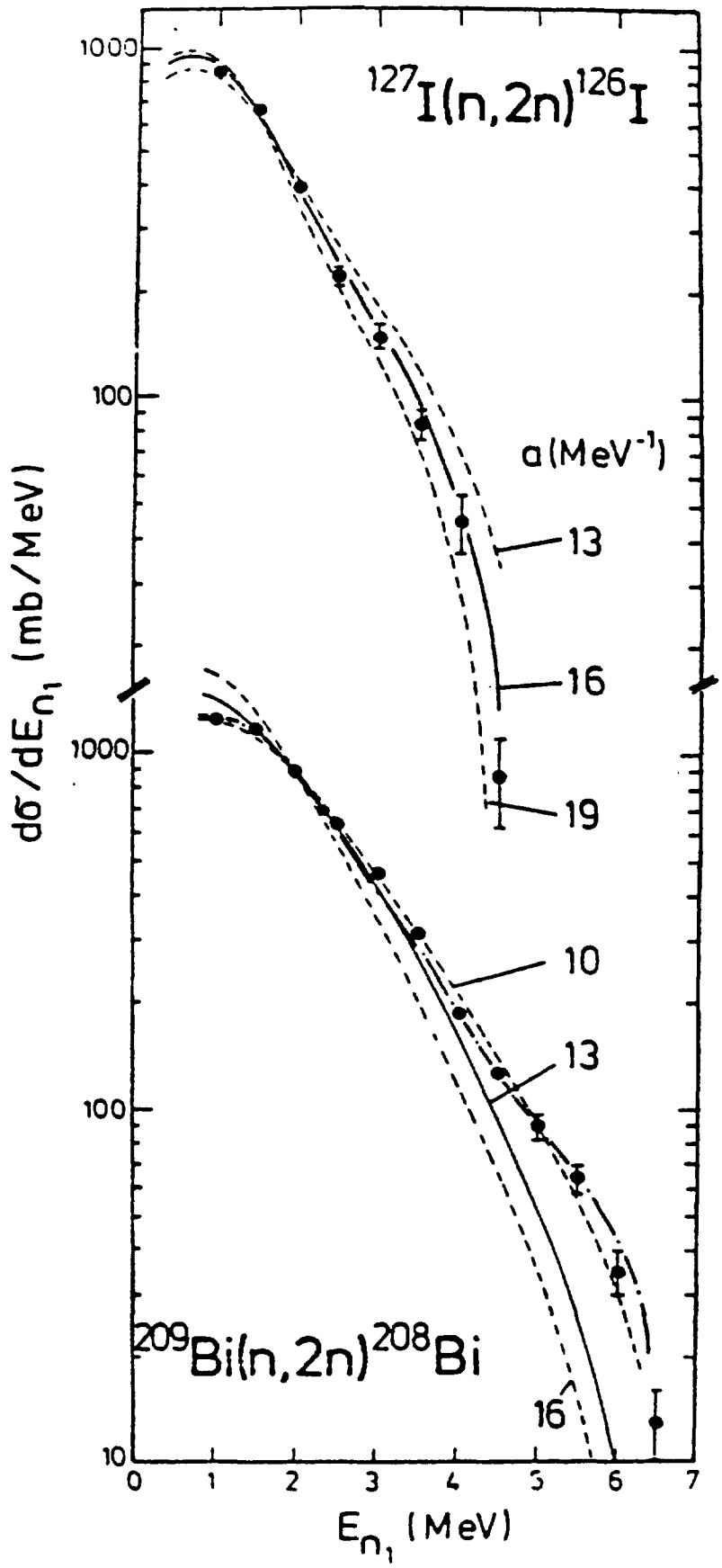

fig. 5 Spectra of the first neutrons from the n,2n reaction determined from fig 4 calculations by statistical model with different level density parameters [32]

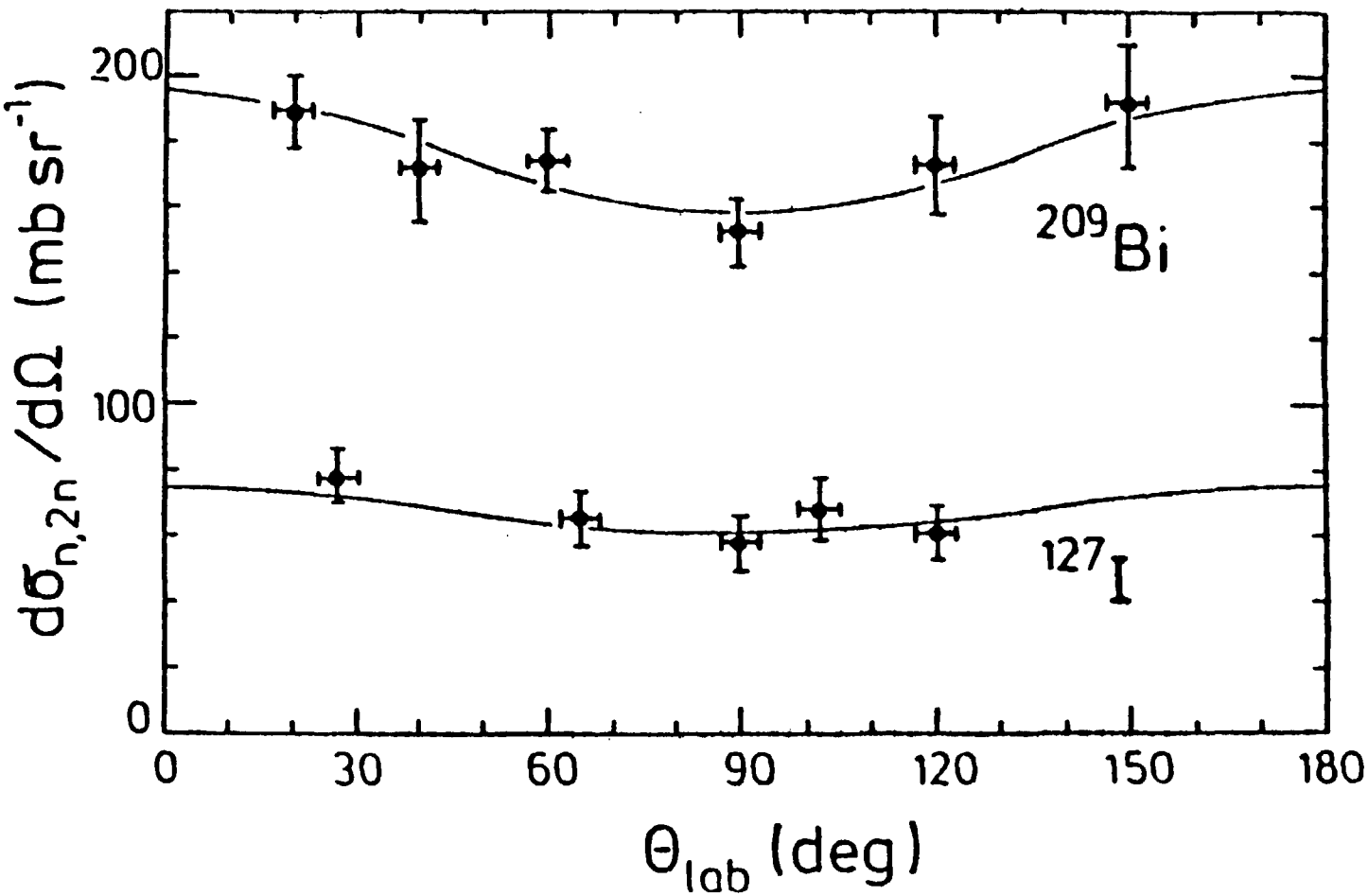

fig. 6 Angulardependence of (n,2n) cross sections for ^{127}I and ^{209}Bi [32]

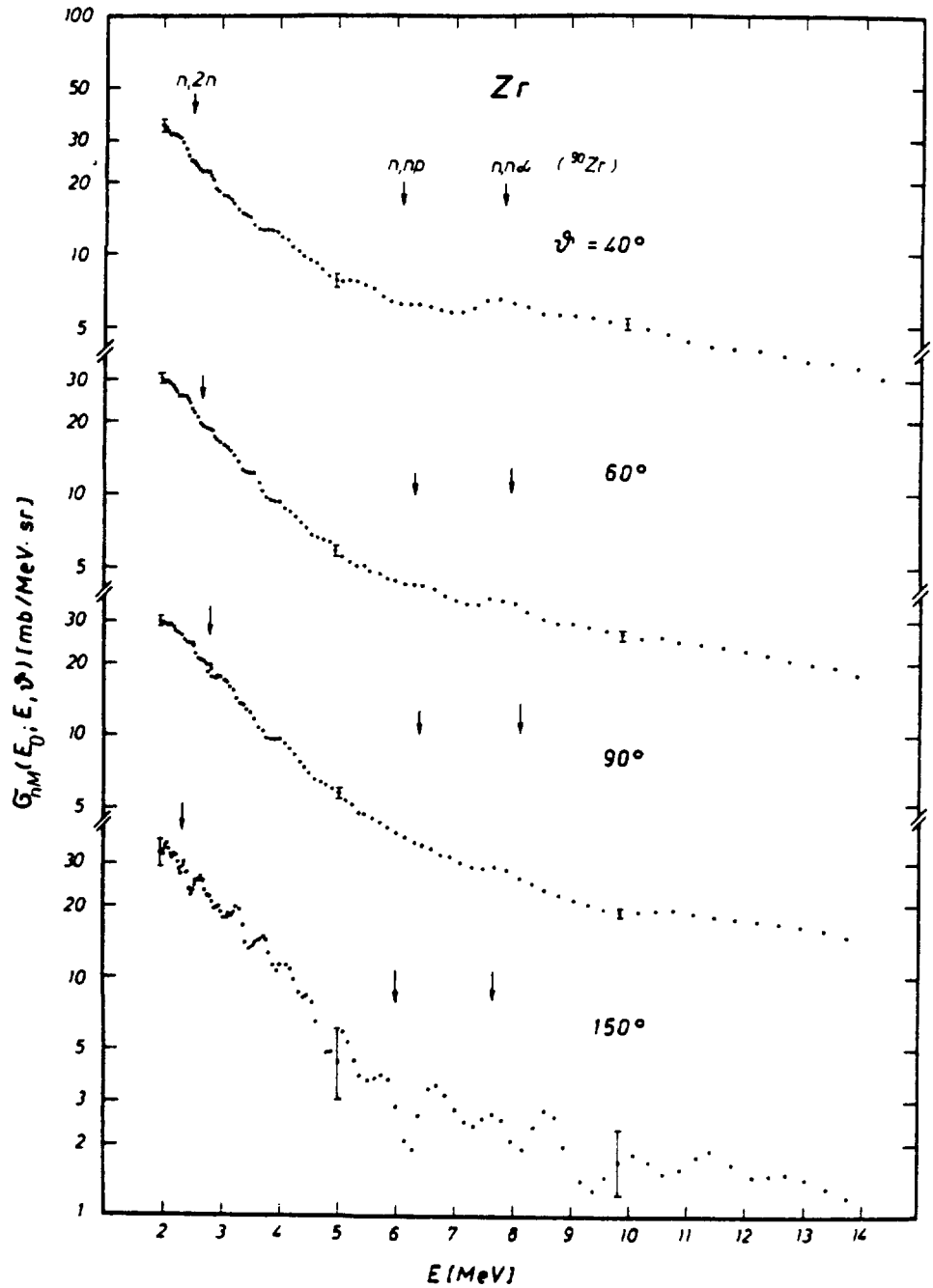

fig. 7 Double-differential neutron emission spectra at 14.6 MeV incident energy [6].
a) for Zr

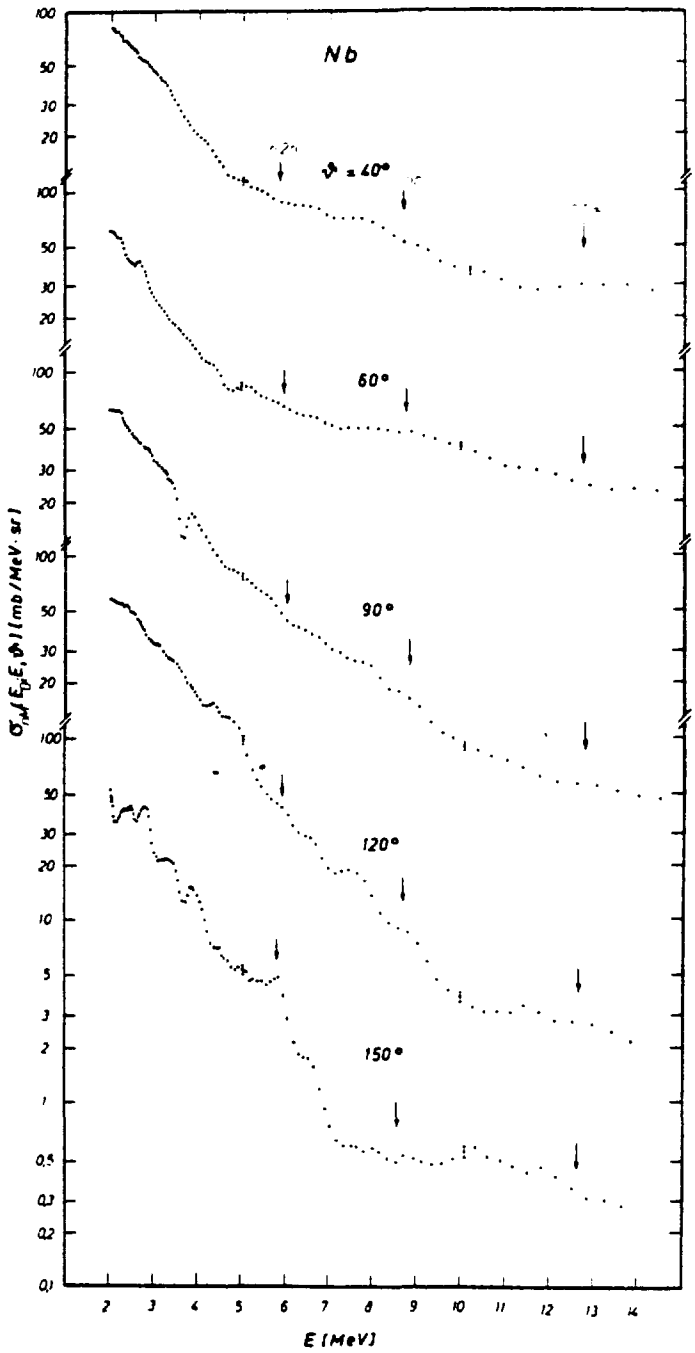

fig. 7 Double-differential neutron emission spectra at 14.6 MeV incident energy [6]

b) for Nb

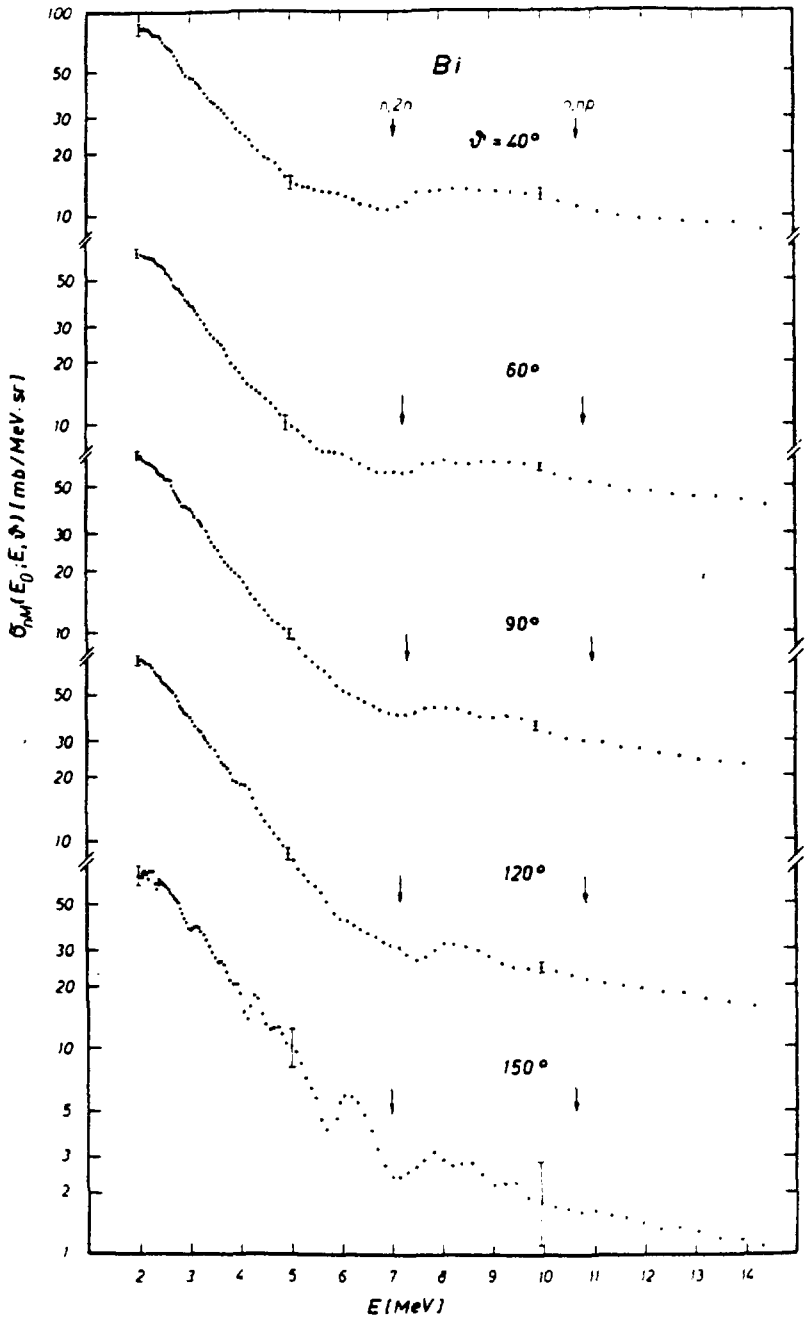

fig. 7 Double-differential neutron emission spectra at 14.6 MeV incident energy [6]

c) for Bi

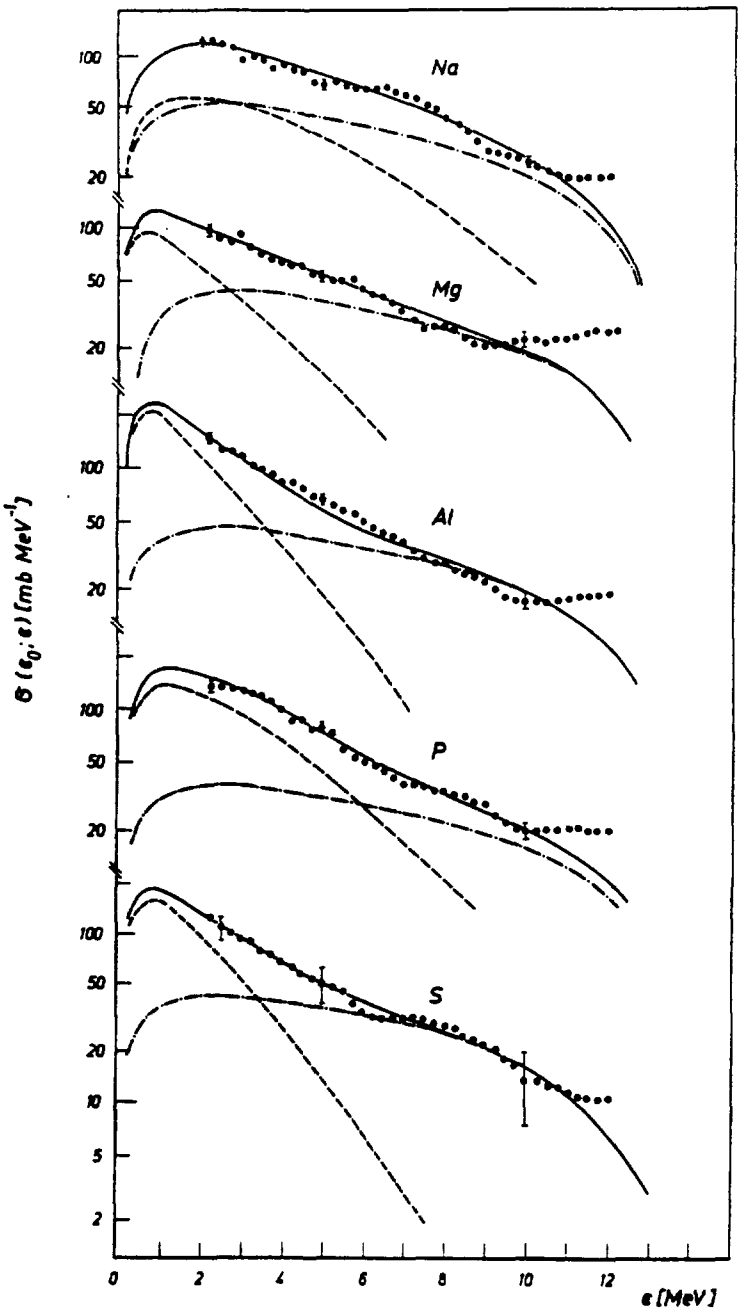

fig. 8 Angle integrated neutron emission spectra at 14.6 MeV incident energy [6]
a) for Na, Mg, Al, P, S

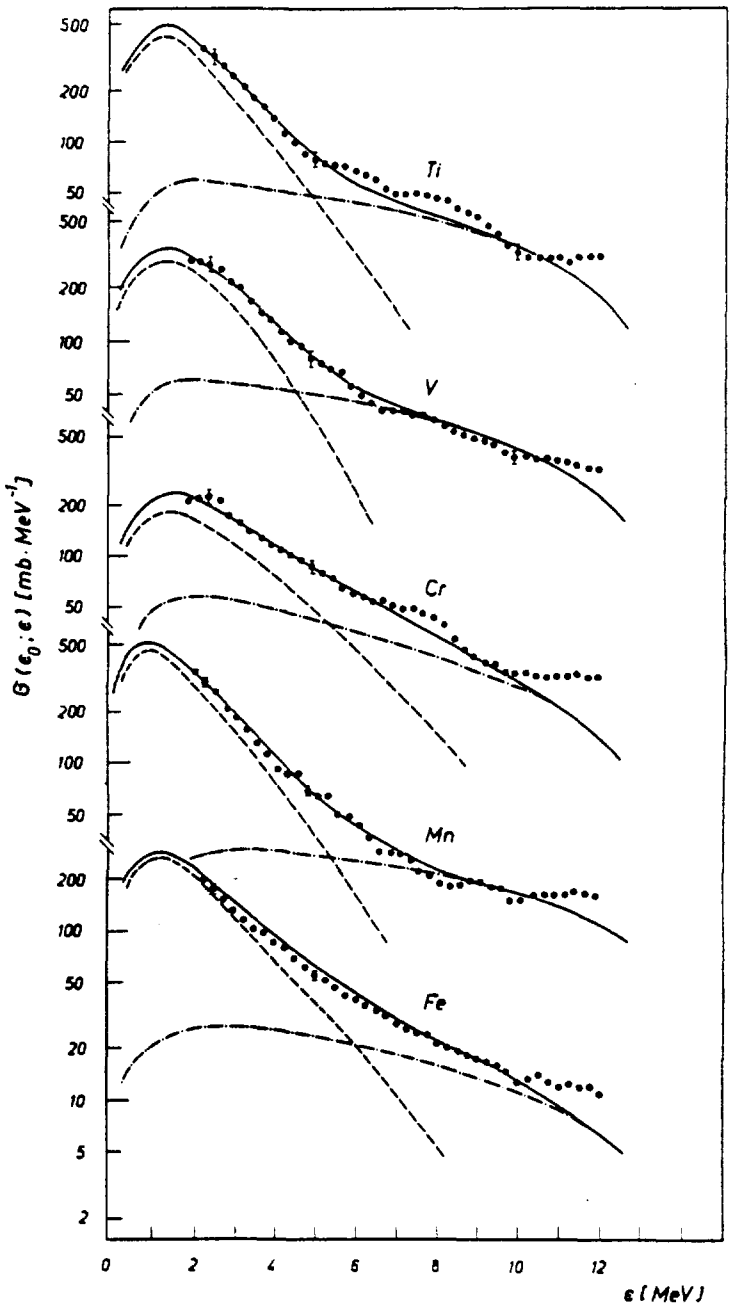

fig. 8 Angle integrated neutron emission spectra at 14.6 MeV incident energy [6]

b) for Ti, V, Cr, Mu, Fe

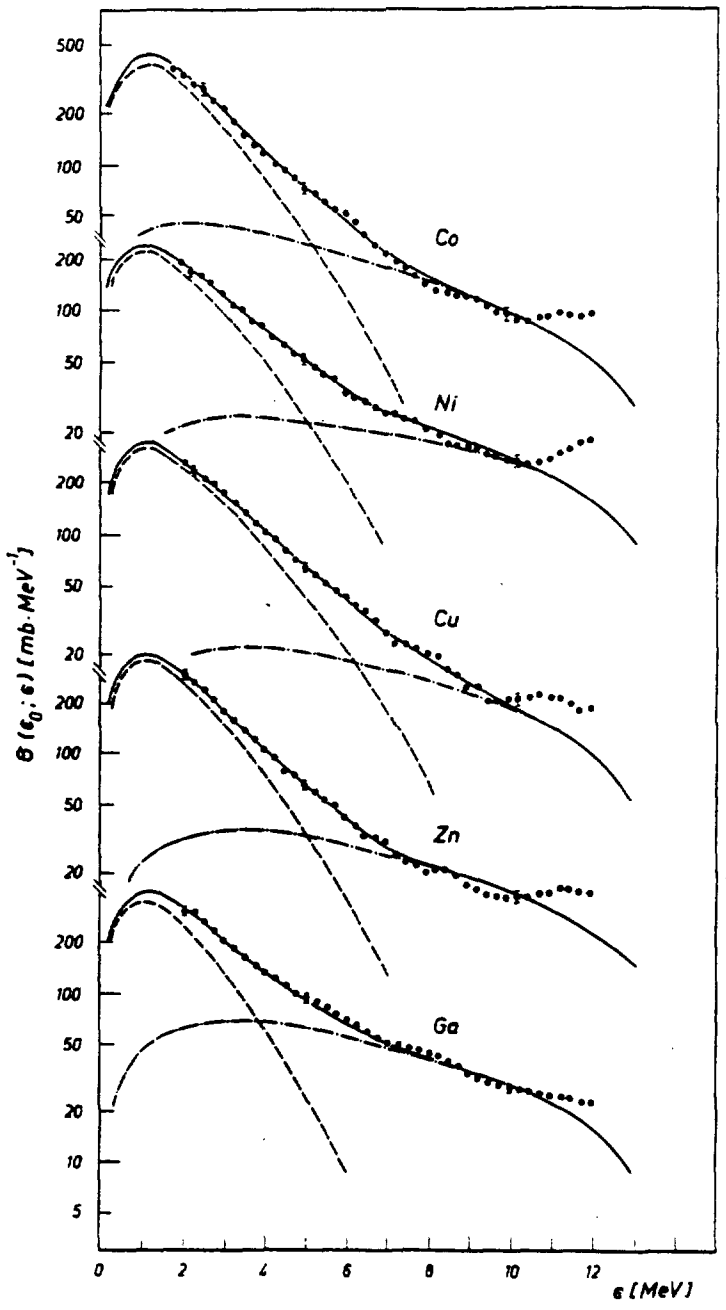

fig. 8 Angle integrated neutron emission spectra at 14.6 MeV incident energy [6]

c) for Co, Ni, Cu, Zn, Ga

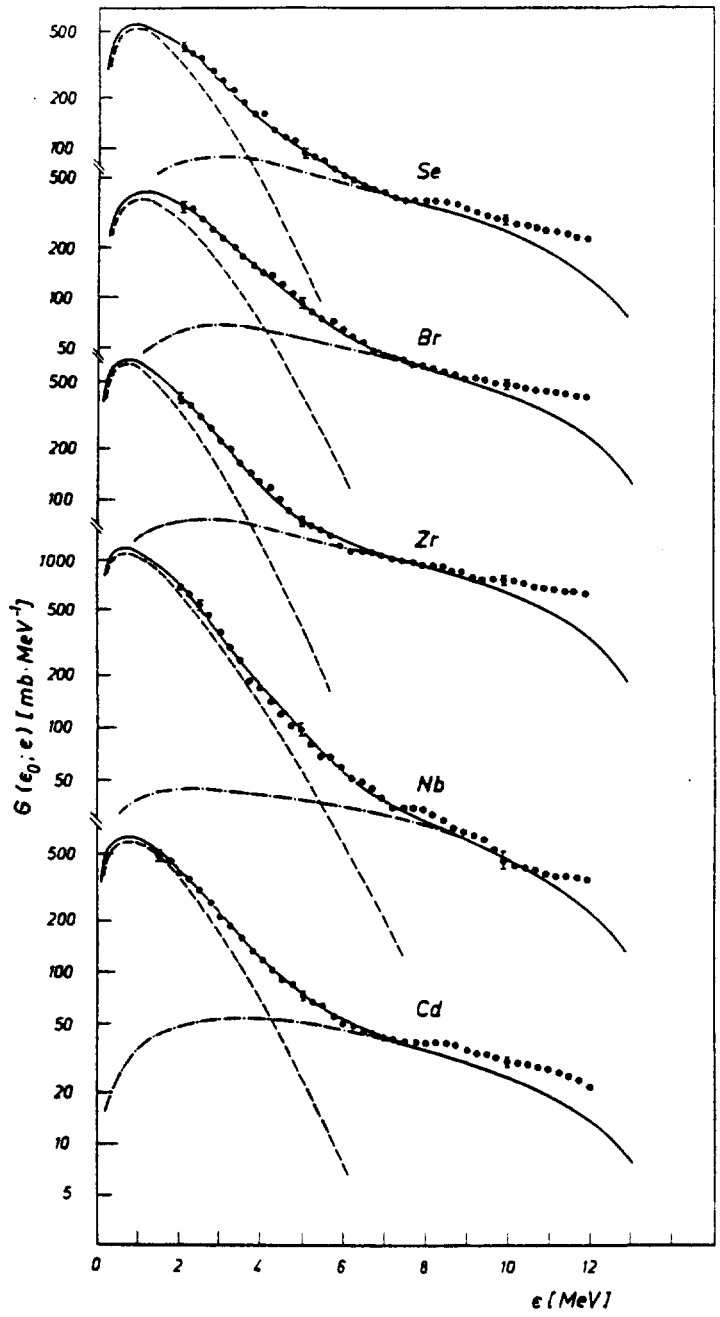

fig. 8 Angle integrated neutron emission spectra at 14.6 MeV incident energy [6]

d) for Se, Br. Zr, Nb, Cd

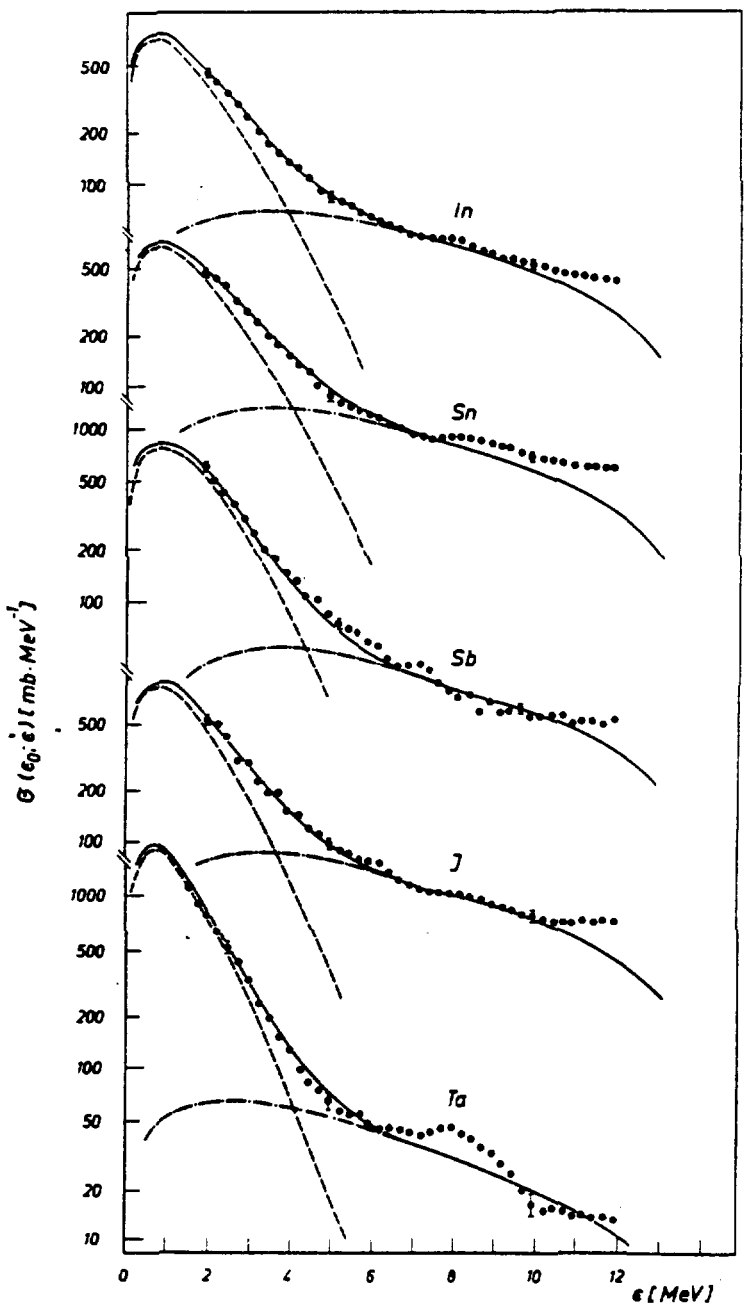

fig. 8 Angle integrated neutron emission spectra at 14.6 MeV incident energy [6]

e) for In, Sn, Sb, J, Ta

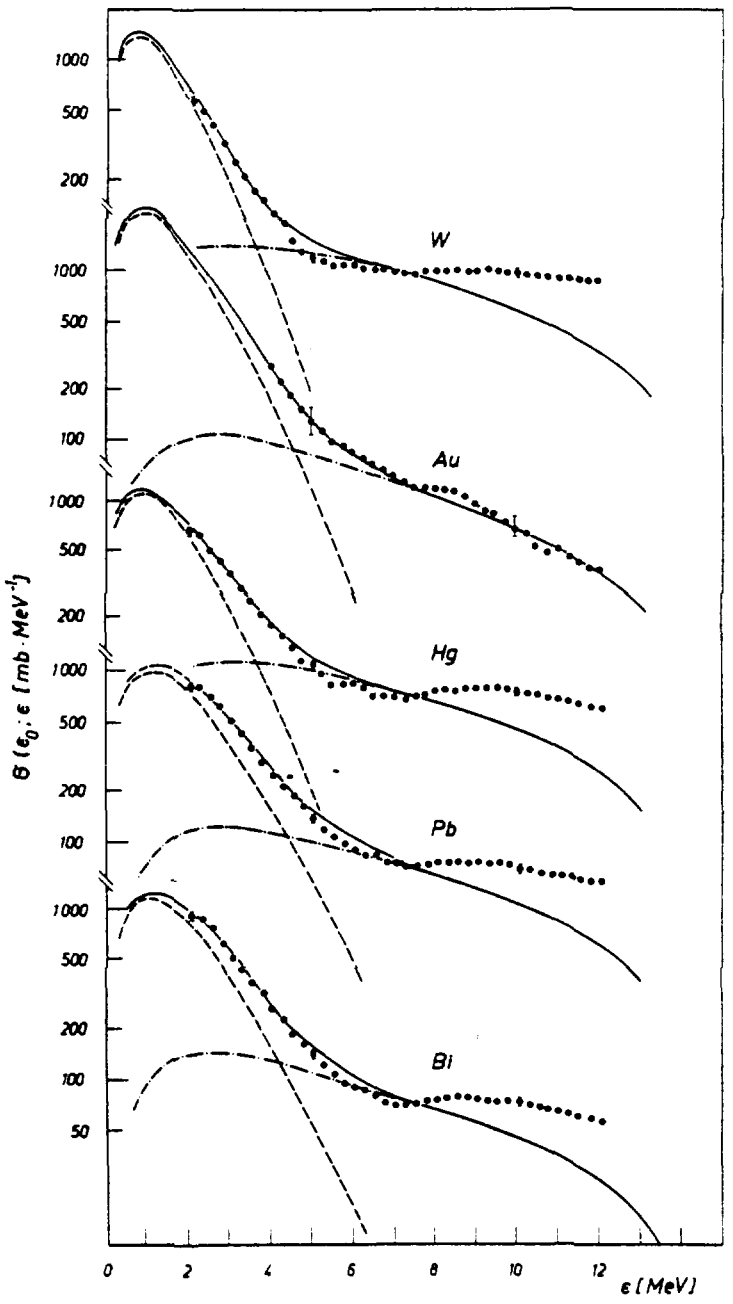

fig. 8 Angle integrated neutron emission spectra at 14.6 MeV incident energy [6]

f) for W, Au, Hg, Pb, Bi

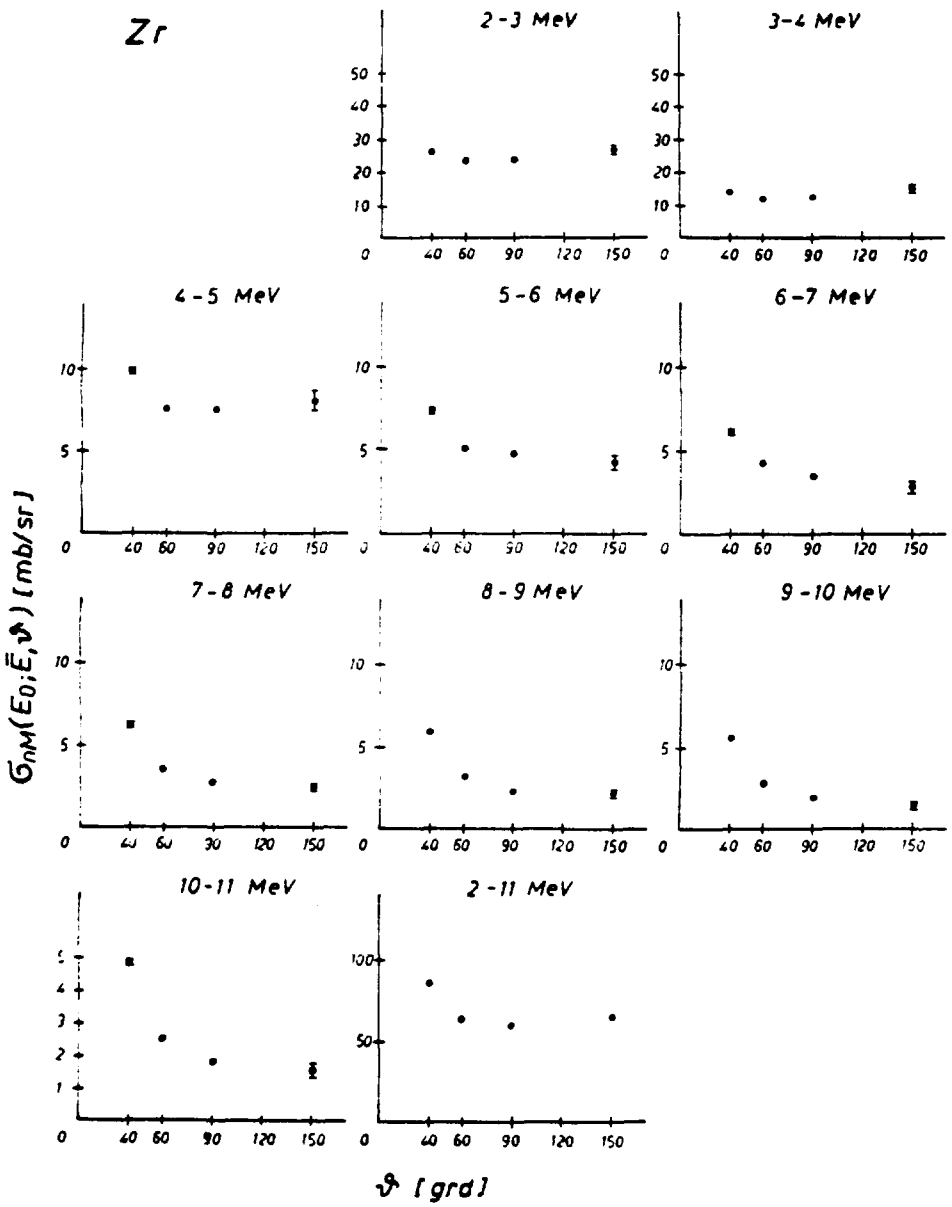

fig. 9 Differential neutron emission cross sctions for 1 MeV emission energy bins [6]
a) for Zr

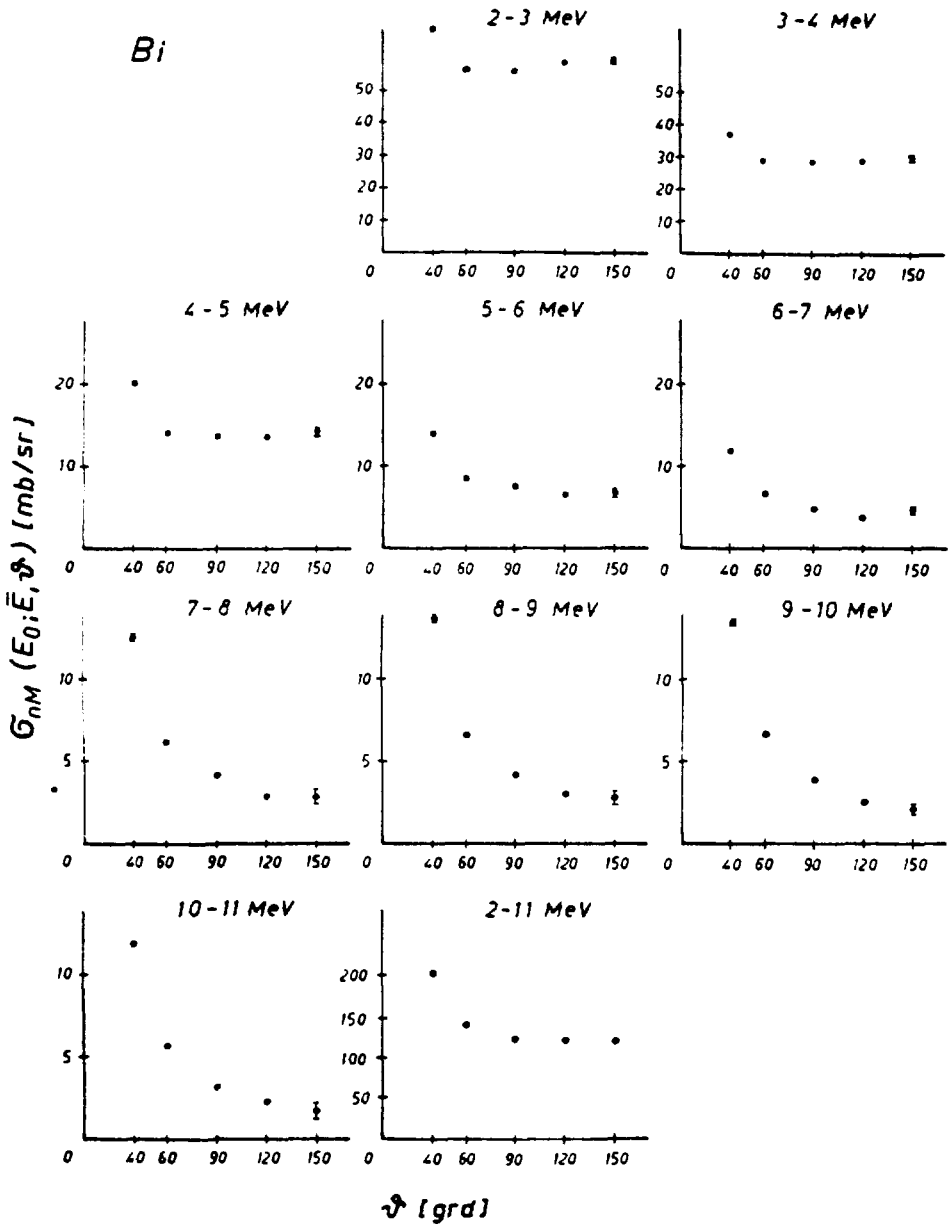

fig. 9 Differential neutron emission cross sctions for 1 MeV emission energy bins [6]

b) for Bi

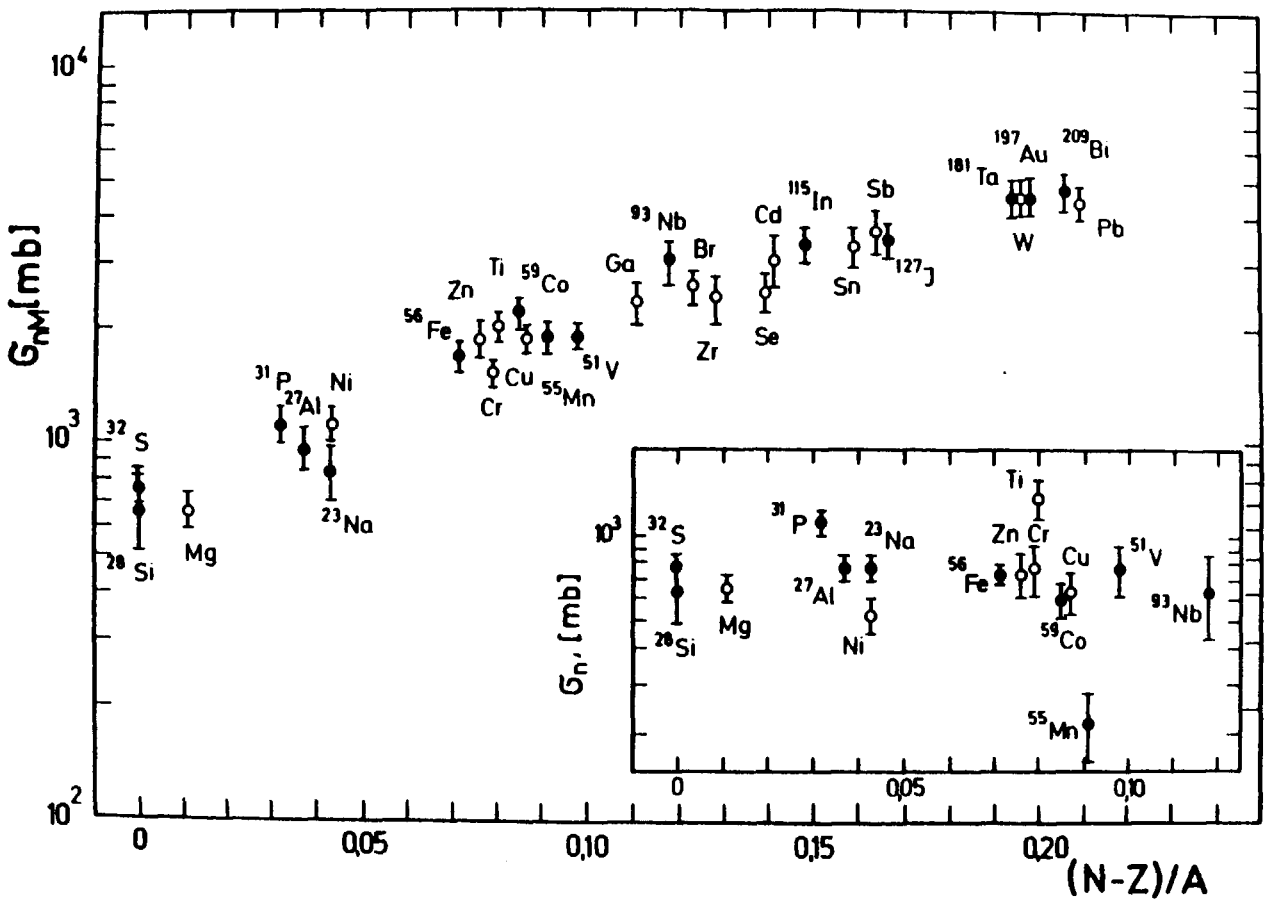

fig.10 Systematics of the neutron production cross sections σ_{nM} determined by theoretical extrapolation of the integrated spectra presented on fig. 8 [6]; insert: $\sigma_{nn'}$ cross sections estimated by the rule $\sigma_{nn'} \simeq (\sigma_{nM} + 100\ mb) - 2\sigma_{n,2n}$; points-isotopes; circles-elements

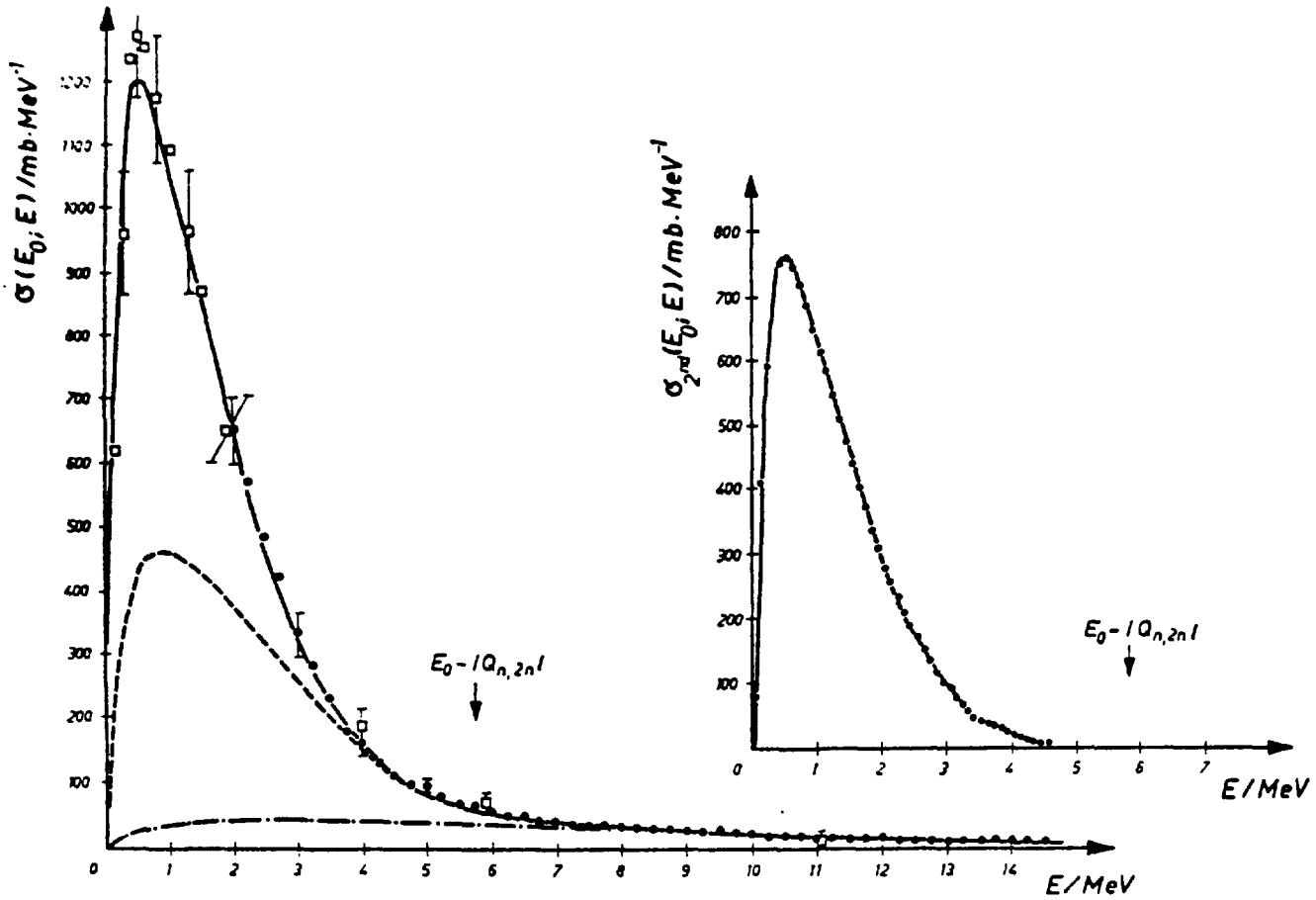

fig.11 Separation of the spectrum of second neutrons (right hand insert) from the difference between The experimental spectrum (solid line) and the calculated emission spectrum for the first neutrons (broken line) for ^{93}Nb [35]

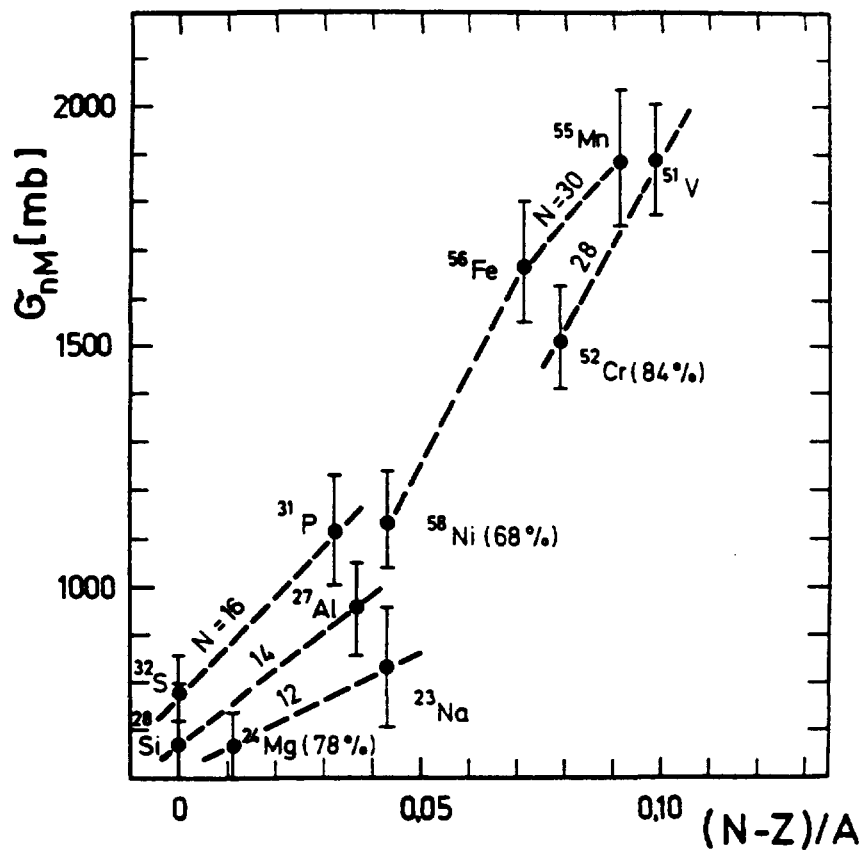

fig.12 Systematical dependence of σ_{nM} cross sections for nuclei with the same neutron number N [6].

Measurements of cross sections and spectra by in-beam γ ray spectroscopy[+]

P. Obložinský

Institute of Physics, Electro-Physical Research Centre of the Slovak Academy of Sciences, 842 28 Bratislava, Czechoslovakia

Abstract: In-beam γ ray cross sections and spectra measurements at 14 MeV neutron incident energy are reviewed. First, we discuss experimental techniques used systematically in these investigations. Indispensable features of such techniques are time-of-flight discrimination, massive shielding of spectrometers and heavy samples. Basic devices are NaI(Tl) and Ge(Li) spectrometers, though important piece of data was obtained also by NE213 used as γ spectrometer, telescopic scintillation pair spectrometer as well as recently introduced γ-γ and n-γ coincidence spectrometer systems. Second, we deal with variety of $(n_{14\ MeV}, x\gamma)$ cross sections and spectra measurements and illuminate them on selected examples. We touch on systematics of yields, total spectra including continuum components, population of discrete levels and angular distributions, specifics of capture spectra and recently initiated studies on γ ray multiplicities.

+) Invited talk at the 13th Inter. Symp. on Nuclear Physics--Fast Neutron Reactions, 21-25 November 1983, Gaussig, GDR

1. Introduction

Our task is nontraditional and perhaps even pioneering: to review in-beam γ ray spectroscopy techniques and measurements at 14 MeV neutron incident energy. In fact, there are only a few laboratories throughout the world dealing with in-beam γ ray measurements at neutron incident energies exceeding 10 MeV and still less of those concentrated on 14 MeV region. One reason is probably historical and valid for γ spectroscopy more generally. Its second man position has changed dramatically relatively recently only, when in-beam techniques were developed [1]. Real highlight is 162-fold NaI(Tl) crystal ball designed for heavy ion physics [2].

In (n,xγ) reactions at 14 MeV bulk of γ rays follow emission of 1 - 2 nucleons. Average excitation energy and angular momentum is $\lesssim$ 7 MeV and $\lesssim$ 4 $\hbar$, respectively. Consequently, cascades are short and experimental techniques are relatively simple, single NaI(Tl) or single Ge(Li) spectrometer.

Objectives of such works are twofold. First, data needed for calculations of shielding and nuclear heating in fission as well as fusion reactors. Second, it is physics concentrated mainly on understanding of reaction mechanims and γ decay processes.

The plan of the review is following. In sect.2 we discuss experimental techniques and procedures, variety of experimental results is examined in sect. 3 and conclusions are drawn in sect.4.

2. Experimental techniques and procedures

An obvious question is: What can one observe when studying (n_{14MeV},xγ) reactions? The answer is partly given in fig.1 where we show typical γ ray production spectrum for the target mass A$\sim$60. Dominant is smooth intermediate component originating in statistical (n,n'γ) transitions. Superimposed on this component are discrete γ rays, well pronounced in low energy region, $E_\gamma \lesssim$ 3 MeV, coming presumably from (n,n'γ) and (n,2nγ) channels. High energy component, $E_\gamma \gtrsim$ 14 MeV, which is very weak and rather smooth is due to capture.

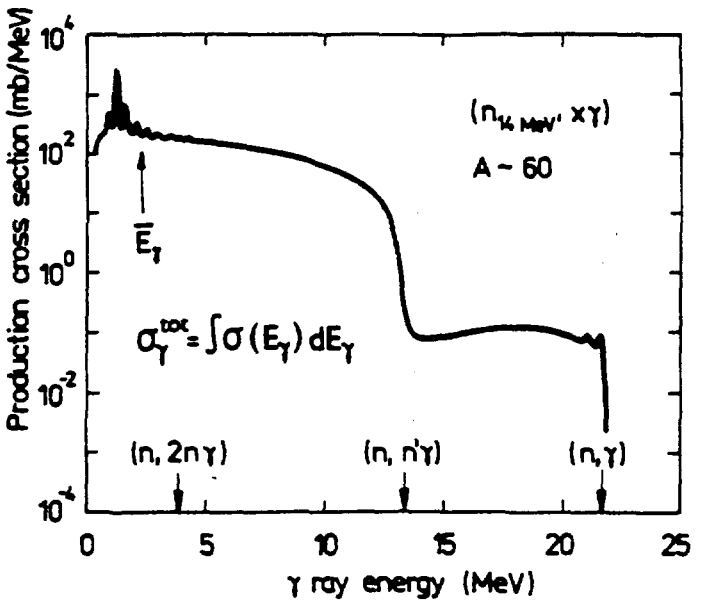

Fig.1. Typical γ ray production spectrum from reactions with 14 MeV neutrons. Shown by arrows are end-point energies of γ rays for 3 important reaction channels.

Production of γ rays can be most simply characterized by 2 integral numbers, namely γ ray yield, σ_γ^{tot}, and average energy per one γ ray emitted $\bar{E}_\gamma$. More detailed information can be obtained if one observes full γ ray production spectrum. In low spectral energy region of primary interest is population of discrete γ rays. Angular distribution of γ rays can be rather generally expressed via Legendre polynomials as [3]

$$\frac{d\sigma(\vartheta)}{d\omega} = a_0 + a_2 P_2(\cos\vartheta) + a_4 P_4(\cos\vartheta)$$

Often, one can neglect the last term and observe only at $\vartheta = 55^\circ$ or 125° where the second term vanishes. Angle integrated cross section in this approximation is simply

$$\sigma \approx 4\pi \frac{d\sigma(55^\circ)}{d\omega}$$

Finally, one can observe γ rays in coincidence with other simultaneously emitted γ rays or neutrons. These γ-γ and n-γ coincidence techniques seem be rather powerful in disclosing

γ decay processes of both bound and unbound excited states.

In-beam γ ray spectroscopy techniques applied to 14 MeV incident neutrons must cope with several limitations imposed basically by neutron sources. It is high background rate due to 4π character of a source, extremely low beam intensity (pour 1.5 nA proton beam, for example, providing beam intensity 10^{10} p/cm^{2}s by far exceeds its neutron counterpart from standard 10^{10} n/4πs D+T machine) and high sensitivity of γ spectrometers to neutrons, specifically to those scattered elastically from the sample. One, therefore, has to use heavy shielding of spectrometers, time-of-flight techniques for background suppression as well as for n-γ discrimination and massive samples to compensate for low counting rates. Typical sample weight is about 100 grams although the range is as broad as 10g - 3kg.

So far, variety of spectrometers were used to observe γ rays from $(n_{14\,MeV}, x\gamma)$ reactions. Representative selection of systems which cover broad range of ideas and techniques applied is given in tab.1. NaI(Tl) and Ge(Li) given in the first 2 columns represent basic tools. Last 3 columns show less common techniques. They include liquid scintillator NE 213 for γ ray spectra and integral characteristics, telescopic pair spectrometer for capture spectra and combined spectroscopy system for coincidence measurements.

Tab.1. Variety of spectrometers and techniques used in in-beam studies of $(n,x\gamma)$ reactions at 14 MeV incident neutron energy.

Spectrometer	NaI(Tl)	Ge(Li)	NE213	Pair	Combined
Laboratory	Los Alamos[4]	Bruyères[5]	Oak Ridge[6]	Ljubljana[7]	Bratislava[8]
Measured γ	continuum	discrete	integral	capture	γ-γ, n-γ
Source	T+D	D+T	ORELA	D+T	D+T
Timing	pulsed n	associated α	pulsed n	—	associated α
Bkg suppression	tof,shield	tof,shield	tof,collimator	telescope	tof,collimator
Sample	cylinder	cylinder	ring	4π	cylinder
Data acquisition	2-parametric	1-parametric	2-parametric	1-parametric	multi-parametric
Data analysis	unfolding	peak fitting	unfolding	unfolding	combined

In subsequent figures we illuminate in more detail some of the above systems. Shown in fig. 2 is the NaI(Tl) spectrometer developed by Drake et al.[4]. The ø 6cm x 15 cm NaI(Tl) detector is in anticompton ø 25 cm x 31 cm NaI(Tl) annulus. The spectrometer is shielded by lead, borated polyethylene and by tungsten shadow bar. Lithium hydrid plug is used to decrease number of fast neutrons scattered on the sample and flying towards the spectrometer.

We point out that sensitivity of NaI(Tl) to fast neutrons is rather high, mainly due to $^{127}I(n,n'\gamma)$ reactions. For example, measured total efficiency of ø 16 cm x 10 cm NaI(Tl) to 14.6 MeV neutrons is about 45% and average pulse height detected is 2.6 MeV [9]. Also, it was suggested to monitor fast neutrons with a NaI(Tl) by observing strong 57 keV and 202 keV γ lines from ^{127}I [10].

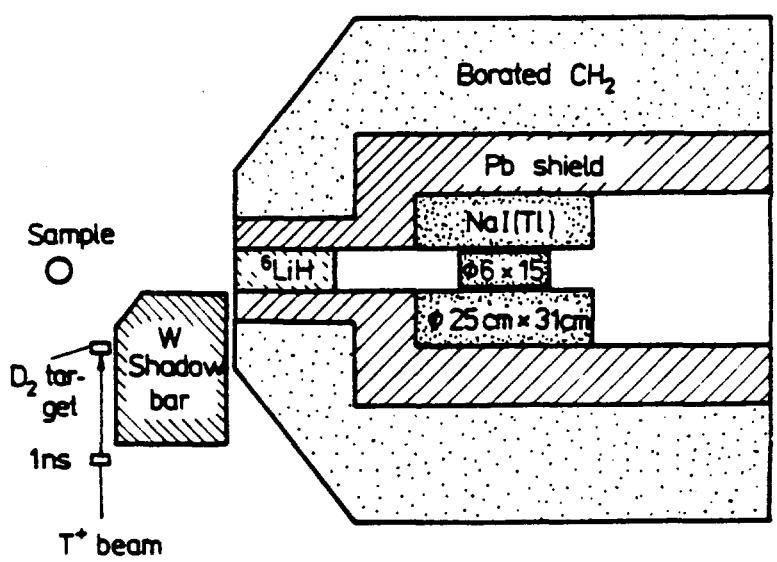

Fig.2. NaI(Tl) spectroscopy system with anticompton shielding (Drake et al.[4]).

Shown in fig.3 is Ge(Li) spectroscopy system developed by Lachkar et al.[5]. The 67 cm^3 Ge(Li) is surrounded by an anticompton ø 30 cm x 30 cm NaI(Tl) annulus. Unless time-of-flight separation between neutrons and γ rays is performed, even in a well shielded Ge(Li) one can observe several background lines due to interactions of fast neutrons with Ge isotopes and also

with surrounding materials like Al, Pb etc. Peaks from intra-detector reactions are very broad, most typical is ~600 keV one from $^{74}Ge(n,n'\gamma)$ reaction.

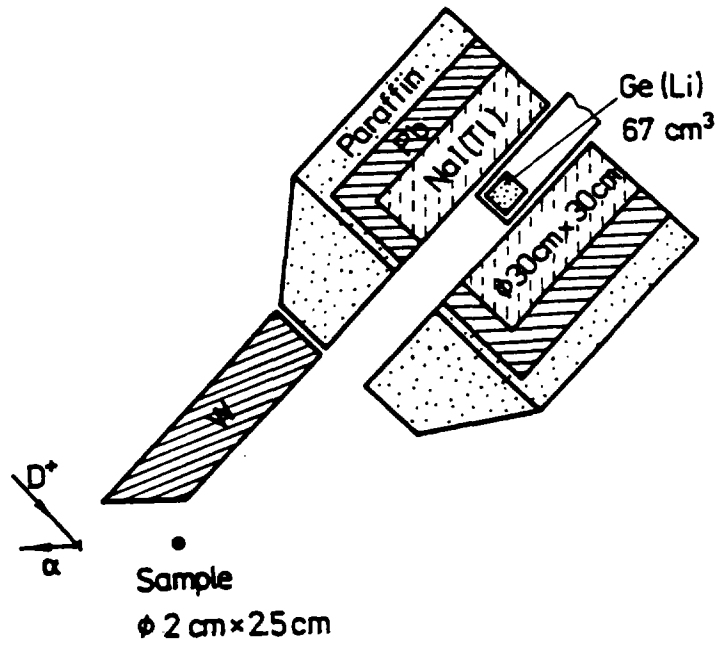

Fig.3. Ge(Li) spectroscopy system with anticompton shielding (Lachkar et al.[5]).

Shown in fig. 4 is a multidetector system developed by Hlaváč et al.[8] comprising of NaI(Tl), Ge(Li) and a neutron tof spectrometer. Significant background reduction is achieved by applying both mechanical and electronical collimation. Front-face shielding of the NaI(Tl) serves as a passive anticompton arrangement. The system allows simultaneous measurement of singles γ ray and neutron spectra as well as coincidence γ-γ and n-γ spectra. These data often allows transparent presentation in terms of average γ ray multiplicities.

Accumulation of γ ray spectra should be accompanied by neutron monitoring and followed by analysis of raw spectra. We briefly commented on the first point and make only very few remarks about the rest.

In-beam monitoring of 14 MeV neutrons is rather delicate task and it is useful to apply simultaneously 2 independent methods. An obvious choice is the associated α particle counting combined with counting by an absolutely calibrated neutron spectrometer.

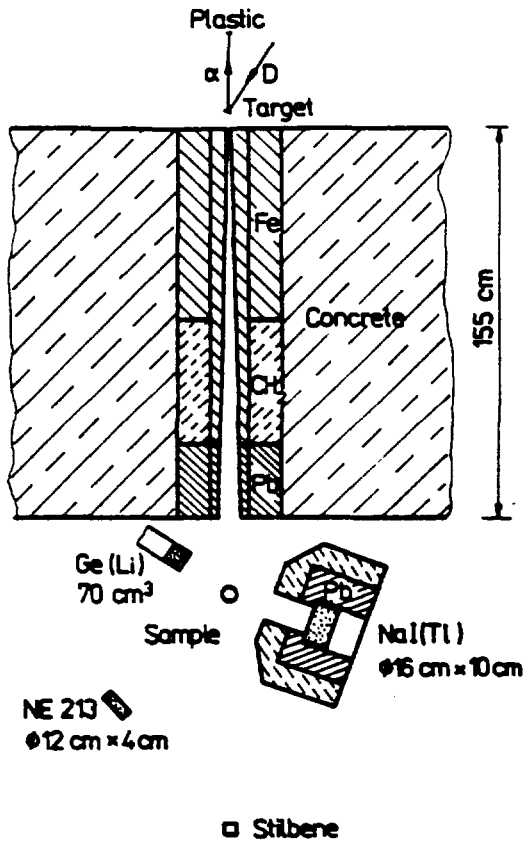

Fig.4. NaI(Tl) - Ge(Li) - NE 213 spectroscopy system for singles as well as γ-γ and n-γ coincidence measurements (Hlaváč et al.[8]).

Analysis of raw spectra includes peak fitting procedure for discrete γ lines as observed by Ge(Li) detectors and unfolding of continuum spectra detected e.g. by a NaI(Tl). Also, one has to apply absolute efficiency of the spectrometer and corrections due to unavoidably large dimensions of a sample.

Unfolding procedure solves equation [11,12]

$$S_{exp} = R \times S_{true} ,$$

where R is the response matrix of the spectrometer. Usually, one extracts response matrix from several spot energy measurements. Sources of high energy γ rays, useful for this purpose and available by a low energy accelerator, are listed in tab.2.

Tab.2. Simple sources of high energy γ rays for response measurements.

Source	Incident enegy (MeV)	E_γ (MeV)
$^{12}C(n,n'\gamma)$	14	4.44
$^{16}O(n,p)$, $T_{1/2} \sim 7s$	14	6.13
$^{11}B(p,\gamma)$	0.163	11.67
		16.11
$^{3}H(p,\gamma)$	0.1	19.8

3. γ ray production cross sections and spectra

Limited scope of this review does not allow us to present comprehensive discussion of all results. Rather, we briefly touch upon basic aspects of γ ray cross sections and spectra and try to demonstrate variety and complexity of observed γ rays at 14 MeV neutron incident energy. We start our discussion with integral characteristics and proceed to continuum spectra, discrete γ ray cross sections and coincident spectroscopy. We shall use ^{56}Fe as an illustrative example since it is probably best studied nucleus in this region.

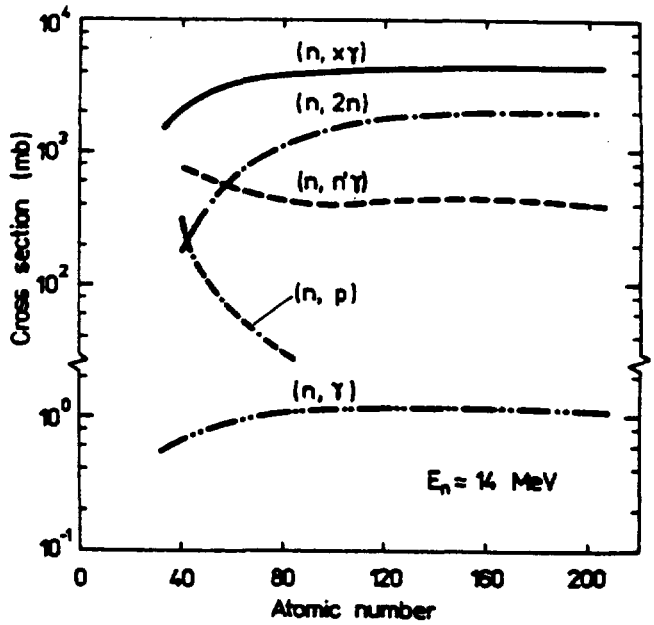

Fig.5. Gross trend in $(n_{14\,MeV}, x\gamma)$ total cross sections. Shown for comparison are trends in some other channels from activation measurements. ($(n,x\gamma)$ deduced from[13], activation from[14]).

Integral characteristics. Gross trend in total γ ray production cross sections as a function of target mass number is shown in fig.5. Shown for comparison are trends in (n,2n), (n,n'γ), (n,p) and (n,γ) cross sections from activation measurements. Seen is that (n, totγ) is the strongest reaction channel and it exceeds (n,2n) cross section by a factor of $\approx$ 2 - 5 and activation (n,n'γ) cross section even by an order of magnitude. The reason is that in average more than one γ ray is emitted in a cascade especially in the (n,n'γ) channel. Activation (n,n'γ) cross section reflects population of one specific γ transition only.

The second integral characteristics of γ ray production is the average energy per one γ ray emitted. Values observed on several target elements are given in tab.3. Based on these numbers one could expect that $\overline{E}_\gamma$ may vary from about 1.5 MeV up to about 2.5 MeV throughout the whole mass region. This indicates important contribution of high energy statistical γ rays in (n,n'γ) cascades.

Tab.3. Observed average γ ray energy from (n_{14MeV},xγ) reactions on several elements.

Element	Ti	Cr	Fe	Cu	Nb
$\overline{E}_\gamma$(MeV)	2.2	2.4	2.2	1.9	1.7

Continuum spectra. Total γ ray production spectrum on ^{56}Fe as observed by various authors is compared with theoretical calculations in fig.6. Shown are calculated contributions from (n,2nγ), (n,n'γ) as well as (n,γ) channels. The first two components as calculated within the statistical model seem describe basic features, though not all details of the observed spectrum. Of special physical interest is capture where the statistical component (dash-double dott line) is several orders of magnitude below the experiment. It is seen that the direct-semidirect model calculations[16] accounts reasonably well for the hardest part of the the capture spectrum. Also shown are two attempts (full lines) to account for the capture spectrum in a frame of the preequilibrium models. Though neither of these latter attempts seem to be without criticism, they suggest that preequilibrium [17] or multistep direct process*es* do play important role in

fast neutron capture.

So far, few groups have measured continuum γ ray spectra at 14 MeV neutron incident energy systematically. Dickens et al. [13] measured spectra on 22 elements, $7 \leq A \leq 208$, with a NaI(Tl) in the spectral energy region $E_\gamma \leq 10$ MeV at $E_n = 1 - 20$ MeV. Similarly, Morgan [18] measured on a number of elements with a NE 213. Drake et al.[4] obtained spectra on 15 elements, $8 \leq A \leq 238$, up to $E_\gamma \leq 8.5$ MeV at $E_n = 14.2$ MeV. Finally, Budnar et al. [7] reported capture spectra, $E_\gamma \gtrsim 14$ MeV, on 28 elements, $12 \leq A \leq 208$, with a telescopic pair spectrometer at $E_n = 14$ MeV.

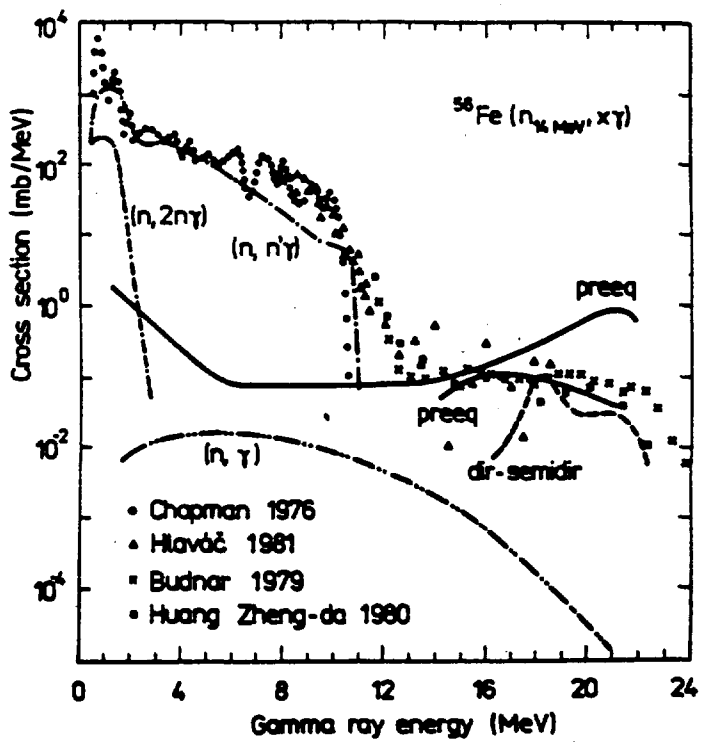

Fig.6. γ ray production spectrum from $^{56}Fe(n_{14\,MeV}, x\gamma)$ is compared with theoretical calculations (compiled by Hermsdorf et al.[15]).

Discrete γ rays. From discrete γ ray production cross sections one can easily obtain population of discrete levels of a given nucleus. It turns out that this way of presentation of the data is rather useful.

Shown in fig. 7 is observed and calculated population of discrete levels of ^{55}Fe in $^{56}Fe(n, 2n\gamma)$ reactions at 14.6 MeV. It is seen that these cross sections exhibit rather regular pattern with increasing J^π. Since the ground state is $3/2^-$

the population of the first excited $1/2^-$ state is suppressed. Important point in theoretical calculations was realistic treatment of the ^{55}Fe decay scheme. Still, agreement between the experiment and calculations is rather impressive.

Of interest is population of the ^{55}Fe ground state. Calculated (n, 2n) total cross section is substantially higher than γ ray feeding of the ground state. It means that as much as 60% of secondary neutrons is not accompanied by γ rays at all and feed directly the ground state.

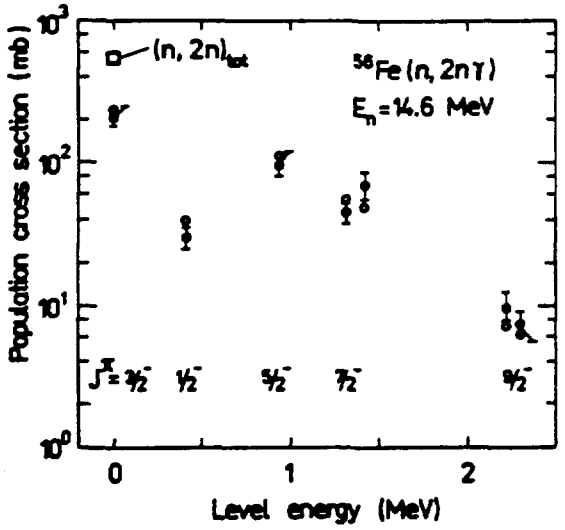

Fig.7. Observed population of discrete levels in ^{55}Fe is compared with calculated values (code STAPRE). About 60% of secondary neutrons feed directly g.s. of ^{55}Fe (Hlaváč[19]).

Probably most often measured production cross section of a discrete γ line at 14 MeV neutron incident energy is strong $2^+ \rightarrow 0^+$ g.s. transition of 847 keV in ^{56}Fe(n,n'γ) reaction. Values reported from various laboratories, however, differ substantially. This indicates that often important systematic errors are involved in some of these measurements.

Shown in fig. 8 are production cross sections of the above γ line at about 90-deg towards the neutron beam and at E_n = 14 - 15 MeV as observed in many laboratories during last 20 years. Cross sections go from 40 mb/sr up to 86 mb/sr. Only a small part of these discrepancies can be explained by 1 MeV spread of the incident neutron energy. This is seen in fig. 9 showing excitation curve measured by Dickens et al.[23]. Similar conclusion concerns also possible contribution from the spread due to angular distributions.

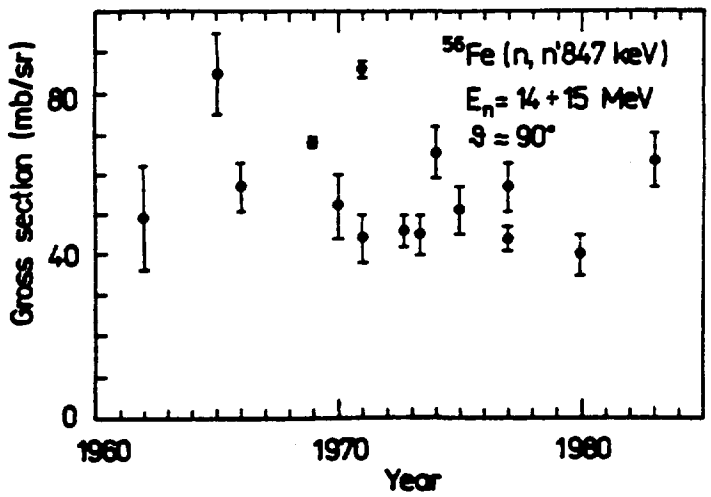

Fig.8. Production cross section for the 847 keV γ line at 90-deg from ^{56}Fe(n,n'γ) as observed in various laboratories during the last 20 years (data from refs.[4,5,19,20,21,22]).

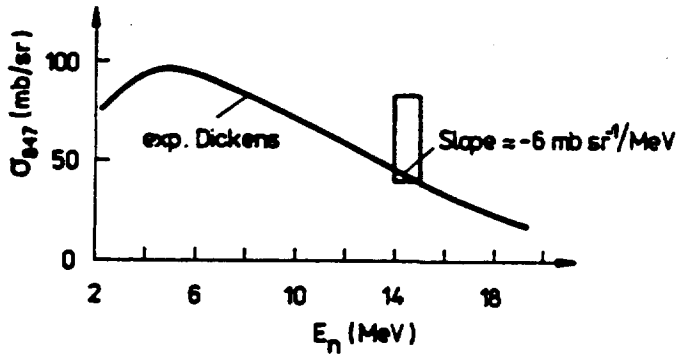

Fig.9. Excitation curve for the 847 keV γ line from ^{56}Fe(n, n'γ). The slope in 14 MeV region is about - 6 mb/sr per 1 MeV of neutron energy.

Angular distributions of γ rays at 14 MeV neutron incident energy were measured practically for discrete γ rays only. Available are data mostly for (n, 2nγ) and (n,n'γ) reactions but really rare are e.g. (n,γ) data.

Shown in fig. 10 are observed angular distributions for 3 specific instances. Ground state capture transition on ^{40}Ca indicates weak fore-aft asymmetry. Angular distributions in (n, n'γ) and (n, 2nγ) are, however, symmetric around 90-deg. It is seen that the strongest transition in ^{56}Fe(n,n'γ), 847 keV, $2^+ \rightarrow 0^+$ g.s., E2, as well as the strongest one in ^{56}Fe(n, 2nγ), 932 keV, $5/2^- \rightarrow 3/2^-$ g.s., M1+10%E2, do show significant forward-

backward enhancement. This means that the final nucleus still preserve memory about orientation of the original compound nucleus, although the average angular momentum of the latter is rather low, $\overline{J}_c \approx 4\ \hbar$.

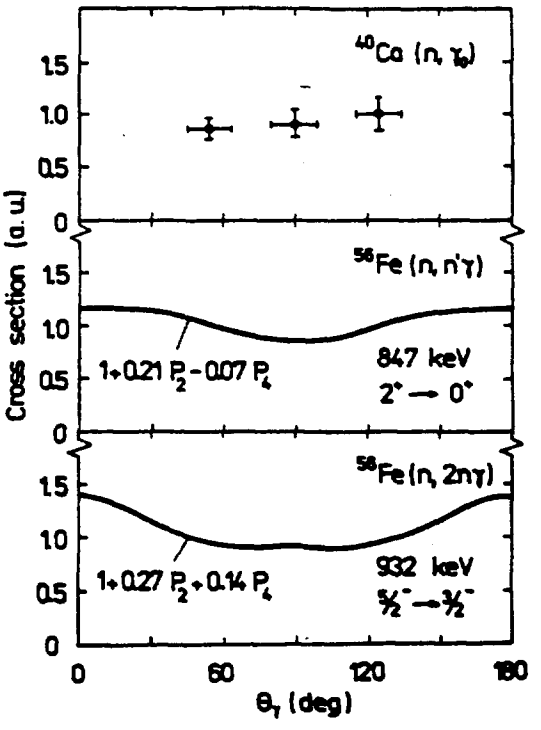

Fig.10. Observed angular distributions of discrete transitions in (n,γ), (n,n'γ) and (n, 2nγ) reactions at 14 MeV (^{40}Ca:Arthur [24], ^{56}Fe:Degtyarev [21]).

Coincidence spectroscopy. Coincidence spectroscopy seems to be of special physical interest. At 14 MeV neutron incident energy n-γ spectroscopy measurements, for example, can provide information about γ decay of unbound states, $E_{exc} > B_n$, formed in (n,n'γ) reactions.

One technique is to observe neutron spectrum in coincidence with a discrete γ transition in (n,n'γ) channel [25]. Low energy part of the spectrum reflects γ competition with emission of secondary neutrons. Relative radiative width $\Gamma_\gamma / \Gamma_{tot}$ can be extracted from theoretical fit to the spectrum. Another technique [19] is to measure singles as well as coincident neutron spectra which can be presented in terms of average multiplicity of γ ray cascades following emission of neutrons with a given energy [8]. It can be seen in fig. 11 displaying results for ^{56}Fe target that at low neutron energies

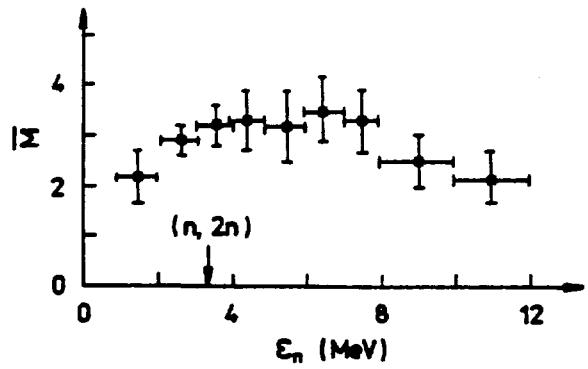

Fig.11. Average γ ray multiplicity as a function of energy of emitted neutrons from ^{56}Fe bombarded with 14.6 MeV neutrons [26].

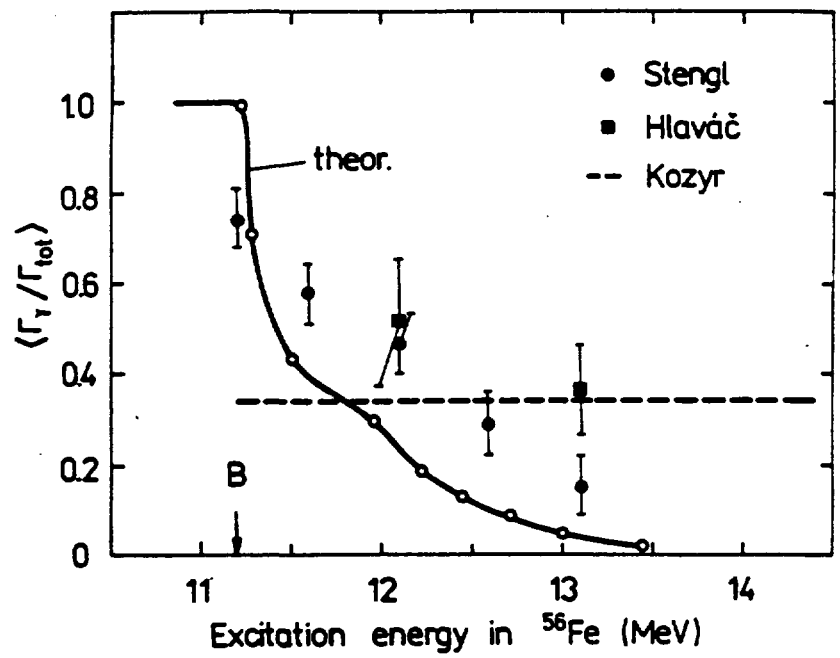

Fig.12. Relative radiative width of unbound states in ^{56}Fe as deduced from ($n_{14\,MeV}$,n'γ) spectra measured by the n-γ coincidence technique (refs. [25,19,27]).

the multiplicities bent down. This is due to a mixture of long (n,n'γ) cascades and short (n, 2nγ) ones. Observed multiplicity is

$$\overline{M} \approx \frac{M' \frac{\Gamma_\gamma}{\Gamma_{tot}} + 2\,M''\left(1 - \frac{\Gamma_\gamma}{\Gamma_{tot}}\right)}{2 - \frac{\Gamma_\gamma}{\Gamma_{tot}}} ,$$

where M' refers to $(n,n'\gamma)$ and M'' to $(n,2n\gamma)$ cascades. An advantage of this method is its independence on absolute values of (n,n') cross sections.

Shown in fig. 12 is average relative radiative width $\langle \Gamma_\gamma / \Gamma_{tot} \rangle$ as a function of excitation energy in ^{56}Fe. The averaging refers to angular momentum of the compound nucleus. Theoretical curve was obtained by statistical model calculations with Γ_γ normalized to realistic 2 eV at $E_{exc} = B_n$ [25], experimental values are from refs.[25,19] and also from Kozyr et al.[27] who report one average value only. The results indicate that γ competition, in the region of excitation energies and angular momenta studied, is about 1.5 - 2 times stronger than suggested by the statistical model.

4. Conclusions

Until now, γ ray production spectra at 14 MeV neutron incident energy have been measured for many elements of practical importance. Unsatisfactory measured, however, is intermediate spectral energy region $E_\gamma \approx 6$ - 14 MeV. Also, the spread in data reported by various groups is often significant. Practically not measured were angular distributions of continuum parts of spectra. WRENDA, for example, lists some 50 - 70 requests for various in-beam γ spectroscopy measurements at 14 MeV, usually with 10 - 20% precision and priority 2.

Of special physical interest seems to be coincidence spectroscopy, where only little has been done until now. Development of experimental systems comprising of at least 2 spectrometers seems, therefore, useful. Also, it seems that new bismuth germanate scintillator, $Bi_4Ge_3O_{12}$ (BGO), with superior efficiency and spatial resolution to NaI(Tl), should be used on a larger scale [28].

Systematic analyses of γ ray production at 14 MeV neutron incident energy are scarce, especially when compared with activation measurements and also with neutron and charged particle spectroscopy. Majority of nuclei have never been measured offering an interesting option for a research programme of a new generation of D+T neutron sources.

Theoretical analysis should include still missing formulation of preequilibrium γ ray emission with angular momentum

conservation. Another interesting point would concern γ competition in decay of unbound nuclear states.

The author is indebted to R. Antalík, S. Hlaváč and E. Běták for valuable discussions.

References

1) H.Morinaga and T.Yamazaki, In-beam gamma-ray spectroscopy (North Holland, Amsterdam 1976) preface
2) V.Metag et al., in Detectors in Heavy-Ion Reactions, ed. W.v.Oertzen (Springer Berlin 1983, Lecture Notes in Physics 178) p. 163
3) Z.W.Bell, J.K.Dickens, D.C.Larson and J.H.Todd, Nucl.Sci. Eng. 84(1983)12
4) D.M.Drake, E.D.Arthur and M.G.Silbert, Report LA-5983-MS (Los Alamos 1975)
I.Bergqvist, D.M.Drake and D.K.McDaniels, Nucl.Phys. A 191(1972)641
5) J.Lachkar, J.Sigaud, Y.Patin and G.Haouat, Nucl.Sci.Eng. 55(1974)168
6) G.L.Morgan, T.A.Love and F.G.Perey, Nucl.Instr.Meth. 128 (1975)125
7) M.Budnar et al., Report INDC(YUG-6/L) (IAEA Vienna 1979)
F.Cvelbar et al., Nucl.Instr.Meth. 44(1966)292
8) S.Hlaváč and P.Obložinský, Nucl.Instr.Meth. 206(1983)127
9) P.Obložinský and S.Hlaváč, in Neutron Induced Reactions, Proc. Europhysics Topical Conference (ed. P. Obložinský, Bratislava 1982) p. 397
10) F.E.Cecil, K.Killian and M.Rymes, Phys.Rev. C19(1979)2414
11) J.F.Mollenauer, Phys.Rev. 127(1962)867
12) E.Sjøntoft, Nucl.Instr.Meth. 163(1979)519
13) J.K.Dickens et al., Nucl.Sci.Eng. 62(1977)515
14) S.M.Qaim, in Handbook of Spectroscopy (CRC Press, Florida) vol.3, p.141
15) B.Barragatscha, D.Hermsdorf and E.Paffrath, J.Phys.G:Nucl. Phys. 8(1982)275
16) F.Rigaud, Nucl.Phys. A173(1971)551
17) E.Běták and J.Dobeš, Phys.Lett. 84B(1979)368
18) G.L.Morgan, Report ORNL 5563 (Oak Ridge 1979) and referen-

ces therein
19) S.Hlaváč, Thesis (Bratislava 1982) unpublished
20) G.Grenier, Kiev Neutron Conference´73 (Obninsk 1974) vol. 3, p.216
21) A.P.Degtyarev et al., Kiev Neutron Conference´77 (Moscow 1977) vol. 2, p.3 and p. 57
22) Al-Shalabi and A.J.Cox, Nucl.Instr.Meth. 205(1983)495
23) J.K.Dickens, G.L.Morgan and F.G.Perey, Nucl.Sci.Eng. 50 (1973)311
24) E.D.Arthur, D.M.Drake and I.Halpern, Phys.Rev.Lett. 35(1975) 914
25) G.Stengl, M.Uhl and H.Vonach, Nucl.Phys. A290(1977)109
26) S.Hlaváč, P.Obložinský and R.Antalík, Bull.Acad.Sci. USSR, Ser. Phys. 46(1982)903
27) Yu.E.Kozyr and G.A.Prokopec, Yad.Fiz. 27(1978)616
28) S.A.Wender et al., Nucl.Instr.Meth., submitted

THEORETICAL MODELS AND COMPUTER CODES FOR 14 MEV NEUTRON NUCLEAR DATA CALCULATION

D. Hermsdorf
Technical University of Dresden, Department of Physics
GDR - 8027 Dresden, Mommsenstr. 13

Abstract:

In this paper, a review of various empirical and theoretical models for representation and interpretation of 14 MeV neutron nuclear data is presented.

Computer codes embodying the principles of the relevant nuclear reaction models are summarized.

Some problems of application of different codes for a consistent calculation of neutron nuclear data are discussed including numerical problems and the choice of convenient parameters.

Results of code intercomparisons are given along conclusions for future demands.

1. Introduction

In 1965, S. Pearlstein formulated a question addressed to physicists active in the field of neutron nuclear data evaluation:

> 'Can you give me the cross section information I need to know for a nucleus that has not been measured if I give you two facts, the atomic number and the atomic mass?'

(cited by V. Benzi in 'Evolution in Evaluation' /1/).

Meanwhile 18 years have gone. But can we answer this question now?

The present review is aimed to discuss the situation of neutron nuclear data prediction around 14 MeV.

The importance of 14 MeV data are quite out of question for practical applications but they are of extremly high interest for fundamental scientific research in nuclear physics too. This relevance results from the facts that at 14 MeV

(i) a very large amount of experimental data has been measured and compiled in CINDA;

(ii) quite different experimental techniques including integral and differential as well as relative and absolute measurements are applied (see reviews given by Csikai, Qaim, Seeliger, Takahashi, Vonach and others at this Symposium and formerly /2/);

(iii) all kinds of reaction products including n, p, d, t, τ, α, fission products and γ's have been investigated.

What can be done with 14 MeV data in nuclear physics?

The bulky material can be used for

(i) mass systematics to predict unmeasured cross sections by empirical formulae

and

(ii) normalization of calculations in the frame of semi-empirical and theoretically founded models for data prediction at energies $E < 13$ and $E > 15$ by extrapolation.

So, all 14 MeV data are extremly interesting for testing nuclear reaction mechanism models. But any model is as useful as it can be treated by convenient numerical methods applicable for computer codes.

The relations between models, codes and calculations will be discussed now.

2. Models used for neutron nuclear data interpretation and prediction

2.1. Empirical and semi-empirical formulae derived from mass systematics at 14 MeV

2.1.1. Derivation of formulae

At a very early stage in neutron physics, in the late fiftees, the collection of 14 MeV data was initiated by systematics for $\tilde{\sigma}_{nX}$ (Flerov, Talyzin /3/) and $\tilde{\sigma}_{n,p}$ (Gardner /4/, Levkovskij /5/).

Fig. 1
Mass systematics of total cross sections $\tilde{\sigma}_{nT}$ in units of the Black-Nucleus-Model cross section at 14 MeV (taken from ref. /6/).

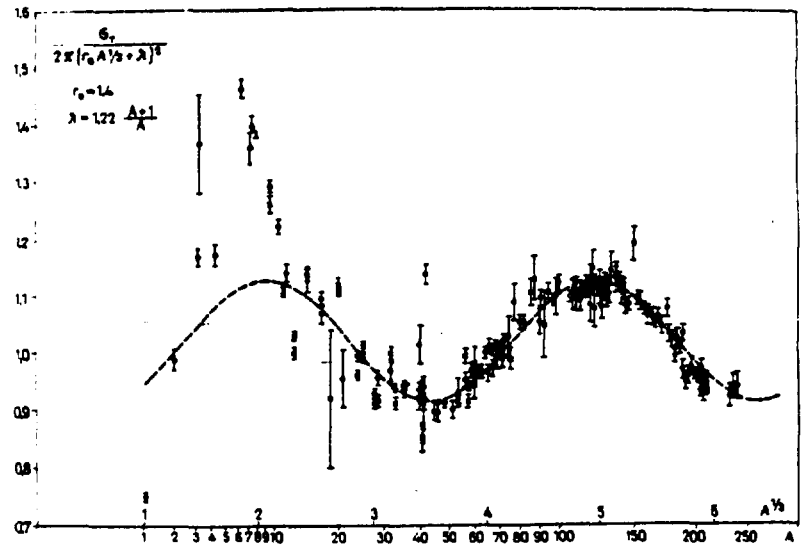

Any more sophisticated systematics was only possible after appearance of more reliable data.

Several attempts to establish mass systematics in terms

of empirical formulae are based on simple nuclear models like the "Black Nucleus Model" and the "Evaporation Model" (Weisskopf-Ewing-Model). For example we refer to formulae derived for the total cross section by Angeli and Csikai /6/ yielding (see fig. 1)

$$\frac{\sigma^{exp}_{nT}}{2\pi(R+\lambda)^2} = 1.021 - 0.104 \cos(2.18\, A^{1/3} - 1.25) \qquad (1)$$

and

$R = r_o A^{1/3}$, $r_o = 1.4$ fm , $\lambda = 1.22\,(A+1)/A$.

In terms of the same model that systematic has been extended to elastic and nonelastic scattering by Angeli and Csikai /7/. However, Flerov and Talyzin /3/ had obtained

$$\sigma_{nX} = \pi(0.12\, A^{1/3} + 0.21)^2 \qquad (2)$$

corresponding to the black nucleus formula

$$\sigma_{nX} = \pi(R\,(A) + \lambda)^2.$$

Fig. 2
Mass systematics of nonelastic cross section σ_{nX} at 14 MeV(taken from ref. /3/).

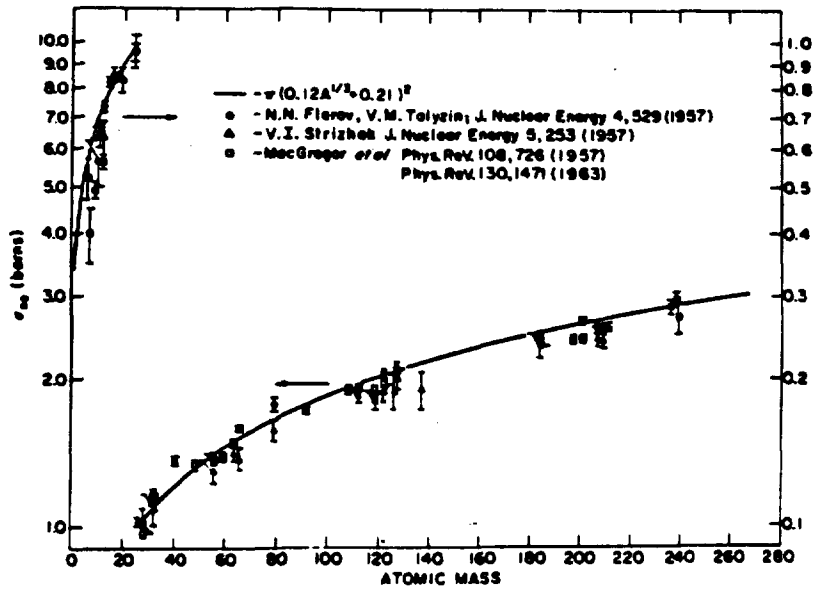

On the other hand, cross sections for neutron-induced reactions clearly show isotopic effects represented more pronounced by the (N-Z)-dependence. Such (N-Z)-dependences have been observed by Pearlstein /8/ and Hankla /9/ for neutron emission and Csikai / Petö /10/ and Qaim /11/ for (n,2n) resulting in

$$\tilde{\sigma}_{nM} = \begin{cases} \tilde{\sigma}_{nX} \left(1 - 1.764 \exp\left(-18.14 \left(\frac{N-Z}{A}\right)\right)\right) & /8/ \\ \tilde{\sigma}_{nX} \,/\left(1 + 11.5 \exp\left(-32.5 \left(\frac{N-Z}{A}\right)\right)\right) & /9/ \end{cases}$$

and

$$\tilde{\sigma}_{n,2n} = 61.6 \left(A^{1/3}+1\right)^2 \left[1 - 1.319 \exp\left(-8.744 \frac{(N-Z)}{A}\right)\right] \quad /10,11/$$

correspondingly and shown in fig. 3.

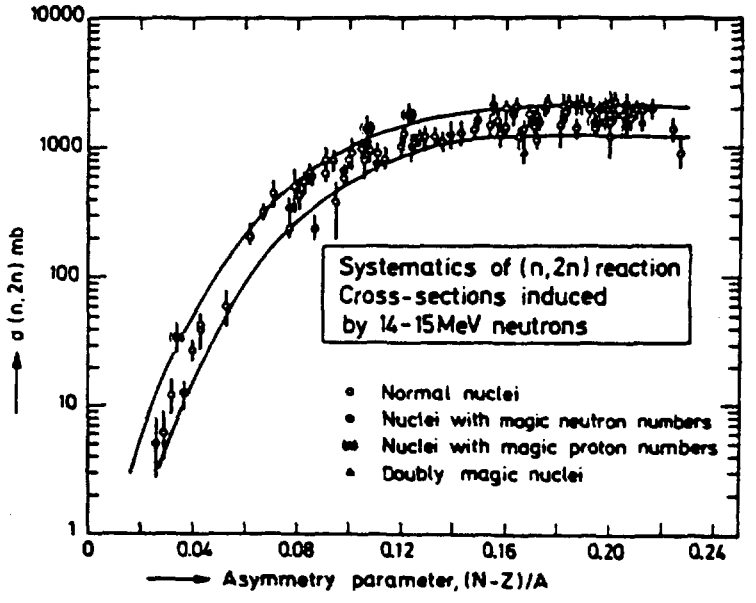

Fig. 3
(N-Z) systematics of cross section for (n,2n) reactions at 14 MeV (taken from ref. /11/).

A carefully study of such regularities (for (n,2n) known as Csikai-Petö effect) has been carried out by Bödy / Csikai /12/ and Holub / Cindro /13/. Also at very early times the systematics of (n,z) reactions have been compiled. For (n,p) some authors received

$$\tilde{\sigma}_{n,p} = 45.2 \left(A^{1/3}+1\right)^2 \exp\left(-33 \frac{(N-Z)}{A}\right) \text{ mb} \quad /5/ \qquad (3)$$

or

$$\log_{10}\left(\frac{\tilde{\sigma}_{n,p}}{mb}\right) = 0.2 + 0.4\sqrt{A} - 4.6 \frac{(N-Z)}{A^{2/3}} \quad /14/. \qquad (4)$$

Whereas for more complex particles following formulae are available

$$\tilde{\sigma}_{n,t} = \begin{cases} 4.52 \left(A^{1/3}+1\right)^2 \exp\left(-10 \frac{(N-Z)}{A}\right) \text{ /ub} & /15/ \qquad (5) \\ 7.684 \left(A^{1/3}+1\right)^2 \exp\left(-13 \frac{(N-Z)}{A}\right) \text{ /ub} & /16/ \qquad (6) \end{cases}$$

$$\tilde{\sigma}_{n,^3He} = 0.54 \left(A^{1/3}+1\right)^2 \exp\left(-10 \frac{(N-Z)}{A}\right) \text{ /ub} \quad /15/. \qquad (7)$$

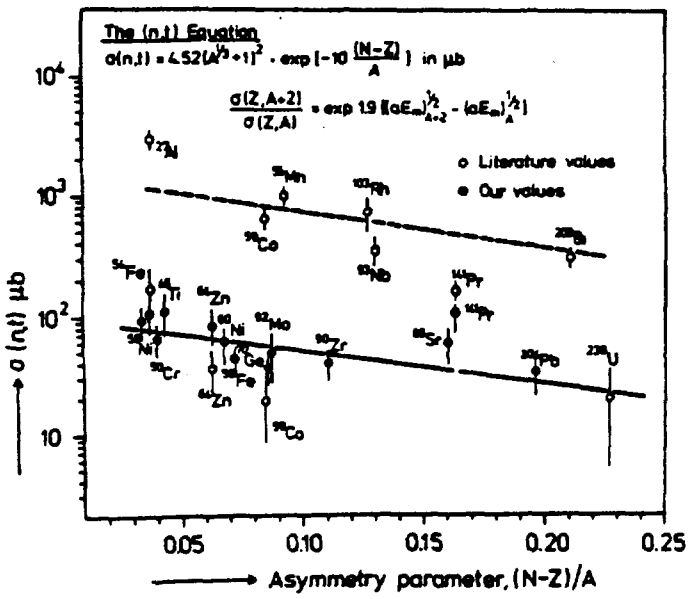

Fig. 4
(N-Z) systematics of cross sections for (n,t) reactions at 14 MeV (taken from ref. /15/).

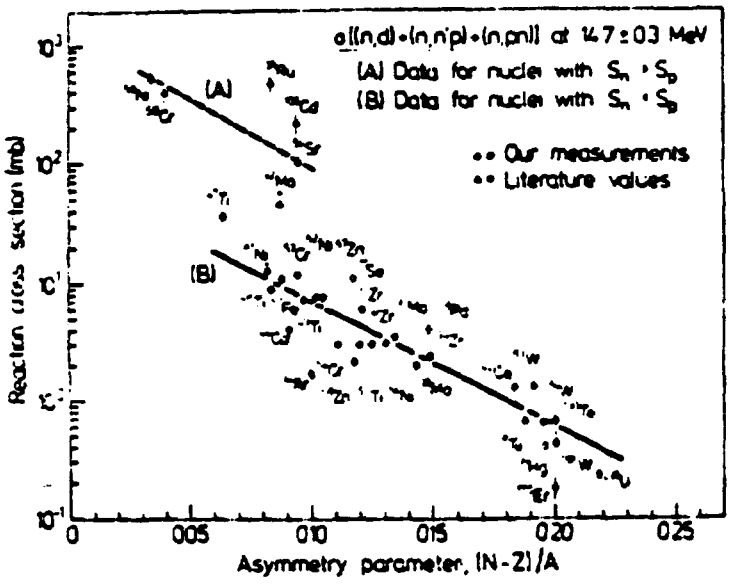

Fig. 5
(N-Z) systematics of cross sections for (n,d), (n,pn) and (n,np) reactions at 14 MeV (taken from ref. /15/).

Furthermore, analogous formulae have been obtained for (n,α), (n,d), (n,np) and (n,pn) reactions by Qaim /15/(see figs. 4 and 5).

Excellent review papers have been published by Csikai /2,17/ and Bychkov et al. /18/.

2.1.2. Problems of application of empirical formulae

Any empirical formula has a "Janus-head" including advantages and drawbacks.

As advantages we assume:

(i) a very quick but rough prediction of unmeasured cross sections (integrals only);
(ii) test of mass dependences of models more theoretically refined.

The formulae will be limited by
(i) their range of validity in the range $A \gtrsim 30$ and $Z \gtrsim 20$;
(ii) failure to extrapolate to $N-Z \to 0$.

These limitations restrict the application of empirical formulae for medium and heavy nuclei mainly. In contrast, the (n,z)-cross sections are competing with neutron scattering and reaction data for light nuclei especially.

But in this limitations, equations 1 to 7 (and other one not mentioned here) can really be used to estimate unknown cross sections with an accuracy of about an order of magnitude or better.

2.2. Derivation of semi-empirical models

The (N-Z)-dependence of reaction cross sections at 14 MeV has been derived easily from the statistical model introducing the constant-nuclear-temperature approximation for level densities and a semi-empirical mass formula /18,19/. In addition, some empirical equations (partly for re-normalization) have to be applied.

Such simple models have been also used at other energies than 14 MeV.

One of the best-known example of such extensions is Pearlstein's formalism /20/ for the computer code TRESH.

The concept of interpretation of 14 MeV data by underlying theoretically founded models has been widely used in the early seventees. Besides the crude Evaporation Model, more refined Preequilibrium Models became available.

A large body of 14 MeV data for (n,n') /21/, (n,p) /22/, (n,α) /23/ and (n,2n) /24,25/ have been analyzed to investigate contributions of pre-equilibrium particle emission and to fix some free parameters of the models.

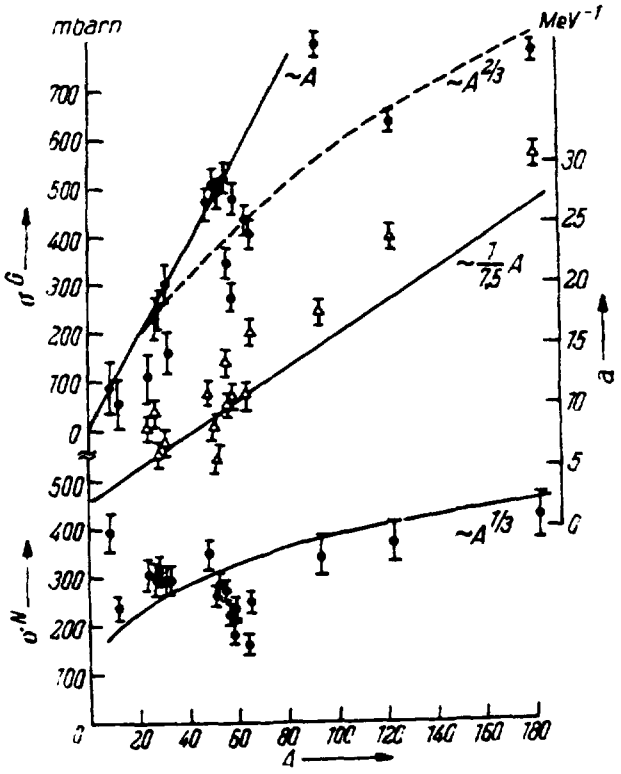

Fig. 6
Mass dependences of parameters a, $\tilde{\sigma}^G$ and $\tilde{\sigma}^N$ for parametrization of energy spectra of inelastically scattered 14 MeV neutrons (taken from ref. /26/).

Fig. 7
Example for application of parametrization of the energy spectrum of neutrons emitted from ^{93}Nb+n at 14 MeV (taken from ref. /27/).

Also differential cross sections (particle spectra) could be interpreted in terms of an incoherent superposition of Equilibrium and Pre-equilibrium Models. So, the neutron spectra from inelastic scattering at 14 MeV can be well understood within the simple ansatz /26/

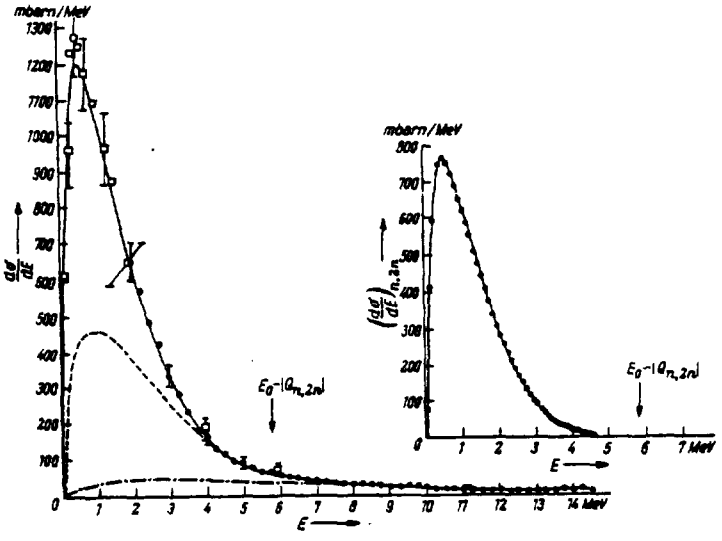

$$\frac{d\tilde{\sigma}_{n,n'}}{dE'} = \tilde{\sigma}^G(E') + \tilde{\sigma}^N(E') \qquad (8)$$

and $$\sigma^{G}(E') = K_1 E' \sigma^{inv} \exp(2\sqrt{aU})/(U+T)^2$$

$$\sigma^{N}(E') = K_2 E' \sigma^{inv} \sum_{n=3,5,7} n(n-1)\left(\frac{U}{E'}\right)^{n-2}$$

The constants K_1 and K_2 have been fitted over a broad range of nuclear masses (see fig. 6). This method has been successfully applied also for description of secondary neutron emission from (n,2n) /27/. This is shown in fig. 7.

2.3. Theoretically founded models

One of the fundamental problems attacked by theoretical nuclear physics is the investigation of the nuclear reaction mechanism. An exact solution is equivalent to the treatment of the time-dependent Schroedinger-equation for many-particle systems.

Obviously, any practicable solution can only be obtained by more or less stringent and decisive simplifications. According to the approximations applied different models can classified into three groups

(i) statistical treatment of the many-body problem by thermodynamical methods (Evaporation Model (EM), Hauser-Feshbach Model (HFM)) including Monte-Carlo Simulation of intranuclear processes (MM);

(ii) statistical treatment of the many-body problem including relaxation processes within the nucleus (Pre-equilibrium Models (PEM), in several formalisms of Exciton Model, Hybrid Model, Master-Equation Approach, Monte-Carlo Methods);

(iii) reduction of the many-body problem into a two-body problem by introduction of an effective nuclear potential and possible residual (disturbing) interactions (Optical Model (OM), Direct Reaction Models (PWBA, DWBA, CCBA)).

However, recently there are several attempts for derivation of unified models /28,29/. As first practicable applications we should mention encouraging results of the Generalized Exciton Model (GEM) as well as formulation of Multi-Step-Direct (MSDR) and Multi-Step-Compound Reaction Models (MSCR).

More detailed considerations of the theoretical background of the models should be taken from review papers (also in this symposium) or standard text books.

In the present paper, more attention should be paid to computer codes basing on theoretical models.

3. Review on computer codes for neutron nuclear data calculation

3.1. Remarks on relations between theoretical formalisms and their applicability by convenient numerical methods

There is a well-known fact in quantum mechanics and nuclear physics for a time-delay between derivation of formal solutions of fundamental problems and their numerical treatment, which is often hindered by inadequate numerical methods and by limitations of computers in operational speed and/or memory capacity.

Also for nuclear reaction models and computer codes related with them some examples are given in table 1.

Table 1: Delay between derivation of a theoretical solution and its application in terms of rigorous, convenient or fast numerical methods.

Formalism/ Model	Derived by/ Year	Numerical method by / Year	Computer code by/ Year
Hauser-Feshbach Model (HFM)	W. Hauser H. Feshbach /30/ 1952	calculation of T_{lj} by Optical Model (OM)	ABACUS E.H. Auerbach /31/ 1964
Exciton Model (PEM)	J.J. Griffin /32/ 1966	transformation of the set of coupled differential equations (Master-equations) by an algebraic set of equations J. Dobeš/E. Betâk /33/ 1977	AMALTHEE O, Bersillon, L. Faugere /34/ 1977
Multi-Step-Direct-Reactions (MSDR)	T. Tamura,1977 et al. /35/ H. Feshbach et al. /28/ 1980	first attempts by R. Reif /36/ 1976, I. Kumabe /37/1980, R. Bonetti /38/1981	first attempt by ORION-TRISTAR-1 T. Tamura T. Udagawa M. Benhamou /39/ 1983

Table 1 clearly reflects the fact that an access to fast and big computers is a necessary condition but not the only one. This is confirmed by the first attempts to solve MSDR-formalisms on computers. Although adopting additional simplifying assumptions the calculations consume such a lot of computer time that only a very few examples have been investigated up to now /37,38/. On the contrary, the results can be regarded of only formal value for further discussions.

In theoretical nuclear physics, a rapid progress is hindered by the computer generation presently installed with wide dessimination and can be overcome with supercomputers of the CRAY-1 or analogous types only.

Nevertheless, a great variety of computer codes for a wide range of applicationsis available in nearly free exchange.

3.2. Compilation of well-known computer codes for nuclear reaction models

On this subject several excellent and comprehensive reviews have been given by Benzi /40/, Prince /41/ and Young /42/ in the past. This paper will only include some most recent codes which became presently available.

Generally, the abbreviations given in section 2.3 are used. Additionally following terms are introduced in tables 2 to 4:

MPE...Multi-Particle-Emission
DC....Direct capture
F.....FORTRAN
K.....Kilobyte
CPL...Computer Program Library, Belfast
NEA-CPL..Computer Program Library of NEA Data Bank, Saclay

Table 2: Optical Model codes

Code/Year	Authors	Remarks on Formalism	Language/size	Availability
SCAT 1961	M.A. Melkanoff J.S. Nodvik D.S. Saxon D.G. Cantor		F	NEA-CPL
SMOG 1963	V. Benzi F. Fabbri A.M. Sarnis		F	NEA-CPL
GENOA 1975	F.G. Perey	parameter search	F 270 K	author
CERBERO 1977	F. Fabbri G. Fratamico G. Reffo		F 240 K	NEA-CPL

CRAPONE 1977	F. Fabbri	local, non-local potentials	F	NEA-CPL
RAROMP	G.J. Pyle	reformulated op. potential, search	F 32 K	author

Table 3: Statistical Model computer codes.

Code/Year	Authors	Remarks on Formalisms	Language/Size	Quantities $\frac{d\sigma}{d\Omega}$	$\frac{d\sigma}{dE}$	$\frac{d^2\sigma}{d\Omega dE}$	Availability
ABACUS 1964	E.H. Auerbach	HFM+ OM	F 32 K	X	-	-	NEA-CPL
NEARREX 1964	P.A. Moldauer S. Zawadski	HFM+ OM	F 55 K	X	-	-	NEA-CPL
SASSI 1967	V. Benzi F. Fabbri L. Zuffi	HFM	F	X	-	-	NEA-CPL
FISPRO 1969	V. Benzi G.C. Panini G. Reffo	HFM (for f^1's) DC	F 13 K	-	-	-	NEA-CPL
STAX 1970	Y. Tomita	HFM+ OM	F	X	-	-	NEA-CPL
COMNUC 1970	C.L. Dunford		F				NEA-CPL
CASCADE 1970	C.L. Dunford		F				NEA-CPL
NNTC	R.C. Alsmiller T.A. Gabriel	EM MM (intran. cascade)	F	X	X	X	RSIC
THRESH 1971	S. Pearlstein	EM	F 12 K	-	-	-	NEA-CPL

ELIESE 1972	S. Igarasi	HFM+ OM	F 80 K	X	-	-	NEA-CPL
OVERLAID ALICE 1975	M. Blann	EM+ MPE+ PEM	F 180 K	- -	X	-	author
STAPRE 1976	M. Uhl B. Strohmaier	HFM+ MPE+ PEM	F 400 K	-	X	-	NEA-CPL
ERRINNI 1977	F. Fabbri G. Reffo	HFM+ MPE	F 240 K	-	-	-	NEA-CPL
GNASH 1977	P.G. Young E.D. Arthur	HFM+ MPE+ PEM	F	-	X	-	NEA-CPL
TNG 1977	C.Y. Fu	HFM+ MPE+ PEM	F 300 K	X	X	X	NEA-CPL
AMALTHEE 1977	O. Bersillon L. Faugere	GEM	F 440 K	-	X	-	NEA-CPL
HAUSER 1978	F. Mann	HFM+ MPE+ PEM	F 170 K	X	X	X	NEA-CPL
MODESTY	M. Matthes	HFM+ MPE	PL/1 130 K	-	X	-	NEA-CPL
HELGA	S.K. Penny	HFM+ OM	F 740 K	X	-	-	
PRECO	C. Kalbach	PEM	F 20 K	-	X	X	author
PREANG 1979	J.M. Akkermans H. Gruppelaar F.J. Luider	GEM	F 1600 cards	-	X	X	NEA-CPL

EMPIRE 1980	M. Herman A. Marcinkowski	HFM+ MPE+ PEM	F	-	X	-	author
PREM 1982	S. Koshita G. Keeni	EM+ MPE+PEM	F	-	X	-	NEA-CPL
PEQGM 1983	E. Beták J. Dobeš	EM+ MPE+ PEM (for A's)	F	-	X	-	authors
ALAPRE 1983	H. Kalka D. Hermsdorf	GEM	F	-	X	X	author

Table 4: Direct Reaction Model Codes.

Code/ Year	Authors	Formalism	Remarks on Language/ Size	Quantities $\frac{d\tilde{\sigma}}{d\Omega}$	$\frac{d\tilde{\sigma}}{dE}$	$\frac{d^2\tilde{\sigma}}{d\Omega dE}$	Availability
JULIE 1962	R.H. Bassel R.M. Drisco C.R. Satchler	DWBA	F 500 K	X	-	-	NEA-CPL
TWO PLUS 1966	C.L. Dunford	DWBA	F	X	-	-	author
JUPITOR 1967	T. Tamura	CCBA	F 72 K	X	-	-	NEA-CPL
DIRCO 1971	F. Fabbri G. Longo F. Saporetti	DC	F	X			author
DWUCK 1978	P. Kunz	DWBA	F	X	-	-	NEA-CPL
CHUCK 1978	P. Kunz	CCBA	F	X	-	-	NEA-CPL

LOLA	R. de Vries	DWBA (finite range)	F	X	-	-	author
ECIS (1968) 1979	J. Raynal	CCBA+ OM (de-formed p.)	F 14 250 cards	X	-	-	NEA-CPL
ORION-TRISTAR-1 1983	T. Tamura T. Udagawa M. Benhamou	MSDR (one step only, zero range approx.)	F 20 224 words	X	X	X	CPL

Of course, such a compilation must be incomplete because of lot of computer codes are not available or the reviewer is'nt aware of their existence.

3.3. Remarks on computer code statistics and availability

Interpreting tables 2 to 4 we can found that FORTRAN is the mostly applied computer language in nuclear physics. This is in total agreement with Brainerd's opinion that a higher level language must remain an efficient tool for producing results /43/.

However, this doesn't negotiate the appearance of any new slang or modification of high-level computer language in physics (FORTRAN-77, PASCAL) in the nearest future.

The sizes of codes are in general in the order of 100 to 300 Kbyte (partly with overlay structure).

The computer times necessary for calculations strongly depents on the example and the computer used and cannot be compared directly.

Nearly all codes are available from the computer program library at the NEA Data Bank, Saclay. It is the policy of this NEA-DB to serve any customer with the tested source deck and an example run of any code stored in the CPL. The scope of CPL is in steady development and will reviewed by a Newsletter regularly issued by the NEA Data Bank /44/

From such a great variety of different codes for a very limited class of tasks two problems arise for authors and users:

(i) to ensure the consistency of different codes for one problem;
(ii) to choose the most adequate code for a special aim.

This aspects have to be discussed in the next sections.

3.4. Nuclear Model codes intercomparison

As stated in the preceding section, there are several codes for calculation of cross sections basing on the same model. Nevertheless, significant differences may arise from numerical methods applied. Also the conversion of codes from one computer typ to another can result in deviations in the calculations. Stronger deviations will occur if other physical constants or models are used for calculations.

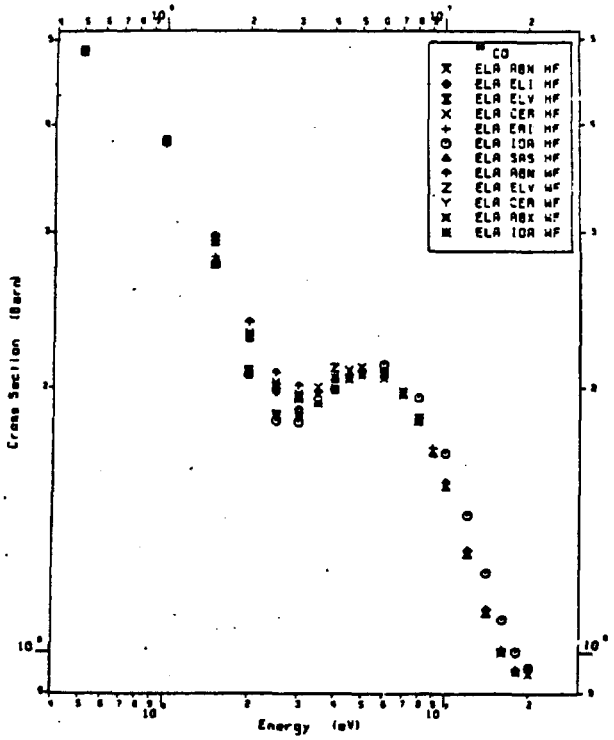

Fig. 8
Comparison of calculations of elastic scattering cross sections obtained by use of different codes (taken from ref. /46/).

So, code intercomparisons have to be carried out in two steps:

(i) comparison of codes basing on the same formalism;
(ii) comparison of codes basing on different formalisms but using a consistent set of physical constants ("benchmark" calculations).

Internal (laboratory) code comparisons have been carried out in an early stage already in CNEN Bologna /40,45/, in LLL and LASL /42/ as well as in BNL /41/. An overall agreement of ≤ 5 % have been obtained from typ (i) intercomparisons /42/. (Such errors are within the experimental uncertainties!).

At present a series of typ (ii) intercomparisons have been stimulated by the NEA-CPL on an international level. Results for a benchmark calculation of reaction cross sections for ^{59}Co by Spherical Optical Mo-

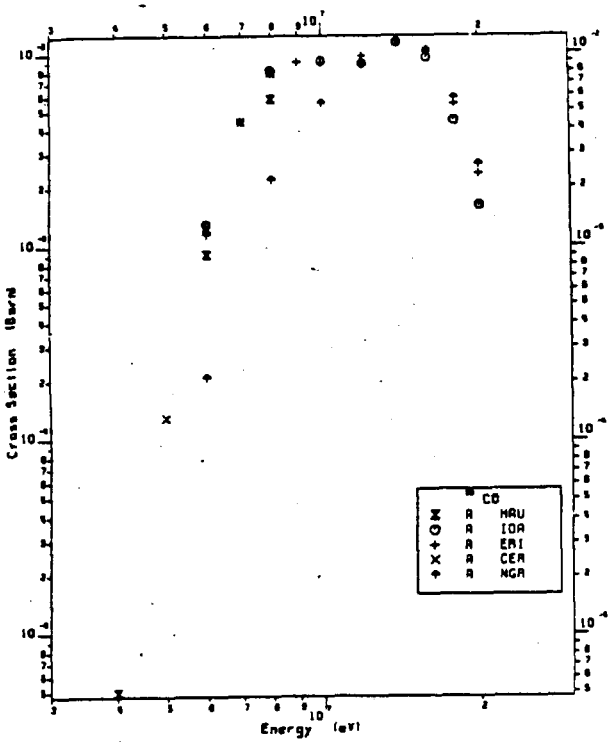

Fig. 9
Comparison of calculations of (n,α) cross sections obtained by use of different codes (taken from ref. /46/).

dels and Statistical Models including pre-equilibrium effects were published recently by Prince, Reffo and Sartori /46/. An analoguos project including formalisms for calculations of double differential cross sections in the frame of Pre-equilibrium Models (GEM) initiated by Nagel and Gruppelaar /47/ is underway. Finally, a Spherical Optical Model code comparison for charged particles is announced by Hodgson /48/. In all three cases proposed stronger discrepancies are expected. Especially, this is true for cross section calculations for γ, charged particle and multi-particle emission. Some examples are shown in figs. 8 to 10.

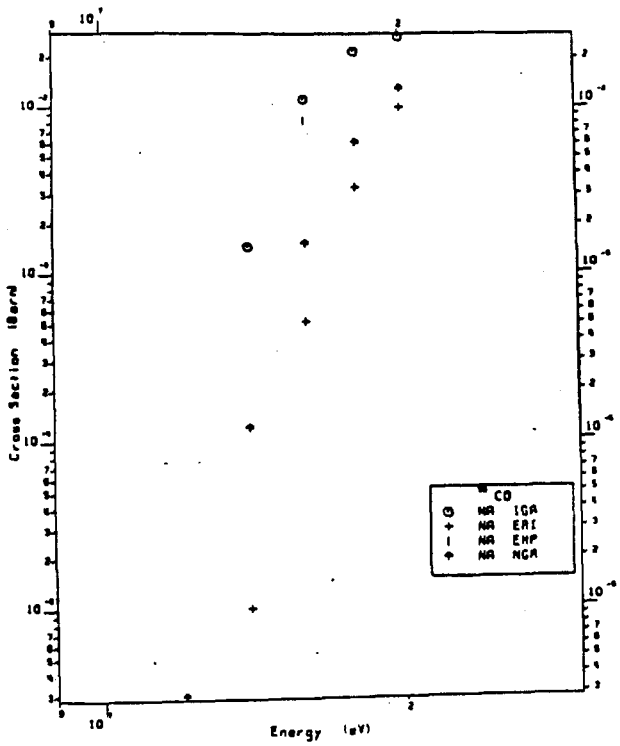

Fig. 10
Comparison of calculations of (n,nα) cross sections obtained by use of different codes (taken from ref. /46/).

It is of high interest for future developments to analyze possible reasons for discrepant results by examining

- computer used;
- physical limits adopted (e.g. R_{max}, l_{max}, etc.);
- numerical methods;
- fundamental constants

etc.

3.5. Recommendations for the choice of appropriate codes

The availability of quite different codes via a computer program library (NEA-CPL, LASL Code Centre, RSIC etc.) makes the decision met by non-experienced physicists or engineers difficult.

All arguments concerning

(i) the adequacy of the code to treat the problem under discussion (reaction type, energy range, reaction mechanism etc.);

(ii) the portability of the code (original computer, speed and memory size of computer aimed to run the code, versions of original language, effectivity of compiler, peripheral devices etc.);

(iii) the compatibility with other codes existing (modular technique, combination of codes, consistency of input parameters etc.)

should be proved very carefully before an adoption of any computer code.

4. Some problems of application of nuclear model codes around 14 MeV

4.1. Basic physical problems

The application of any nuclear reaction model at 14 MeV neutron incidence energy should be done very cautious because that energy is really an intermediate one. That means

(i) the number of reaction channels involved is not sufficient for a statistical description at least for light nuclei or for some residual nuclei
but
this number is in all cases to high for an individual description.

This is equivalent to the fact that

(ii) competing reaction mechanisms including interference effects have to be expected.

Therefore, to achieve a reasonable agreement with experiments

(iii) different reaction models have to be applied including a consistent set of nuclear parameters.

These three general conditions imply the application of computer codes which take into account correct normalization conditions by

- matching the individual (discrete) level statistics to a level density formula;
- consideration of all competing reaction channels including charged particle and γ-ray emission;
- reduction of compound nucleus formation cross section by non-statistical energy release in every stage of a nuclear reaction;
- consideration of possible channel enhancements or strong channel coupling in direct reaction modes.

Up to now, there is nearly no computer code which fulfills those pretensions simultaneously. If any code takes into account the necessary normalization conditions partially then the problem arise that any other code which has to be used for supplementary calculations must base on the same nuclear parameters for consistency.

Repeating the statement given in the preceding section, the choice of a set of computer codes among a great variety offered should be guided by a unique parameter set the codes relying on.

4.2. Remarks on a procedure to adjust a consistent set of parameters for application of nuclear reaction models

In fig. 11 a system is shown which demonstrates a combination of different reaction models using an as consistent as possible set of parameters adjusted by well-established experimental and basic physical data. In such a procedure, also 14 MeV data are of great importance keeping in mind the lot of experimental investigations concerning differential and double differential cross sections for all kinds of particles and γ's which are mostly sensitive against parameter changes in the frame of different models.

4.3. Remarks on most crucial parameters in nuclear model calculations

4.3.1. Optical Model parameters and related quantities

In accordance with the parameter flow shown in fig. 11 the preparation of reaction model calculations starts from the OM studies.

Input/Output data	Adjusted parameters	Additional parameters	Model
σ_{nT}, σ_{n,n_0} (Θ)	optical.pot. parameters for n, p, α, d ...	compilations (standard pot., strength func.)	optical model (spherical-deformed, local-non-local)
	↓ transmission coefficients, inverse cross sections		
σ_{n,n_i}, $\sigma_{n,p}$, $\sigma_{n,\alpha}$, $\sigma_{n,d}$, $\sigma_{n,2n}$, $\sigma_{n,n'\gamma}$ ang. distrib., particle and γ-spectra	level densities (a, Δ)	compilations (a, Δ, J) level schemes binding energ. $\overline{\Gamma_\gamma}$, branchings GDR-param.	Hauser-Feshbach inclusive - level continuum - multi-step - γ-deexcitation
deviations ↕ (non-statistical effects)			
$\sigma_{n,n_i}(\Theta)$, σ_{n,α_i}, σ_{n,p_i} ang. distrib. spectra of high-energetic particles and γ's	S_L, $S_\nu \lvert M \rvert^2$	spectroscop. informations (S_L, $S_\nu \lvert M \rvert^2$) single-particle structure	Pre-equilibr. models DWBA CCBA

Fig. 11: Flow chard for nuclear model parameter adjustment procedure (taken from ref. /59/).

Generally, neutron optical potentials are known for a wide energy range from some 100 keV to tens of MeV. Any parameter search can proceed from

as well as standard potentials or best-fit parameters obtained in preceding investigations.

A very comprehensive compilation of individual (best-fit) parameter sets has been carried out by Perey and Perey /50/.

On the other hand, well-substantiated standard potentials valid for definite energy and/or mass ranges have been derived by several authors. For application at 14 MeV the parameters found by Holmqvist and Wiedling /51/, Becchetti-Greenless /52/ or Rapaport et al. /53/ may be recommended. Such standard potentials are of the spherical type $V_{opt}(r)$ usually. If any other type of optical potential seems desirable convenient OM-codes have to be runned for parameter search. A search procedure should be performed according to the "SPRT-Method" proposed and successfully used by Delaroche et al. /54/ especially for determining of parameters of non-spherical (deformed) potentials $V_{opt}(r, \Theta, \varphi)$ necessary for DWBA or CCBA calculations.

Parameter searches can be done by computer codes ELIESE, GENOA, ECIS etc. at a very different level of Optical Model type, automatization and accuracy. However, any parameter set obtained according to a minimizing technique is ambigeous. From such studies results a supplementary behaviour of potential strength and radial dependences. Therefore, non-local effects has been assumed in optical potentials to simulate the finite size of the incidence particles and dispersive properties of the nucleus.

In studying such ambiguouities from inter-relation-ship between various potential parameters derived from multiparameter search already H. Feshbach /55/ proposed in 1958 the use of the volume integral

$$J = \int V(\bar{r})\, d\bar{r} \qquad (3)$$

including contributions from the well depths along with the geometry. This results in the Reformulated Optical Model by folding with nucleon and matter distribution in the target nucleus. Such a procedure is realized in the code RAROMP.

The folding model concept is not fully tested up to now. However, it constitutes a rather meaningfull approach to parametrizing the Optical Model not only for neutrons and protons but also for composite projectiles as found by Jackson /56/ and Hodgson /57/. Predictions of more reliable potentials for d, t, ^{3}He and α's may be expected in the future.

The most important quantities related to the OM are transmission coefficients T_{lj} and inverse cross sections normally obtained from Optical Model calculations.

A lot of different statistical model codes are based on predetermined (taken as input data) quantities T_{lj}, $\bar{T}_l$ or σ^{inv} for every kind of incident or emergent particles. Keeping in mind the equation

$$\sigma^{inv} = \pi\lambda^2 \sum_{l=0}^{\infty} ((l+1)\, T^{+}_{lj} + l\, T^{-}_{lj}) \qquad (9)$$

the relation between Optical Models and those quantities are immediately visible.

But also the descrepancy can be obviously seen. The OM is determined from the elastic scattering of any particle (including the ground state U=0 only).

Contrary, the inverse cross section is needed for excitation energies $U > 0$. To solve the question of simplification of $\sigma^{inv}(E,U)$ by $\sigma^{inv}(E,U=0)$ and their influence on calculations in the frame of statistical models some new approaches has been introduced by Ignatyuk et al. /58/.

4.3.2. Nuclear level density formulae

Most of the computer codes reviewed in the preceding section 3. use different models to describe the nuclear level density.

Sometimes, codes implies two (or three) different models simultaneously (i.e. model of constant nuclear temperature, Fermi-Gas-Model, Back-Shifted-Fermi-Gas-Model, Superconductivity Model) for a convenient representation of the well-established dependence of level density on the excitation energy U.

Prospects for better level density models are now under wide discussion and experimental as well as theoretical investigation. One of the most substantiated proposals have been made by Ignatyuk et al. /59,60/ taking

$$a(U) = \tilde{a}\,(1 + f(U)\,\frac{\tilde{W}}{U}). \qquad (10)$$

In this ansatz a converges to $\tilde{a}$ for $U \to \infty$ and to $a = \text{const} \leq a$ for $U \to 0$. The energy dependence is described by

$$f(U) = 1 - \exp(-\gamma U). \qquad (11)$$

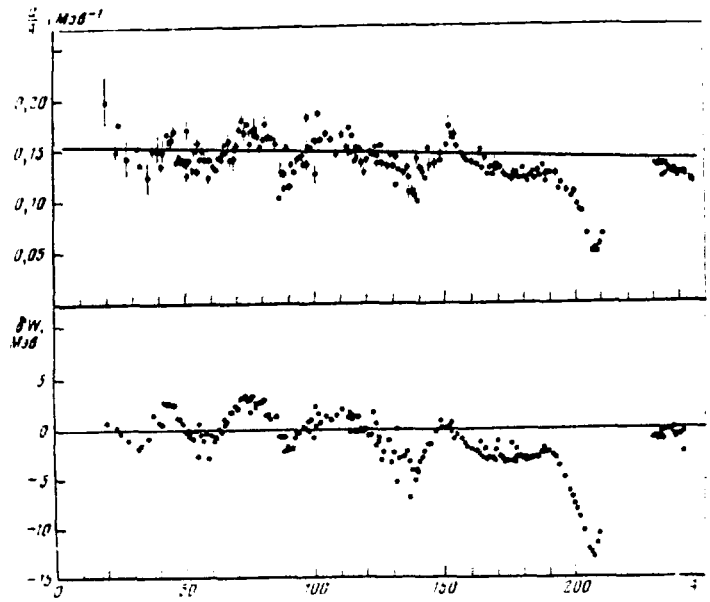

Fig. 12
Mass systematics for nuclear level density parameter a/A and the related quantity δW used in Ignatyuk's semi-empirical formula for the energy dependence a(U) (taken from ref. /59/).

Equation (10) simulates the shell effects obtained experimentally in the level density parameter a. From theoretical considerations such effects should be reduced with increasing energy U resulting in ansatz (11). The magnitude of the influence of nuclear shells is expressed in terms of δW by

$$\delta W = M_{exp} - M_{LDM}\,(Z,\ A, \varepsilon) \qquad (12)$$

using the difference of experimentally determined nuclear masses and their prediction by the Liquid-Drop-Model (LDM) in dependence on mass number Z, mass A and the ground state (static) deformation parameter ε. Values of δW can be easily gotten from a compilation /61/. This dependence can also be seen in fig. 12.

From inspection of the experimental data base the constants used in these equations are in the order of

$$\tilde{a} = \begin{cases} (0.154A - 3\cdot10^{-5}\ A^2)/\mathrm{MeV} & /59/ \\ (0.094\ A)/\mathrm{MeV} & /60/ \end{cases} \qquad (13)$$

and

$$\gamma = \begin{cases} 0.064/\mathrm{MeV} & /60/ \\ \tilde{a}/0.4\ A^{4/3} & /62/. \end{cases} \qquad (14)$$

Other, slightly different approaches have been reviewed some years ago by Ramamurthy /63/.

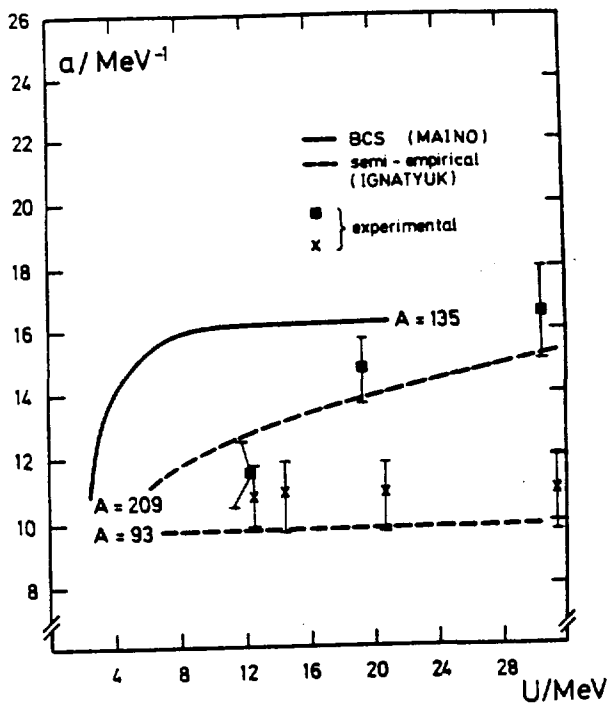

Fig. 13
Examples of energy dependence a(U) obtained from experiments (ref. /64/), semi-empirical formula (ref. /60/) and purely from BCS calculations (ref. /65/).

Basing on most recent results derived from an analysis of differential neutron emission cross sections the dependence of a over U has been proved as well as experimentally /64/ and pure theoretically adopting the BCS-Model /65/ and the Semi-Empirical Model of Ignatyuk et al. /60/.

Some results for different nuclei are shown in fig. 13.

4.3.3. Strengths of collective enhancements in Direct Reaction Models

The cross section for excitation of an individual state f is given by

$$\frac{d\sigma_f}{d\Omega} = \hat{\sigma}(\Theta)\, S_f \qquad (15)$$

if the DWBA-Method is applied. Whereas $\hat{\sigma}(\Theta)$ represents the angular distribution of reaction products, the spectroscopical factor S_f carries all information on the structure of the excited state.

According to the approach to be made for calculation of S_f different Direct Reaction Models can be characterized.

In terms of the Collective Model equation (15) is developed to read

$$\frac{d\hat{\sigma}}{d\Omega} = \sum_{\lambda\mu} \Big| \sum_{ll'} C^{\lambda\mu}_{ll'}(\Theta) \int_0^\infty U_{l'}(r)\, U_l(r)\, F_\lambda(r)\, r^2 dr \Big|^2 \qquad (16)$$

where $C^{\lambda\mu}_{ll'}$, ... Kinematical coefficients

U_l, $U_{l'}(r)$... Radial parts of Optical Model wave functions for incidence and emitted particles

$F_\lambda(r)$ ...Formfactor for collective excitation derived for a multipolarity λ .

Generally a phenomenological approach is used for F_λ by introducing

$$F_\lambda(r) = \frac{\beta_\lambda}{\sqrt{(2\lambda+1)}} R_o \frac{d}{dr} V_{opt}(r) \qquad (17)$$

with β_λ ...parameter for dynamical deformation of the excited state
V_{opt}..optical potential.

From this, for calculation of DI contributions to reaction cross sections the knowledge of the spectral distribution of the amplitude β_λ of one-phonon transitions in the whole range of excitation energy is necessary. The determination of deformation parameters is a very complex problem. There is no general solution up to now. Some values can be obtained from the excitation of lowest-lying levels (β_2 for 2_1^+ levels) derived from (p,p') or (e,e') experiments.

In a more microscopical approximation of equation (15) we get

$$\frac{d\sigma_f}{d\Omega} \sim \sigma(\Theta)\ S\ (\text{target})\ S\ (\text{projectile})\ D_o^2 \qquad (18)$$

using spectroscopical factors for the target and the projectile and an interaction strenght D_o in zero or finite range approach.

Also in that approach the model parameters are not quite well substantiated by experiments or predetermined in terms of other models.

Especially, any uncertainty in D_o will strongly influence the relative importance of contributions from different stages m of MSDR in accordance

$$\left(\frac{d\sigma}{d\Omega}\right)_{MSDR} \sim \sum_m D_o^{2m} \ . \qquad (19)$$

However, for a more powerful use of Direct Reaction Model calculations for cross section prediction a better knowledge of parameters of the internal nuclear structure is necessary.

4.3.4. Some other important parameters

In addition to that said above, some other important quantities appearing as model parameters should be mentioned. Among several, the γ-ray strength function is one of the most interesting. Considerable progress

towards determination and prediction of their values has been achieved through the last years.

5. Summary and conclusions

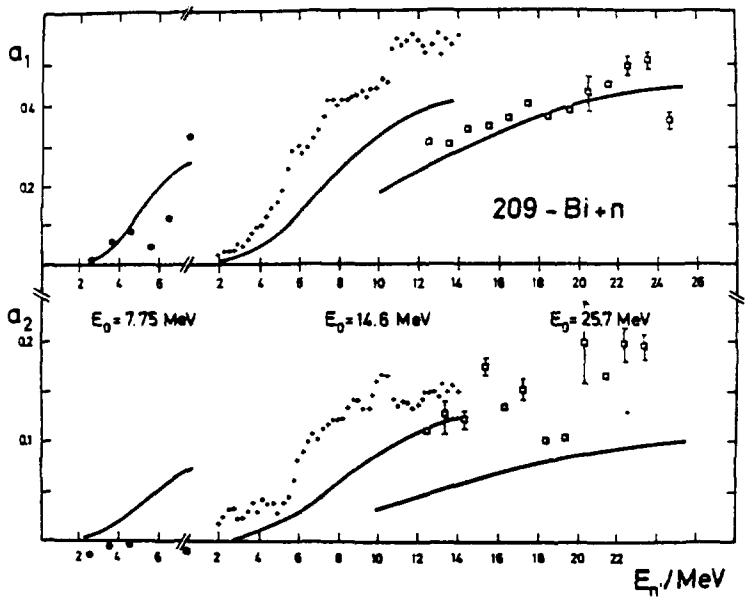

Fig. 14
Relative Legendre coefficients a_1/a_o and a_2/a_o for description of double differential cross sections for ^{209}Bi (taken from ref. /64/).

Fig. 15
Energy spectrum of inelastically scattered neutrons from ^{209}Bi (taken from ref. /64/).

In the summary some results will be given to demonstrate the progress made during the last decade as well as to show problems for future work. Dealing with neutron-induced production of all kinds of particles examples for neutrons, charged particles and γ-quanta can be choosen to prove short-comings and failures of the models applied.

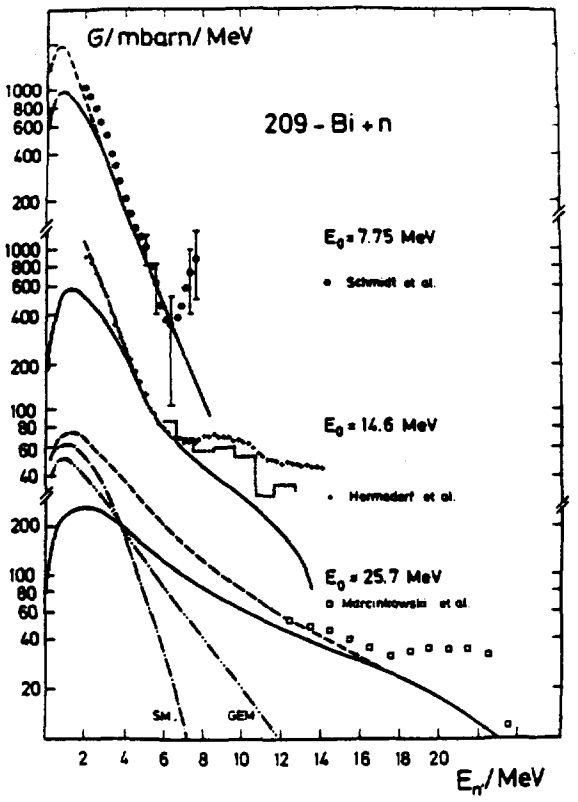

(i) Neutron emission

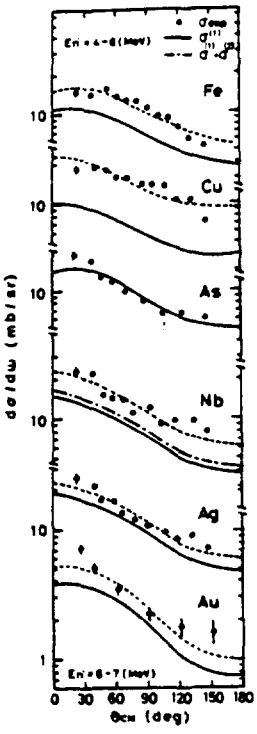

Comparison of the calculated with the experimental angular distributions of the cross sections integrated over 4 MeV bins in $E_{n'}$ = 4–8 MeV except for Au ($E_{n'}$ = 6–7 MeV). The solid and dot–dashed curves present the one-step and two-step cross sections, respectively. The dashed curves present fits to the experimental data for ready comparison.

Fig. 16
Results of MSDR calculations for 14 MeV neutron inelastic scattering on ^{93}Nb (taken from ref. /37/).

Very encouraging results for description of double differential data at 14 MeV have been obtained using the GEM /64/. In general, the relative Legendre coefficients a_1 and a_2 can be predicted in surprinsingly good agreement with experiments (see fig. 14). For a consistent description of the energy spectrum contributions from collective reaction modes not included in GEM have to be added incoherently (see fig. 15). But this is deeply connected with an adjustment of ß parameters.

On the contrary, a more microscopic and unified description in terms of MSDR is at the very beginning only. First results obtained by Kumabe et al. /37/ are shown in fig. 16.

(ii) Charged particle emission

Several systematical attempts have been undertaken to calculate production cross sections of complex charged particles for example for (n,d) and (n,t) reactions by Qaim et al. /15/.

Generally, the theoretical calculations fail in prediction of the right order of magnitude. One reason for this may be due to incomplete knowledge of optical potentials for complex particles.

Further, it is quite well proved that the double differential cross section of emitted charged particles are strongly influenced by non-equilibrium effects. Often their contributions to the spectral distribution were estimated in terms of PEM's, whereas angular distributions are excluded in those models up to now. Some systematical studies have

been carried out for charged particle transitions exciting lowest-lying levels in the residual nuclei in terms of DI. For instance see the review of Turkiewicz /66/ on (n,α) reactions at 14 MeV. Calculations in the frame of particle-knock-out, particle-pick-up or stripping include the adjustment of spectroscopical factors normally unpredicted or undetermined by analogous experiments.

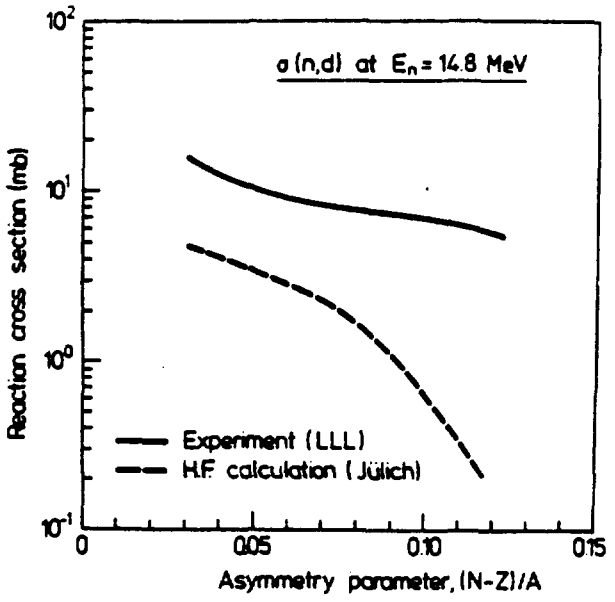

Fig. 17
Comparison between experiments and theoretical calculations for (n,d) reaction cross sections at 14 MeV (taken from ref. /15/).

Fig. 18
Comparison between experiments and theoretical calculations for (n,t) reaction cross sections (taken from ref. /15/).

Theoretical calculations of spectroscopical factors in the frame of the Nuclear-Shell-Model have been done with results deviating from experiments by one order of magnitude or more depending on the simplifications introduced for simulation of the real structure of the nucleus under investigation.

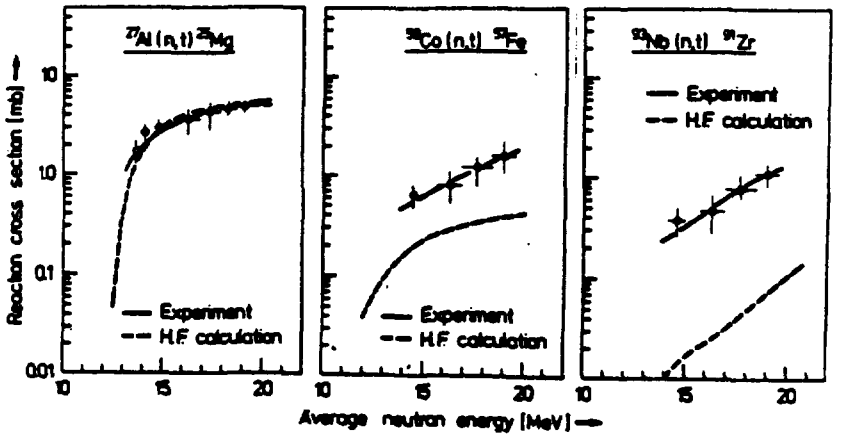

As example in figs. 19 to 21 the cross sections of α-particle transitions to the ground state $\widetilde{\sigma}_{n,\alpha_0}(E_0,\Theta)$ are demonstrated. The superposition of statistical and non-statistical reaction mechanism modes can be seen

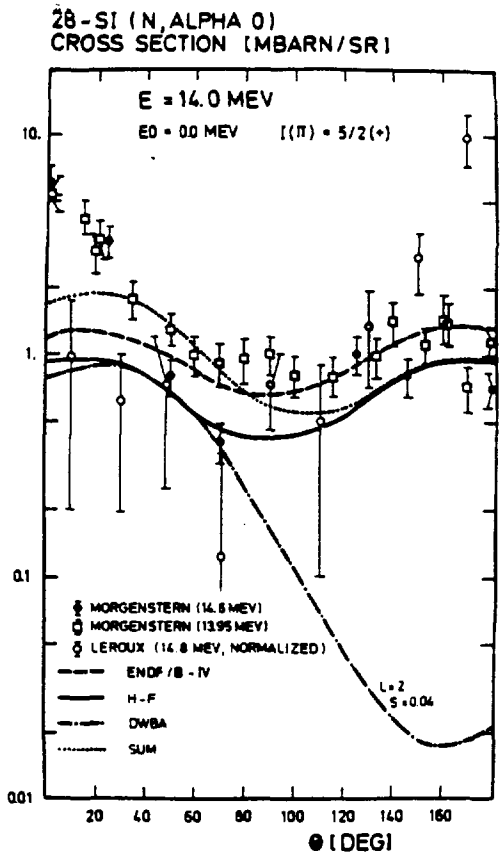

Fig. 19
Angular distribution of α-particles from (n,α_0) at 14 MeV for ^{28}Si in terms of different reaction models (taken from ref. /67/).

Fig. 20
Same as in fig. 19 for 21 MeV (taken from ref. /67/).

as well as in angular distributions (figs. 19, 20) and excitation function (fig. 21). Clearly, any fit for determination of relative contribution of DI components is only possible at energies above 14 MeV expecting the dominance of such modes (fig. 20).

(iii) γ-ray emission

Generally, the reliability of theoretical description of the γ-ray production via neutron-induced reactions (n,γ), (n,n'γ), (n,2nγ) etc. is not quite well up to now at neutron energies in the MeV range.

Bigdifferences in (n,γ) cross section prediction by various codes is shown in fig. 22.

More strong descrepancies arise for description of differential data (γ-ray spectrum).

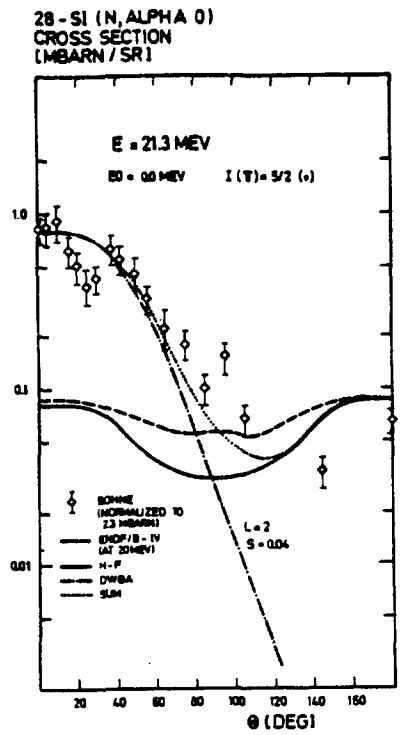

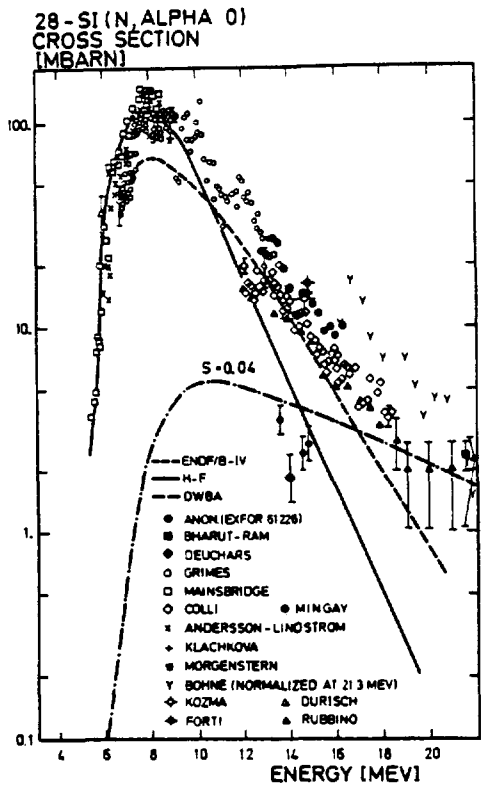

Fig. 21
Excitation function of (n,x_0) reaction for ^{28}Si (taken from ref. /67/).

Fig. 22
Comparison of calculations of neutron capture cross sections obtained by different codes (taken from ref. /46/).

tion from (n,γ') is underestimated by some orders of magnitude. Non-statistical effects are predominant and can be simulated by DI modes (direct capture, direct-semidirect-capture) or also PEM.

Applying Betáks code PEQGM /69/ the γ'-ray spectrum emitted from preequilibrium decay is in quite encouraging agreement with experiments.

The predominance of non-statistical mechanisms in emission of γ'-quanta of high energy ($E_{\gamma'} > B_n$)

A typical picture at 14 MeV is given in fig. 23. The γ'-ray emission spectrum is a very complex one resulting from $(n,n'\gamma')$ and (n,γ'). Whereas the γ'-production by neutron inelastic scattering is in surprisingly good agreement with statistical model (for particles and γ's) predictions the calculation of γ'-produc-

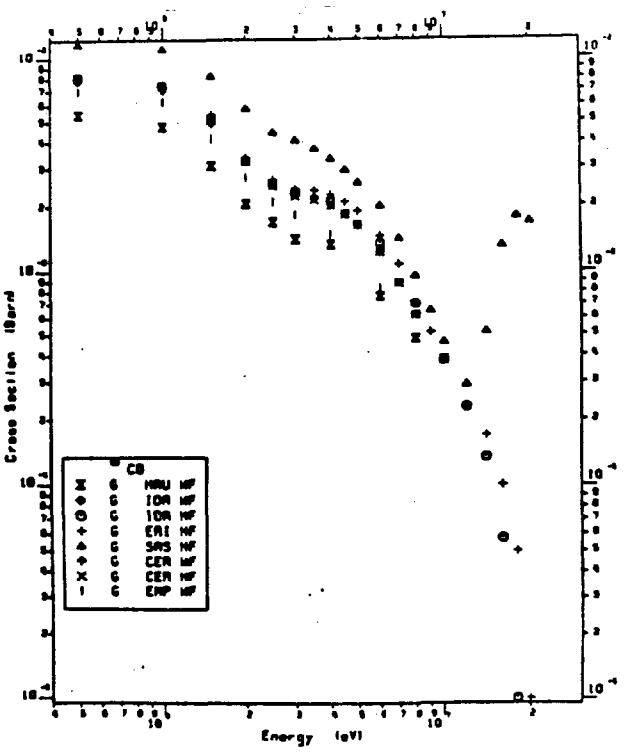

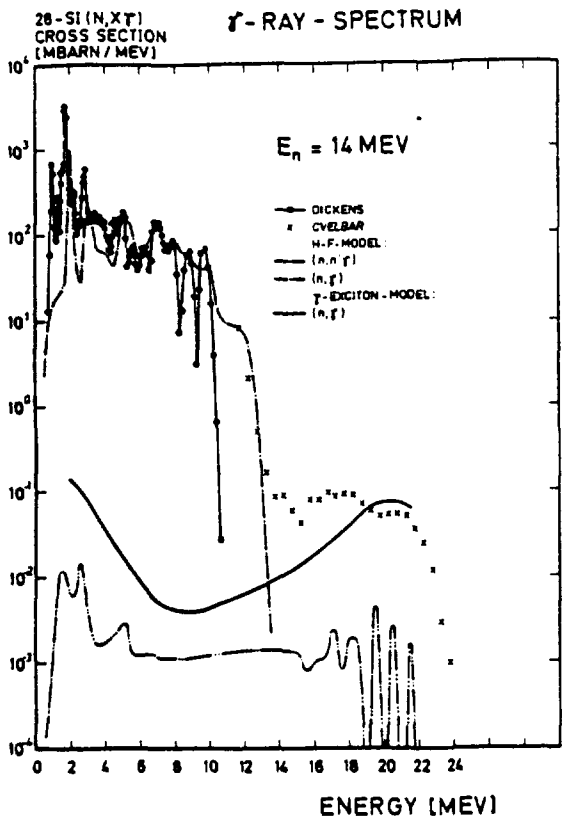

Fig. 23
Description of γ-ray spectrum produced by (n,γ) and (n,n'γ) reactions induced by 14 MeV neutrons on ^{28}Si (taken from ref. /68/).

Fig. 24
Excitation function of the 1.78 MeV γ-line induced by bombardment of ^{28}Si with neutrons (taken from ref. /63/).

can be calculated in very satisfying agreement using simple statistical assumptions on radiation strengths for different multipolarities. Commonly, better results are obtained regarding collective enhancements for E1 in terms of Axel-Brink's approach. An example is shown in fig. 24.

may be understood as the analogon of the enhancement of particle transitions to low-lying levels ($E'_p \sim E_o$).

In contrast to that, the production of γ-quanta emitted from γ-deexcitation of low-lying (discrete) levels in the intermediate or residual nuclei

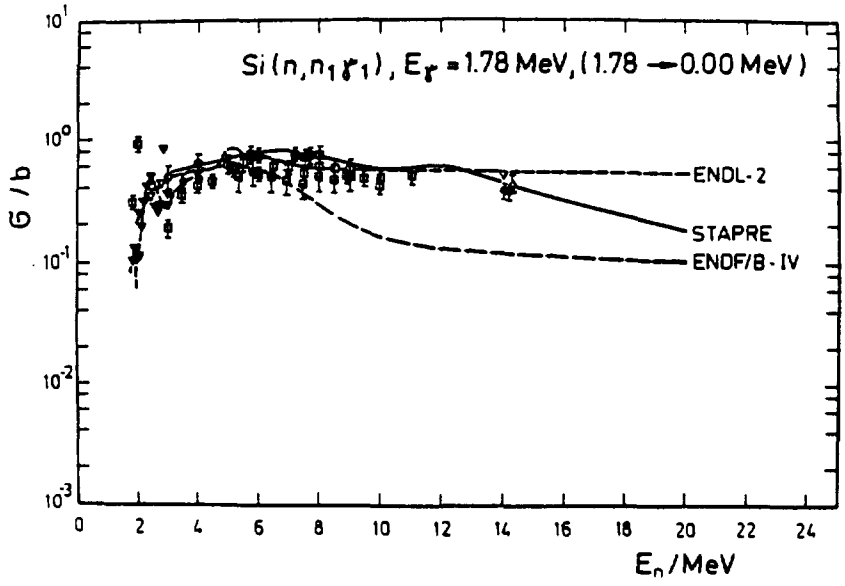

Final remarks

In the conclusions the considerable improvements achieved in application of nuclear theory for nuclear data calculation during the last decade has been reviewed. But also questionable or doubtful results were pointed out to show open problems attacked at present.

For a contineous progress in model calculations in the nearest future more accurate measurements of differential and double differential cross sections have to be carried out at first. These data are urgently demanded for further improvement of consistent parameters related with theoretical or semi-empirical models.

Then we can hope to realize "Pearlstein's experiment" of prediction of any desired quantity to a reasonable (corresponding to the necessary) degree of confidence by given values A, N and Z only.

References

/1/ V. Benzi, 'Evolution in Evaluation', summarizing report TIB/DIR (82) 1, p. 40, 1982

/2/ papers of J. Csikai, D. Seeliger, S.M. Qaim and H. Vonach in "Nuclear Theory for Application", Proc. Int. Trainings Course, Trieste, 1980, IAEA-SMR-68/1, 1981

/3/ N.N. Flerov, V.M. Talyzin, J. Nucl. Energy 4 (1957) 529

/4/ D.G. Gardner, Nucl. Phys. 29 (1962) 373

/5/ V.N. Levkovskij, JETP 45 (1963) 305

/6/ I. Angeli, J. Csikai, Nucl. Phys. A158 (1970) 389

/7/ I. Angeli, J. Csikai, Nucl. Phys. A170 (1971) 577

/8/ S. Pearlstein, Nucl. Sci. Engng. 23 (1965) 238

/9/ A.K. Hankla, R.W. Fink, Nucl. Phys. A180 (1972) 157

/10/ J. Csikai, G. Petö, Phys. Lett. 20 (1966) 52

/11/ S.M. Qaim, Nucl. Phys. A185 (1972) 614

/12/ Z.T. Bödy, J. Csikai, At. Energy Rev. 11 (1973) 1

/13/ E. Holub, N. Cindro, J. Phys. G: Nucl. Phys. 2 (1976) 405

/14/ G. Eder, G. Winkler, P. Hille, Z. Physik 253 (1972) 335

/15/ S.M. Qaim, in Proc. 3rd Conf. on Neutron Induced Reactions, Smolenice, 1982, Physics and Applications Vol. 10, p. 291, 1983

/16/ Z.T. Bödy, K. Mihaly, in Proc. XII. Symp. on Interaction with Fast Neutrons, Gaussig, 1982, ZfK-491, p. 200, 1983

/17/ J. Csikai, in "Nuclear Data for Fusion Reactor Technology", 1978, IAEA-TECDOC-223, p. 199, 1979

/18/ V.M. Bychkov, V.N. Manokhin, A,B. Pashenko, V.I. Plyaskin, INDC(CCP)-146/LJ, 1980

/19/ Men-deh Lu, R.W. Fink, Phys. Rev. C4 (1971) 1173

/20/ S. Pearlstein, J. Nucl. Energy 27 (1973) 81

/21/ D. Hermsdorf, S. Sassonov, D. Seeliger, K. Seidel, in Proc. Conf. on Nuclear Structure Study with Neutrons, Budapest, 1972

/22/ G.M. Braga-Marcazzan, E. Gadioli-Erba, L. Milazzo-Colli, P.G. Sona, Phys. Rev. C6 (1972) 1398

/23/ L. Milazzo-Colli, G.M. Braga-Marcazzan, Nucl. Phys. A210 (1973) 297

/24/ K. Seidel, D. Seeliger, A. Meister, in Proc. 3rd Conf. on Neutron Physics, Kiev, 1975
Proc. Vth Int. Symp. on Interaction of Fast Neutrons with Nuclei, Gaussig, 1975, ZfK-324, p. 32, 1976

/25/ N. Cindro, J. Frehaut, in Proc. Vth Int. Symp. on Interaction of Fast Neutrons with Nuclei, Gaussig, 1975, ZfK-324, p. 6, 1976
E. Holub, O. Počanic, R. Čaplar, N. Cindro, Z. Physik A296 (1980) 341

/26/ D. Hermsdorf, H.-P. Richter, S. Sassonov, D. Seeliger, K. Seidel, Kernenergie 16 (1973) 252

/27/ D. Hermsdorf, S. Sassonov, D. Seeliger, K. Seidel, J. Nucl. Energy 27 (1973) 747

/28/ H. Feshbach, A. Kerman, S. Koonin, Ann. Phys. (N.Y.) 125 (1980) 429

/29/ H.A. Weidenmüller, in Proc. Conf. on Nuclear Data for Science and Technology, Antwerp, 1982

/30/ W. Hauser, H. Feshbach, Phys. Rev. 87 (1952) 336

/31/ E.H. Auerbach, report BNL-6592, 1964

/32/ J.J. Griffin, Phys. Rev. Lett. 17 (1966) 488

/33/ J. Dobeš, E. Beták, in Proc. VIIth Int. Symp. on Interaction of Fast Neutrons with Nuclei, Gaussig, 1977, ZfK-376, p. 5, 1978
Z. Physik A288 (1978) 175

/34/ O. Bersillon, L. Faugere, NEANDC (E) 191"U", 1977
Proc. VIIth Int. Symp. on Interaction of Fast Neutrons with Nuclei, Gaussig, 1977, ZfK-376, p. 8, 1978

/35/ T. Tamura, T. Udagawa, D.H. Feng, K.-K. Kan, Phys. Lett. 66B (1977) 209

/36/ E. Arndt, R. Reif, in Proc. Vth Int. Symp. on Interaction of Fast Neutrons with Nuclei, Gaussig, 1975, ZfK-324, p. 112, 1976

/37/ I. Kumabe, K. Fukuda, M. Matoba, Phys. Lett. 92B (1980) 15
/38/ R. Bonetti, M. Camnasio, L. Milazzo-Colli, P.E. Hodgson, Phys. Rev. C24 (1981) 71
/39/ T. Tamura, T. Udagawa, M. Benhamon, Comp. Phys. Comm. 29 (1983) 391
/40/ V. Benzi, in"The Evaluation of Neutron Nuclear Data", IAEA-153, p.403, 1973
/41/ A. Prince, in "Nuclear Theory in Neutron Nuclear Data Evaluation", Trieste, 1975, IAEA-190, 1976
and "Nuclear Theory for Applications", Trieste, 1978, IAEA-SMR-43, 1980
/42/ P.G. Young, in Proc. Symp. on Neutron Cross Sections from 10 to 50 MeV, Brookhaven, 1980, BNL-NCS-51245, Vol. I., p. 43, 1980
/43/ W. Brainerd, Comm. ACM 21 (1978) 806
/44/ News from the NEA DATA BANK, issued regularly by OECD NEA DATA BANK (any new Newsletter supersedes all older one)
/45/ V. Benzi, in "The Evaluation of Neutron Nuclear Data", IAEA-153, p. 417, 1973
/46/ A. Prince, G. Reffo, E. Sartori, INDC(NEA)-4, 1983
/47/ P. Nagel, H. Gruppelaar, private communication, 1983
/48/ P.E. Hodgson, private communication, 1983
/49/ D. Hermsdorf, Kernenergie 26 (1983) 261
/50/ C.M. Perey, F.G. Perey, Atomic Data and Nucl. Data Tables 13 (1974) 293
/51/ B. Holmqvist, T. Wiedling, J. Nucl. Energy 27 (1973) 543
/52/ F.D. Becchetti, Jr., G.W. Greenless, Phys. Rev. 102 (1969) 1190
/53/ J. Rapaport, V. Kulkawni, R.W. Finlay, Nucl Phys. A330 (1979) 15
/54/ J.P. Delaroche, Ch. Lagrange, J. Salvy, in "Nuclear Theory in Neutron Nuclear Theory", Trieste, 1975, IAEA-190, Vol. I, p. 251, 1976
/55/ H. Feshbach, Ann. Nucl. Sci. 8 (1958) 49
/56/ D.F. Jackson, Reports Prog. Phys. 37 (1974) 55
/57/ P.E. Hodgson, Reports Prog. Phys. 34 (1971) 765
/58/ A.V. Ignatyuk, private communication, 1983
/59/ A.V. Ignatyuk, G.N. Smirenkin, A.S. Tishin, Yad. Fiz. 21 (1975) 485
/60/ A.V. Ignatyuk, K.K. Istekov, G.N. Smirenkin, Yad. Fiz. 29 (1979) 875
/61/ Y. Ando, M. Uno, M. Yamada, JAERI-M83-025, 1983

/62/ K.H. Schmidt, H. Delagrange, J.P. Deufour, N. Carjan, A. Fleury, Z. Physik A308 (1982) 215

/63/ V.S. Ramamurthy, in "Nuclear Theory for Application", Trieste, 1978, IAEA-SMR-43, p. 187, 1980

/64/ D. Hermsdorf, H. Kalka, D. Seeliger, in Proc. Conf. on Neutron Physics, Kiev, 1983, in press
see also contribution to this symposium

/65/ G. Maino, cited in V. Benzi, report TIB/DIR(82)1, 1983
G. Maino, M. Vaccari, A. Ventura, Comp. Phys. Comm. 29 (1983) 375

/66/ J. Turkiewicz, in Proc. 2nd Int. Symp. on Neutron-Induced Reactions, Smolenice, 1979, Physics and Applications, Vol. 6, p. 13, 1980

/67/ D. Hermsdorf, INDC(GDR)-22/L, 1983

/68/ D. Hermsdorf, INDC(GDR)-20/L, 1983
B. Basarragtscha, D. Hermsdorf, E. Paffrath, J. Physics G: Nucl. Phys. 8 (1982) 275

/69/ E. Beták, private communication, 1982

Recent progress in preequilibrium models

Igor Ribanský, Bratislava

Due to lack of time and the reachness of the subject I will not be able to cover really the "recent progress" as indicated by the title. Instead I will concentrate myself to present several remarks on recent progress of microscopic studies of the preequilibrium (PEQ) decay, brief description of the modified exciton model (MEM) recently proposed in Bratislava and a short discussion of one specific problem connected with α-particle emission in the exciton model (EM).

1. Microscopic theories of PEQ decay

To characterize the recent development of PEQ decay specifically its modelling by different phenomenological approaches based on the use of phase spaces one should pay attention to the results of microscopic theories designed to study this problem. The reason is that just those studies sholud give the answer to the question why the phenomenology works so well or where to look for the cause of an enormous success of phenomenological models. At the same time one would like to find out what should be the direction the phenomenology should follow in future.

As is well known there exist three basic theories of PEQ decay due to Feschbach, Kerman and Koonin (FKK) [1], Agassi, Weidenmüller and Mantzouranis (AWM) [2] and Friedman, Hussein, McVoy and Mello (FHMM) [3]. Though these theories are based on quite different assumptions and use different techniques McVoy and Tang [4] succeeded to shown their mutual connection and the equivalence of their basic statistical assumptions. The result is the following scheme (for details see [4]):

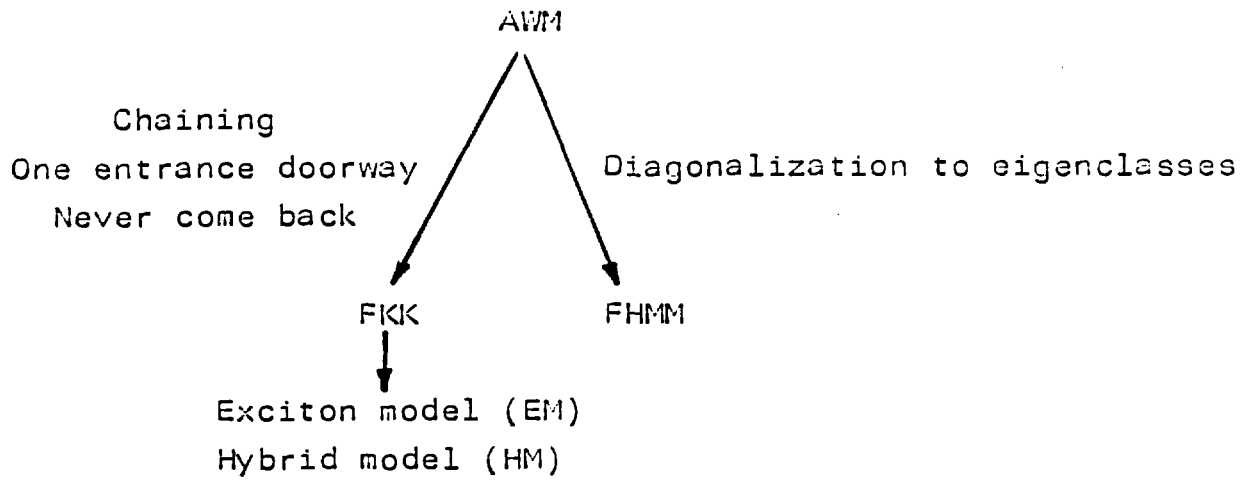

For those who are working with phenomenological models the branch AWM-FKK-EM is especially interesting not only because it makes legitimate the existence of EM but also because it is difficult to understand. The point is that the microscopic theories mentioned are theories of multistep compound (MSC) processes and consequently they predict symmetric angular distributions of emitted particles (in CM). This mere fact implies certain contradictions in current understanding of PEQ mechanism which I would like to characterize by several remarks:

a) It is known that EM si capable to describe the energy distribution also those particles possessing asymmetric angular distribution. As it is widely believed the forward peaking is a sign that direct processes are present. What is than the reason that EM is working well far outside the region indicated by the abovementioned scheme? How it is possible that the factorized form of EM cross section suggesting the unimportance of interference effects is in agreement with the experiment?

b) Many attempts to extend EM for the description of the angular distribution were successful to obtain the augular assymetry (see Dr. Hermsdorf's lecture) while preserving the energy distribution.

c) As a rule EM describes almost the whole PEQ portion of a spectrum as do the statistical theories of multistep direct (MSD) reactions. Are those theories equivalent or why they overlap so much in their results?

d) Kalbach has shown recently [5] that by proper division of EM configurations belonging to n-exciton state EM can be understood as a model describing both MSC and MSD processes.

One can continue to list other questions and problems and to conclude that the answers are not at hand at present. I would stop my discussion of this part of my lecture by citing prof. Weidenmüller [6] : "The microscopic connection between the ranges of validity of random-matrix model, phenomenological models like the exciton model, models using a Boltzman - type collision term, and clasical models are not clear. Direct processes have so far not been included. Statistical assumptions are in need of better justification".

2. The modified exciton model (MEM)

The model I am going to describe rests on the following observation: Consider A~60 nuclei. The shell model predicts [7] a gap d~5 MeV between the last and the next lower lying shells for the ground state of those nuclei. Now consider (nucleon, nucleon) reactions on those nuclei and the portion (ε_{max}-d, ε_{max}) of the spectrum of emitted nucleons, ε_{max} being their maximum energy. We see that this portion can originate only from the interaction of the projectile with the nucleons lying on the last filled shell.

Now the basic assumption of MEM is that in PEQ stage of a reaction only the last shell nucleons are involved. This is certainly an extreme assumption but as we shall see it is not in contradiction with the experiment involving (nucleon, nucleon) reactions and excitation energies E = 20 - 30 MeV.

In the closed form formulation of the exciton model the PEQ nucleon energy distribution in MEM is given by

$$\frac{d\sigma}{d\varepsilon_x} = \sigma_R \sum_{n=3} \frac{a_x(n)\, w_x(n,\varepsilon_x)}{\lambda_+(n) + \sum_{j=\pi,\nu} a_j(n) \int w_j\, d\varepsilon_j} D(n) \qquad (1)$$

where all symbols (except a_j) have their usual meaning (see e.g. [8]) and the coefficients a_j represent the fraction of nucleons of the type j ($= \pi, \nu$; π = proton, ν = neutron) in the n-exciton state

$$a_j(n) = \frac{1}{p} N_j \; j \qquad p = N_\pi + N_\nu \tag{2}$$

where N_π, N_ν is the number of π and ν resp. For example, for neutron induced reaction and n=3 we have

$$N_\nu = \frac{\sigma_{\nu\pi} n_\pi}{\sigma_{\nu\pi} n_\pi + \sigma_{\nu\nu} n_\nu} + 2\,\frac{\sigma_{\nu\nu} n_\nu}{\sigma_{\nu\pi} n_\pi + \sigma_{\nu\nu} n_\nu} = \frac{\alpha n_\pi + 2 n_\nu}{\alpha n_\pi + n_\nu} \tag{3}$$

where $\alpha = \sigma_{\nu\pi}/\sigma_{\nu\nu}$ and $n_\pi (n_\nu)$ is the number of protons (neutrons) lying on the last filled shell. The first term in eq. (3) describes the collision of the incoming neutron with proton and the second term collision with neutron. The quantity λ_+ can also be decomposed in a similar way [9] but we will not consider it now. Instead we treat λ_+ as a fit parameter of MEM and parametrize λ_+ in the usual way [10]

$$\lambda_+ = \frac{2\pi}{\hbar} C E^{-1} A^{-3} \omega_f^+ \tag{4}$$

where ω_f^+ is calculated according to [11] using the state density derived in [12]

$$\omega_{ph}(E) = \frac{g^n}{p!\,h!\,(n-1)!} \sum_{l=0}^{h} \binom{h}{l} (-)^l \left[E - l E_H\right]^{n-1} \theta(E - l E_H) \tag{5}$$

where E_H can be interpreted as a maximum depth of holes excitation [13]. It seems reasonable to approximate E_H in MEM by the energy spread of the last shell due to residual interaction wich is of the order of few MeV [14]. In all calculations to be presented we assumed E_H = 1 MeV, g = A/13 and α =2.5 [15] in eq.(1).

Now we would like to discuss to what extent this model is able to describe the spectra of the first emitted neutrons and protons in neutron induced reactions at 14 MeV. The experimental data were taken from refs. [16,17].

Equation (1) describes only PEQ process and therefore one has to combine it with the evaporation term. To fix the model parameters the following procedure have been adopted. First we determined C in eq. (4) from the high energy portion of neutron spectra ($\varepsilon_n \gtrsim 9$ MeV) since this part is almost free from evaporation. (The proton spectra are not suitable for this purpose because the evaporation peak is shifted to higher energies due to the Coulomb barrier). In this way we fixed PEQ part for both nucleon exit channels and a given target. Then we adjusted the level density parameter a and pairing correction δ in the evaporation term in order to obtain good simultaneous description of both lower energy parts of nucleon spectra (up to the thershold of the second particle emission). In the evaporation term the compound nucleus cross section was determined as $\sigma_{CN} = \sigma_R - \sigma_{PEQ}$, where σ_{PEQ} is the total PEQ emission cross section.

The results of our MEM calculations are presented in figs. 1 to 13. Common to all figs. is the following. The neutron data [16] are represented by full points and the proton data [17] by horizontal bars. At each neutron spectrum the assumed target nucleus shell structure is indicated in the upper-right part of the figure. The open circles indicate next two neutrons in heavier isotope for which the proton spectrum is avaliable; the numbers between topmost shells indicate their distance in units of MeV [7]. The arrows at the energy axis indicate the second particle threshold. The dotted curves always represent MEM PEQ contribution given by eq. (1). Note that the neutron data are avaliable only for target with the natural isotopic composition.

In figs. 1 and 2 we present the comparison of our MEM calculations with the ^{51}V + n experiment. In fig. 2 two sets of calculations are given. The dashed curve represents the calculations with $n_\pi = 3$, $n_\nu = 8$ (see eq. (3)) - the dot-dashed curve is the PEQ contribution. We see that the experiment is overestimated in this case. The corresponding neutron spectrum practically coin-

cides with the full curve in fig. 1. To bring the theory in agreement with the experiment we assumed that odd $f_{7/2}$ proton is preferentially excited. Those calculations are represented by full curves and are in agreement with the experiment. The peak at 12 MeV in fig. 2 represents the transition to the ground state and can not be in principle described by the model used.

In figs 3 to 5 the iron data are compared with our calculations. The full curve in fig. 3 represents the weighted sum of the neutron spectra for 54 and 56 isotopes. We see that the agreement is almost excellent for both neucleon channels and isotopes. To show what is the typical difference between MEM and EM we present also the dashed curves calculated with $n_\pi = Z$, $n_\nu = N$, $\alpha = 1$, $E_H = 20$ MeV and $\lambda_+(3) = 0.5_{10}22\ s^{-1}$ [8]. Other parameters were the same as in MEM calculations. We see that the differences between both models are not large though, clearly, the high energy part of EM does not follow the neutron energy distribution and at lower energies EM slightly overestimates the neutron spectrum.

In figs. 6 to 8 our calculations are compared with N_i+n data. The full curve again is the weighted sum for 58 and 60 Ni isotopes. The agreement between MEM and the experiment is good.

In figs. 9 to 11 the same comparison is made for Cu+n data. The reason for a quite big disagreement of our calculations with ^{63}Cu(n,xp) spectrum is not known to us. We note only that we do not see any possibility to lower the high energy portion of the calculated spectrum without completely destroying the very good agreement with ^{NAT}Cu(n,xn) and ^{65}Cu(n,xp) data.

In figs. 12 and 13 we present the last comparison of MEM calculations with 14 MeV data. The situation here is quite similar to ^{51}V+n case. The dashed curve represents the calculations with $n_\pi = 3$, $n_\nu = 2$ (the dot-dashed curve is PEQ contribution). One can see that the dashed curve does not follow the shape of proton spectrum correctly and generally overstimated the experiment in high energy part. This again indicate that probably only $g_{9/2}$ proton is involved in PEQ stage. The corresponding calculations are represented by full curves which repreduce the data very good except at $\varepsilon_p = 12 \div 13$ MeV. Note however that the (n,p) data from Vienna (see prof. Vonach's lecture) indicate lower cross sec-

tion at this particular energy while in agreement with the rest of the data presented in fig. 13.

Now we want to present the comparison of MEM predictions (parameters were fixed at 14 MeV incident energy) with the neutron spectra measured at 25.7 MeV [18] - figs. 14,15. First we would like to emphasize that the displayed data are practically free from the evaporation contribution and, therefore, only eq. (1) is at work in this region. Next due to the basic assumption of MEM and the incident energy of 26 MeV both 3 and 5-exciton states certainly contain an unbound particle. Those states give the main contribution and consequently eq. (1) essentially describes direct processes.

In fig. 14 the ^{51}V and $^{65}Cu(n,xn)$ data are compared with our calculations. The agreement is quite good both in the shape and the magnitude. In fig. 15 the ^{56}Fe and ^{93}Nb data are confronted with MEM. The iron data are "in average" in agreement with MEM prediction while niobium data are underestimated though the flat shape of MEM curve does follow the frend of the data. In ref. [19] the ^{51}V and ^{93}Nb data were compared with the prediction of the generalized exciton model [20]. Those calculations failed to reproduce the shape and the magnitude of both angle-integrated neutron spectra.

To conclude this part of my discussion I want to stress that MEM is able to describe 14 MeV angle-integrazed spectra as well as EM or even better. "Even better" refers mainly to the high energy part of the neutron spectra where the PEQ process is well pronounced. This and the agreement of MEM with the neutron spectra at 26 MeV - figs. 14.15 - seems to indicate that the preferential excitation of the last shell nucleons is correct. The peculiar feature of MEM which makes it quite different from EM is the average lifetime of the n-exciton states. To obtain that kind of agreement with the data as shown above the required lifetime of n=3 exciton state was shorter by a factor of $\sim$3 compared with EM [8]. This shifts MEM still closer to the direct mechanism which is in complete disagreement with what one would expect from microscopical approaches.

3. Emission of α-particles in EM

Now I will briefly discussed one specific model disigned to describe α-particle emission [21]. In this model (for the present purpose I will call it the formation model (FM)) α-particle is assumed to be formed from the excit nucleons. FM was - rather successfully - used in the analyses of experimental data [22]. However some contraversions exist in the literature [23,24,25] of whether FM is correctly formulated or whether it does not coincides with so called no formation model (NFM) [25,26] which was shown to give too small a number of α-particles especially at higher energies [26]. My aim is to argue that FM is correctly formulated and - as a by product - I will indicate why NFM should not work.

The formation model (FM) is based on the following scheme of the composite nucleus decay

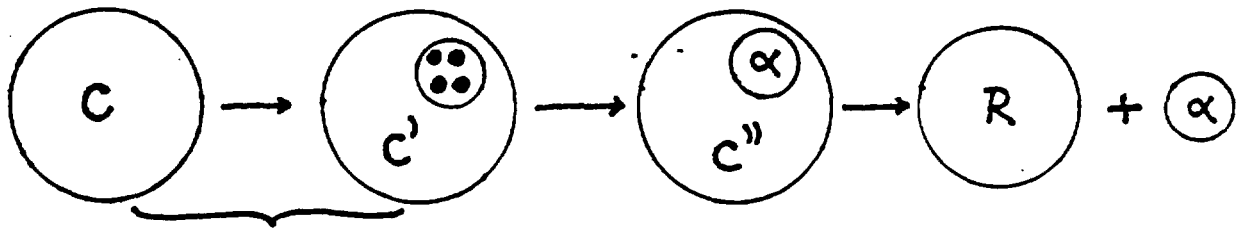

First the composite nucleus characterized by the number of excited particles p holes h and the excitation energy E - (p,h,E) - is devided to two subsystems: four nucleons posessing a total energy ε_α (I will assume that the separation energy of α is zero) and the rest (p-4,h,U=E-ε_α). From the four nucleons α is formed with a certain probability. Once formed it has a chance to be emitted and the residual nucleus plus free α system is created. From the point of view of the perturbation theory [27] the process just described occurs in the second order because the state of the composite nucleus involves only nucleonic states. To use directly the transition rate expression involving the second order matrix element is probably dificult due to its complicated structure [27]. Instead one can calculate the α-particle emission rate $W_{CR,\alpha}$ from the composite nucleus as follows

$$W_{CR,\alpha} = S_\alpha W_{SP,\alpha} \tag{6}$$

where S_α is the number of α-particles in the composite nucleus and $W_{SP,\alpha}$ is the single particle emission rate for α. $W_{SP,\alpha}$ can be calculated using the detailed balance (note that this process occur in a first order because α is treated as an entity)

$$g_\alpha W_{SP,\alpha} = \omega_{f,\alpha} W_{INV,SP,\alpha} \tag{7}$$

where g_α is the α single particle state density in the composite nucleus, $\omega_{f,\alpha}$ is the density of states of the free α and $W_{INN,SP,\alpha}$ is the "capture" rate of α by the residual necleus

$$W_{INV,SP,\alpha} = \frac{v_\alpha \sigma_{INV,\alpha}}{V} \tag{8}$$

where v_α is the relative velocity, $\sigma_{INV,\alpha}$ is the capture cross section and V is the normalisation volume. To calculate S_α is quite easy in EM. First the number of distinquishible quartets in (p,h,E) system in the interval $(\varepsilon_\alpha, \varepsilon_\alpha + d\varepsilon_\alpha)$ is given as [11]

$$dN_4 = \frac{\omega_{p-4,h}(E-\varepsilon_\alpha)\,\omega_{4,0}(\varepsilon_\alpha)}{\omega_{p,h}(E)}\, d\varepsilon_\alpha \tag{9}$$

where ω's are the state densities. Note that $\int_0^E dN_4 = \binom{p}{4}$ which is exactly what one should expect in EM. Now FM assumes that each such quartet can form α with the probability γ_α. Unless further specifications about the state of the quartets are made it is natural to assume γ_α = const. This is certainly a crude assumption but one can avoid it (see e.g. [28,29]). Now the total number of α-particles is given as

$$S_\alpha = \int_0^E dN_4 = \gamma_\alpha \binom{p}{4} \leq \frac{p}{4} \quad (=\text{maximum } N_0 \text{ of } \alpha\text{'s}) \tag{10}$$

Eq. (10) implies that $\gamma_\alpha \leq 1$ for $p \geq 4$. One should expect however that $\gamma_\alpha \ll 1$ because the probability to find an α at the nuclear surface is quite small [30,31] . The final expression for α-particle emission rate in FM then reads

$$W_{CR,\alpha} = \left[\frac{\omega_{p-4,h}(E-\varepsilon_\alpha)\,\omega_{4,0}(\varepsilon_\alpha)\,d\varepsilon_\alpha}{\omega_{p,h}(E)}\,\gamma_\alpha \right] \frac{\nu_\alpha\,\sigma_{INV,\alpha}}{g_\alpha V}\,\omega_{f,\alpha} \qquad (11)$$

where the term in squared brackets is the number of α-particles in the composite nucleus. Now I will briefly discuss eq. (11).

i) An extra factor R_α [26] have to be attached to eq. (11) in order to conserve the charge.

ii) It was suggested [23,24] that eq. (11) should be multiplied by the factor $1/(\frac{p}{4}) = 1/\int dN_4$ (see eq. (9)) in order the ratio $\omega_{p-4,h}(E-\varepsilon_\alpha)\,\omega_{4,0}(\varepsilon_\alpha)/\omega_{p,h}(E)$ could be interpreted as the probability density that E in (p,h,E) system be partitioned between 4 particles having the energy ε_α and p-4+h excitons having the energy $E-\varepsilon_\alpha$. We feel that this is a misunderstanding. First, as clearly seen in eq. (6), one needs to estimate the number of objects in the decaying system and not the probability to find one specific object. Should one apply the above suggestion to the nucleon emission case one shall conclude that in each n-exciton state there is only one excited particle which is in complete disagreement with the philosophy of EM.

iii) It was also suggested [24,32] that $\omega_{4,0}(\varepsilon_\alpha)\gamma_\alpha$ exactly equals g_α and as a result eq. (11) reduces to NFM with known consequences. While the quantity g_α has clear physical meaning the product $\omega_{4,0}(\varepsilon_\alpha)\gamma_\alpha$ has not. It can not be disconnected from the rest of the bracketed term in eq. (11). This term is in fact the estimate of the sum of overlaping integrals between the single-particle components of the composite nucleus and the α-particle wave functions. In FM all nonvanishing overlaping integrals are said to be equal γ_α and what remains is the sum of contributing terms. The last number is

given by eq. (9) in the equidistant spacing model. Clearly, the angular momenta coupling is disregarded.

iv) The peculiar feature of eq. (11) is that it contains the combination of terms $\omega_{4,0}(\varepsilon_\alpha)\,\gamma_\alpha/g_\alpha$ which does not depend on the exciton number. Recalling that the Master equations formulation of EM [33,34] contains both the preequilibrium and the equilibrium contributions this combination has to survive the equilibrium limit and it should appear also in the evaporation cross section. This kind of reasoning is valid for any other EM-type models which explicitely consider the formation of α-particles implying the necessity to modify the usual evaporation cross section formula for α-particles. This gives us further possibility to estimate the values of unknown parameters and - probably - to distinquish contributions from different models. I think that further investigations in this direction would be useful.

Literature

[1] H. Feshbach, A.K. Kerman and S. Koonin, Ann. Phys. 125(1980)429
[2] D. Agassi, H.A. Weidenmüller and G. Mantzouranis, Phys. Rep. 22C (1975)145
[3] W.A. Friedman, M.S. Hussein, K.W. McVoy and P.A. Mello, Phys. Rep. 77(1981)47
[4] K.W. McVoy and X.T. Tang, Phys. Rep. 94(1983)141
[5] C. Kalbach, Phys. Rev. C23 (1981)124
C. Kalbach, Phys. Rev. C24 (1981)819
[6] H.A. Weidenmüller, Conference on Nuclear Data for Science and Technology, Antwerp, 6-11 Sept. 1982
[7] K. Bleuer and M. Beiner, Nuovo Cim. B52 (1967)149
[8] E. Gadioli, Nukleonika 21(1976)385
[9] J. Dobeš and E. Běták, Z. Phys. A310(1983)329
[10] C. Kalbach, S.M. Grimes and C. Wong, Z. Phys. A275(1975)175
[11] P. Obložinský, I. Ribanský and E. Běták, Nucl. Phys. A226 (1974)347
[12] E. Běták and J. Dobeš, Z. Phys. A279(1976)319
[13] Š. Gmuca and I. Ribanský, Neutron Induced Reactions, Ed. I. Ribanský and E. Běták, VEDA Publishing House, Bratislava 1980
[14] D. Wilkinson, Nucl. Instr. Meth. 146(1977)143

[15] K. Kikuchi and M. Kawai, Nuclear Matter and Nuclear Reactions, North-Holland, Amsterdam 1968

[16] D. Hermsdorf, A. Meister, S. Sassonoff, D. Seeliger, K. Seidel and F. Shahin, Rep. ZfK-277(U), Zentralinstitut für Kernforshung Rossendorf bei Dresden, 1975.
Data used in this work were obtained from INDC, IAEA, Vienna

[17] S.M. Grimes, R.C. Haight and J.D. Anderson, Phys. Rev. C17 (1978)508
S.M. Grimes, R.C. Haight, K.R. Alvar, H.H. Barshall and R.R. Borchers, Phys. Rev. C19(1979)2127

[18] A. Marcinkowski, R.W. Finlay, G. Randers-Pehrson, C.E. Brient, R. Kurup, S. Mellema, A. Meigooni and R. Tailor, Nucl. Sci. Eng. 83(1983)13

[19] A. Marcinkowski, R.W. Finlay, G. Randers-Pehrson, C.E. Brient, J.E. O'Donnell and K. Stankiewicz, Nucl. Phys. A402(1983)220

[20] J.M. Akkermans, H. Gruppelaar and G. Reffo, Phys. Rev. C22 (1980)73

[21] I. Ribanský and P. Obložinský, Phys. Lett. 45B(1973)318

[22] J.R. Wu and C.C. Chang, Phys. Rev. C17(1978)1540

[23] M. Blann, Ann. Rev. Nucl. Sci. 25(1975)123

[24] E. Gadioli and E. Gadioli Erba, Nuclear Theory for Applications-1980, IAEA-SMR-68/I, IAEA, Vienna 1981

[25] F.M. Lanzafame and M. Blann, Nucl. Phys. A131(1969)513

[26] C.K. Cline, Nucl. Phys. A193(1972)417

[27] L.I. Schiff, Quantum Mechanics, Mc Graw-Hill, New York-Toronto-London, 1955

[28] H. Machner, Phys. Lett. 86B(1979)129

[29] K. Iwamoto and K. Harada, Phys. Rev. C26(1982)1821

[30] I. Ribanský, Fizika 11(1979) Supplement 2, p.39

[31] S.G. Kadmenski and V.I. Furman, Sov. J. Part. Nucl. 6(1976)469 (in russian)

[32] C. Kalbach, Phys. Rev. C19(1979)1547

[33] C.K. Cline and M. Blann, Nucl. Phys. A172(1969)225

[34] I. Ribanský, P. Obložinský and E. Běták, Nucl. Phys. A205(1973) 545

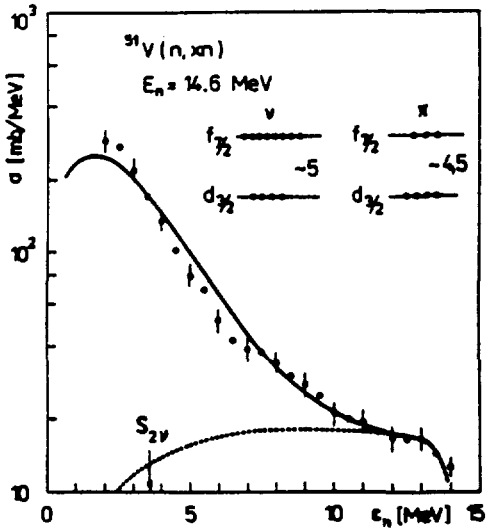

Fig.1

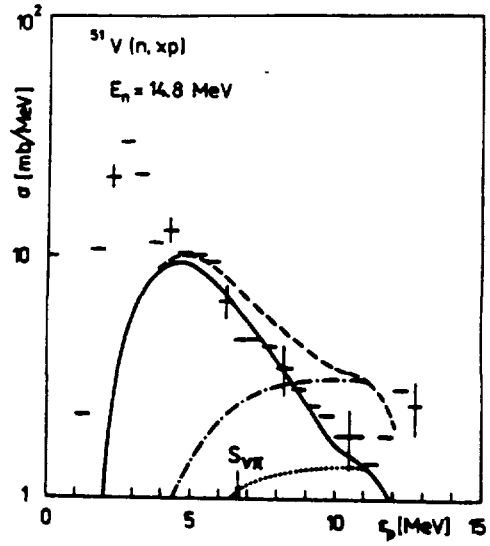

Fig.2

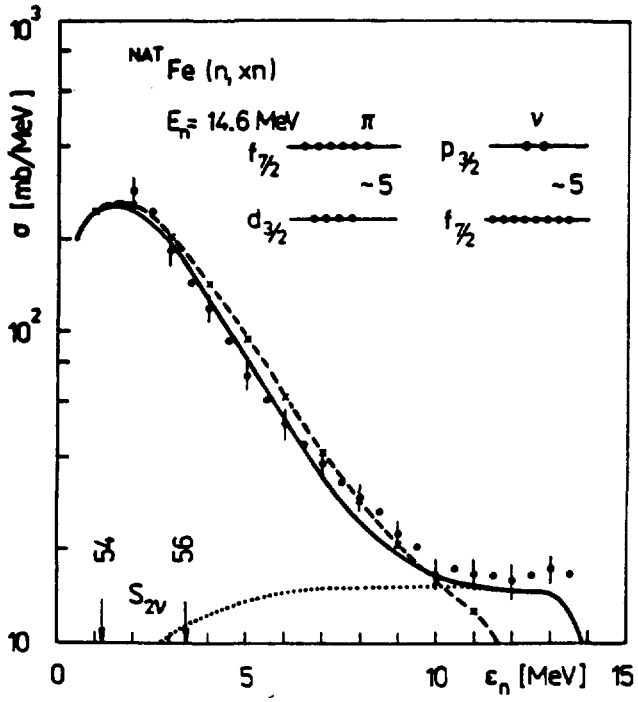

Fig.3

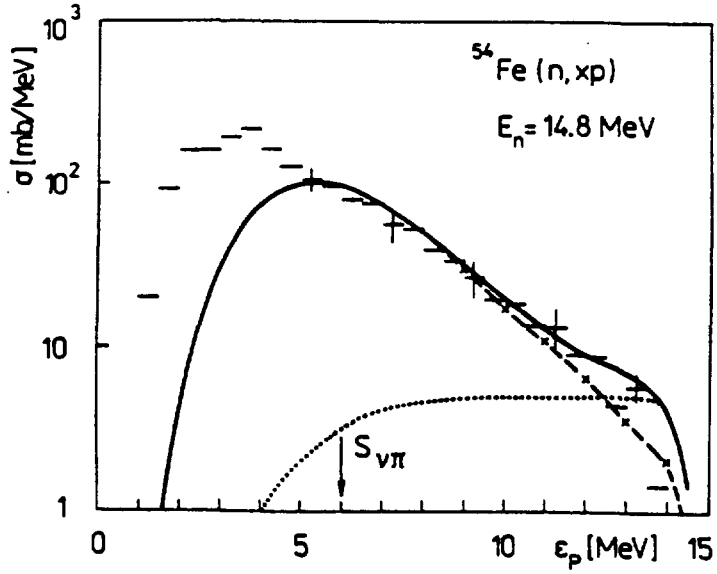
^{54}Fe (n, xp)
E_n= 14.8 MeV
$S_{\nu\pi}$
σ [mb/MeV]
10^3
10^2
10
1
0
5
10
15
ε_p [MeV]

Fig.4

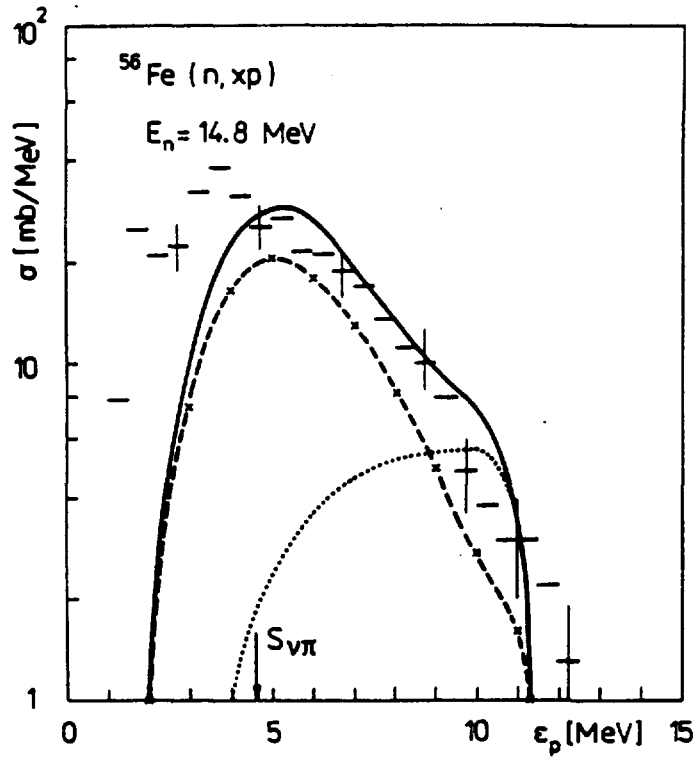
^{56}Fe (n, xp)
E_n= 14.8 MeV
$S_{\nu\pi}$
σ [mb/MeV]
10^2
10
1
0
5
10
15
ε_p [MeV]

Fig.5

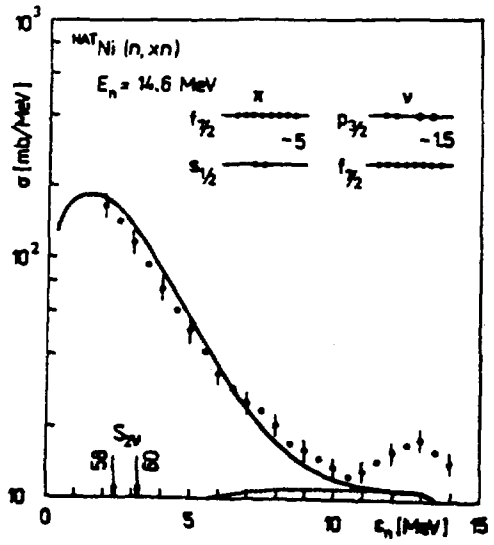

Fig.6

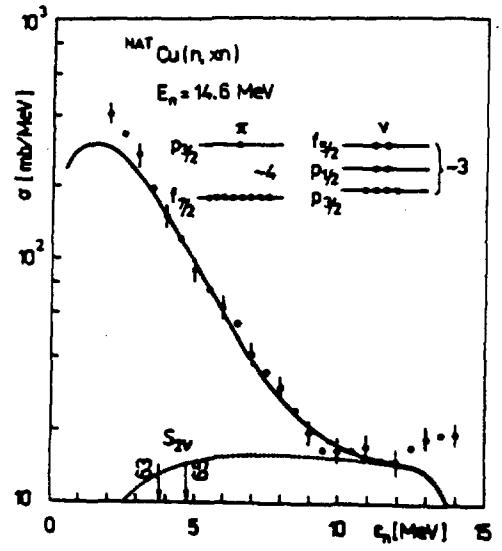

Fig.9

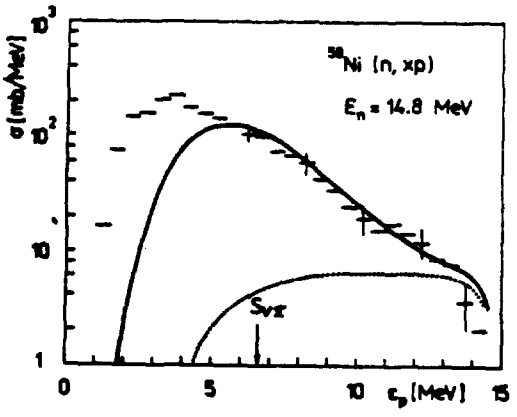

Fig.7

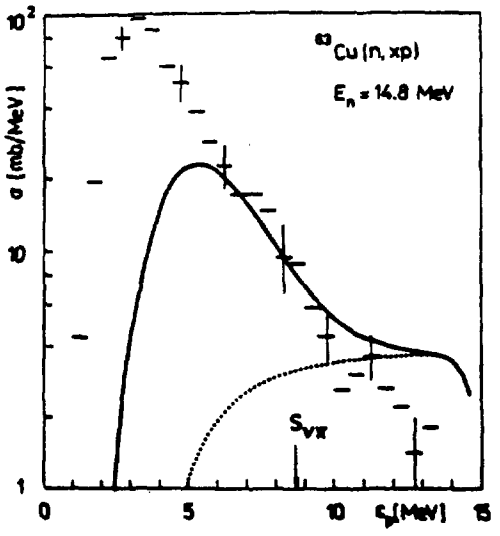

Fig.10

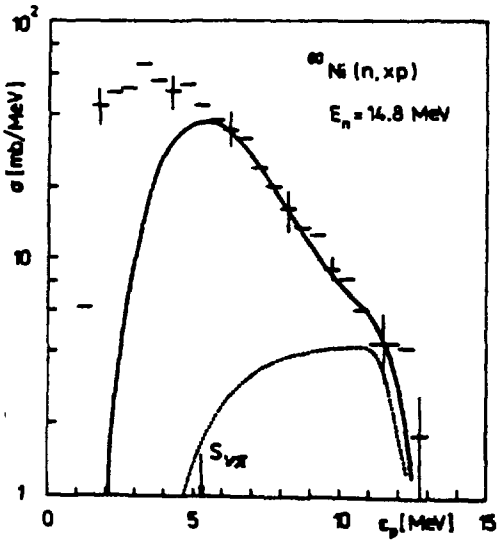

Fig.8

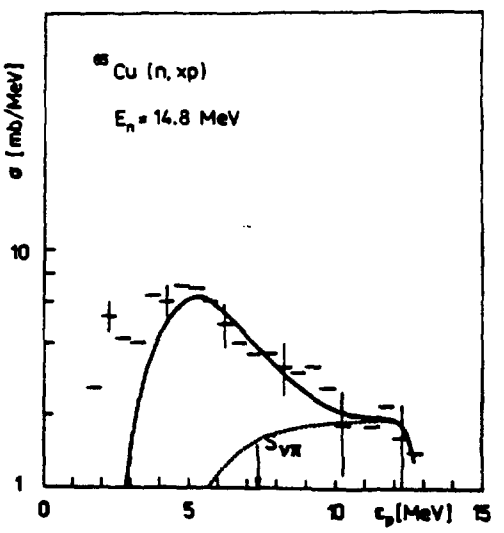

Fig.11

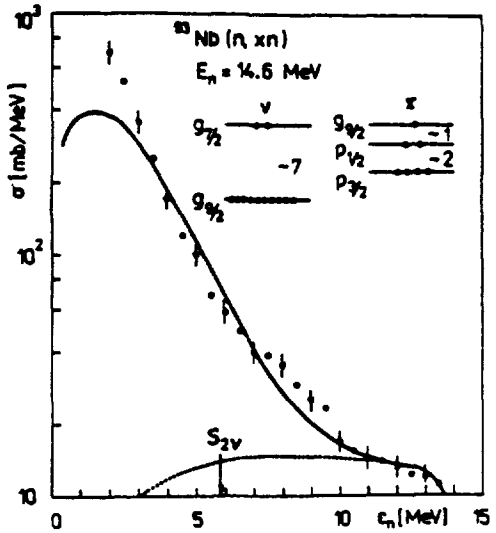

Fig.12

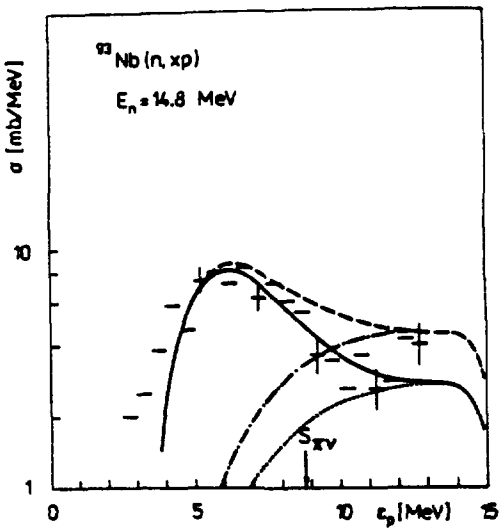

Fig.13

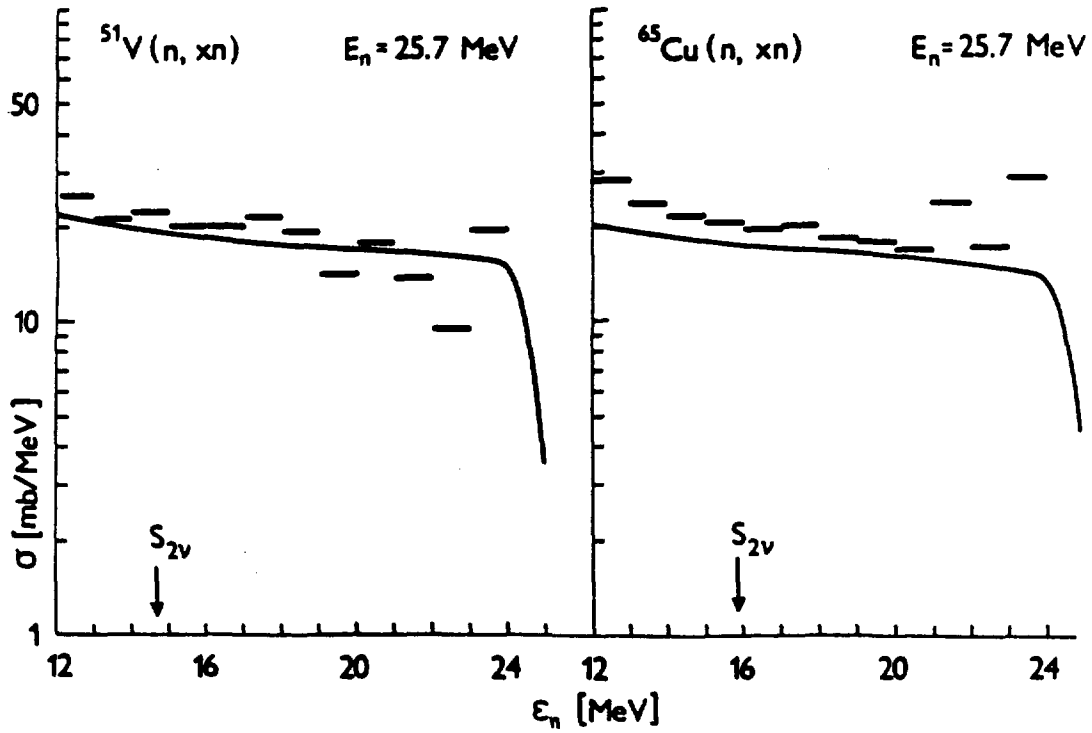

Fig.14

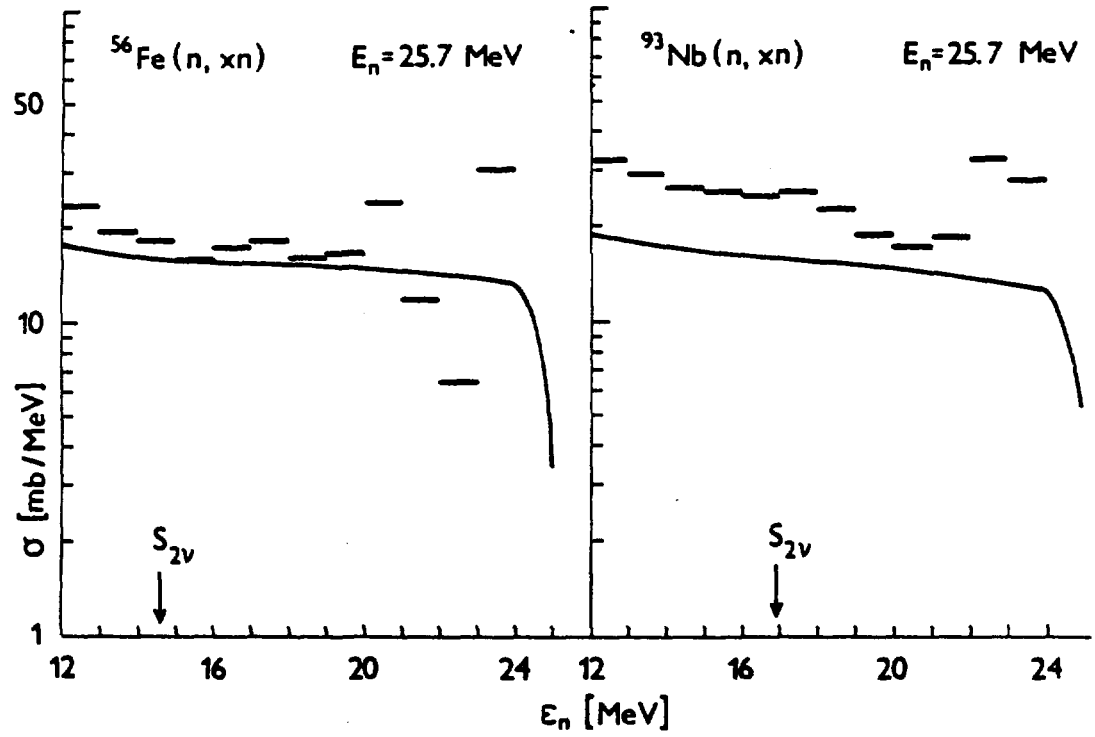
^{56}Fe (n, xn)
E_n = 25.7 MeV
^{93}Nb (n, xn)
E_n = 25.7 MeV
50
10
1
σ [mb/MeV]
$S_{2\nu}$
$S_{2\nu}$
12
16
20
24
12
16
20
24
ε_n [MeV]

Fig.15